



CTU

**CZECH TECHNICAL
UNIVERSITY
IN PRAGUE**

FACULTY OF MECHANICAL ENGINEERING

FAKULTA STROJNÍ

Department of Mechanics, Biomechanics and Mechatronics

Ustav mechaniky, biomechaniky a mechatroniky

Advanced acoustic barriers

Design and evaluation of 3D printed polymer acoustic barriers

Student: Wolf Van Der Bauwhede

Supervisor: prof. Ing. Michael Valášek

Co-supervisor: prof. Ing. Tomáš Vampola

Study program: Erasmus exchange

Academic year: 2021-2022



ABSTRACT

The scope of this thesis project is to design advanced acoustic barriers and to test the acoustic transmissibility. To this goal CAD was used and 3D printing to create innovative structures, subsequently these structures were tested for acoustic performance (absorption and reflectivity) in a 2-microphone impedance tube setup.

The designs were 3D printed using an FDM 3D printer. The design of test samples was inspired by existing studies about acoustic metamaterials. The advanced options in the PrusaSlicer software allowed to determine the impact of different infill structures. The designs varied from basic to advanced geometry. All these structures are of interest to be implemented in future soundproofing applications. Their applications vary from dashboards that reduce the interior sound level to noise-canceling covers for headphones.

To test the various designs, an impedance tube/Kundt tube was used. This test setup worked well to compare different design features and evaluate which design/geometry is better at absorbing or reflecting acoustic energy. This impedance tube was constructed by the university and the input signal is controlled by a MATLAB script that can be customized by the user. The measured results are analysed using another MATLAB script. This script calculates the reflection factor and the absorption coefficient of the tested samples. The calculation is performed by doing a FFT (Fast Fourier Transformation) on the measured microphone signals. The obtained transfer functions and acoustic parameters are then plotted to verify and compare the measurements.

After performing all the measurements, it can be concluded that all the samples are good at reflecting the sound energy. The reflection factor is always high. The 3D printed samples are stiff and are great acoustic reflectors. By comparing the transfer functions determined using the four-microphone method, it can be concluded that the 3D printed acoustic barriers that contain lots of thin and curved features are better at blocking the acoustic energy.

Literature: Valasek, M., Vampola, T.: Acoustic barrier, Utility pattern, 35819, UPV, Prague 2022 [1]

Keywords: CAD, Acoustic barriers, FDM 3D printing, MATLAB, Kundt tube acoustic testing

Supervisor: prof. Ing. Michael Valášek

Co-supervisor: prof. Ing. Tomáš Vampola

ACKNOWLEDGMENTS

This thesis would not have been possible without the large amount of support I have received from the professors of CTU. I would like to thank in particular prof. Valasek and professor Vampola for their patience and guidance. The production of the 3D printed samples was not an easy task. But thanks to the 3D printing lab at the Faculty of Information Technology, I was able to come up with enough samples. That is why I would like to thank professor Sýkora. To print more delicate designs I used the printers of prof. Jan Zavřel and Vít Pawlik at the faculty of Mechanical Engineering, their guidance was excellent. My knowledge of working with MATLAB, data-processing, CAD design and 3D printing has grown substantially during this semester.

This would not have been possible without the Ph.D. students that I have met in the lab here. I am very grateful for this opportunity to write my thesis at the Czech Technical University, thank you to everyone on the International student mobility team both in Belgium and in Prague. I would like to thank my family, my brother Robrecht Van Der Bauwhede for all his support during my thesis and at last, I would like to thank my parents Koen Van Der Bauwhede and Martine Vercruysse for all their love and support.

Wolf Van Der Bauwhede

Prague, 29/05/2022

DECLARATION

This thesis required knowledge of acoustics and mechanical vibrations. Most of this knowledge I retrieved from literature provided by the professors here at CTU. All the calculations and principles that will be used in this thesis are based on existing standards of data processing and measuring principles. The CAD designs/models used in this thesis were made by me. All ideas and major views of the designs were discussed with the professors before they were put into production. I am the sole writer of this thesis, so I am responsible for any miscalculations or uncertainties.

Wolf Van Der Bauwhede

Prague, 12/06/2022

Czech Technical University in Prague

Faculty of Mechanical Engineering

Technická 4

Prague 6, Dejvice

160 00

TABLE OF CONTENTS

Abstract.....	i
Acknowledgments	ii
Declaration	iii
Table of contents.....	iv
List of symbols.....	vi
1 Introduction.....	1
2 Introduction to acoustics	3
2.1 General terms	3
2.1.1 Soundwaves	3
2.1.2 Sound Pressure Level SPL / The decibel dB.....	4
2.1.3 Acoustic sound power and sound pressure	4
2.1.4 Acoustic impedance	4
2.1.5 Absorption, reflection and diffusion.....	5
2.1.6 White noise sound signal	7
2.1.7 Chirp sound signal	8
2.1.8 Standing plane waves	8
3 Introduction to acoustic measurements.....	9
3.1 The Kundt / impedance tube test setup.....	9
3.1.1 Component overview.....	10
3.2 ISO 10534-2 and E2611-19 standards.....	11
3.2.1 Two microphone principle	11
3.2.2 Four microphone principle.....	12
4 Materials and methods to acoustic measurements	13
4.1 Sound source.....	13
4.2 Microphones	14
4.3 Boundary conditions.....	16
4.4 MATLAB script.....	23

4.5 Preferred testing frequencies	25
4.6 Calculating acoustic parameters	26
5 Introduction to 3D Printing.....	29
5.1 FDM 3D printing.....	29
5.2 Important 3D printing terms.....	30
5.3 PrusaSlicer	31
6 Design of acoustic barrier structures.....	32
6.1 Acoustic metamaterials	32
6.2 CAD Models.....	34
6.3 STL conversion	38
7 Production of the acoustic barriers.....	39
8 Data processing.....	43
9 Test results	45
9.1 Results of the two microphone method	45
9.2 Discussion of the two microphone method results.....	55
9.3 Results of the four microphone method.....	56
9.4 Discussion of the four microphone method results	58
Conclusion	59
References.....	60
Appendix	63

LIST OF SYMBOLS

λ	Wavelength	[m]
SPL	Sound pressure level	[dB]
c	Sound speed	[m/s]
f	Frequency	[Hz]
T	Period	[s]
ρ	Density	[kg/m ³]
Z	Characteristic acoustic impedance	[Pa·s/m ³]
r	Reflection factor	From 0 to 1
α	Absorption coefficient	From 0 to 1
CAD	Computer aided design	
CAM	Computer aided manufacturing	
STL	Standard Triangle Language	
FFT	Fast Fourier Transform	
PLA	Polylactic acid	
TPU	Thermoplastic Polyurethane	
PETG	polyethylene terephthalate glycol-modified	

1 INTRODUCTION

The general topic of this thesis is a study around designing, 3D printing and testing 3D printed acoustic barriers. Almost every industrial environment has a lot of unpleasant sound. The acoustic energy produced by machines can be harmful to humans if it's not contained or muted. Most mechanical systems have multiple sound sources that are part of a bigger assembly. So local noise or sound isolation is needed to lower the sound power level and make spaces quieter.

A good example of this issue can be found in the interior of cars. Here the dashboard has to be able to reflect or absorb the sound created by the combustion engine and also other ambient noise, this situation is shown in Figure 1. Here you can observe where acoustic barriers can be used to create spaces with different sound pressure levels.

Designing barriers that block the sound can be difficult. The sound should be reflected or absorbed without creating another mechanical vibration. The best way of doing this when implementing supporting structures like a dashboard is by diffusing or breaking up the sound waves. This is why 3D-printed structures can be interesting.

The design concepts of the barriers are based on the following patent: *Valasek, M., Vampola, T.: Acoustic barrier, Utility pattern, 35819, UPV, Prague 2022* [2]

This patent describes that thin wall structures with lots of curvature are better at cancelling out sound. The geometry sketch of such a design can be seen in Figure 1.

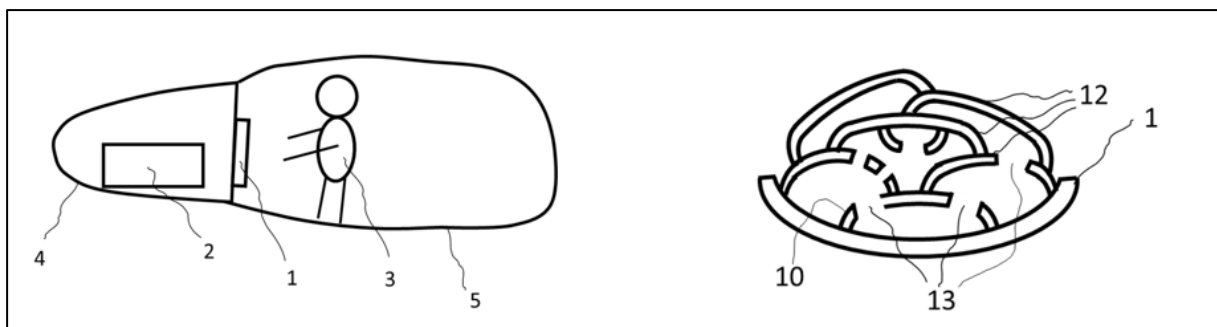


Figure 1: Left: placement of acoustic barrier, Right: thin curved structures used as barriers. [2]

The suggested geometry features in the patent will be tested using 3D printing. The printed samples will be tested using an impedance / Kundt tube. Test setups like this are visible in Figure 9 and Figure 10. This test setup uses a speaker and multiple microphones to determine specific acoustic parameters of the samples. These parameters tell something about the reflection, absorption and acoustic power transmission. [3] The acoustic environment that has

to be blocked by the barriers is always changing. This means that the frequency of the sound that has to be blocked changes as well. That is why the parameters will be determined for a useable and interesting frequency range.

This thesis aims to gain knowledge in the field of 3D printed acoustic barriers. The 3D printing technique used for this study is FDM 3D printing. This technique uses plastic filament that is extruded layer by layer. The main samples will be printed using hard filament like PLA or PETG (not flexible). To create a print, a model has to be converted and sliced into layers. The models for this study are designed using SolidWorks. Prusa FDM 3D Printers will be used to print the samples. The slicer software will be used to create models with different infills.

This thesis aims to answer the following questions:

What is necessary to design and produce 3D printable acoustic barriers?

Is there a notable difference between the absorption or reflection coefficients of FDM 3D printed samples with different geometry or infill types?

There is very little available information about how to design 3D printed barriers, What are the problems that occurred during the study? Are there any issues that can be improved?

The following outline is used to bring the information in a logical way:

- Introduction to acoustics
- Introduction to acoustic measurements
- Materials and methods to acoustic measurements
- Introduction to 3D Printing
- Design of acoustic barrier structures
- Production of the acoustic barriers
- Data processing
- Test results
- Conclusion

2 INTRODUCTION TO ACOUSTICS

This first chapter summarizes the required theory to understand the basics of acoustics and the principles needed to determine the absorption and reflection parameters of an acoustic barrier.

2.1 General terms

2.1.1 Soundwaves

Some terms need to be clarified before explaining how the standards (ISO 10534 or ASTM E2611) determine specific parameters that describe the propagation of sound waves.

A soundwave is a vibration of air molecules. This vibration is visible as a small harmonic pressure wave that is superimposed on the atmospheric pressure.

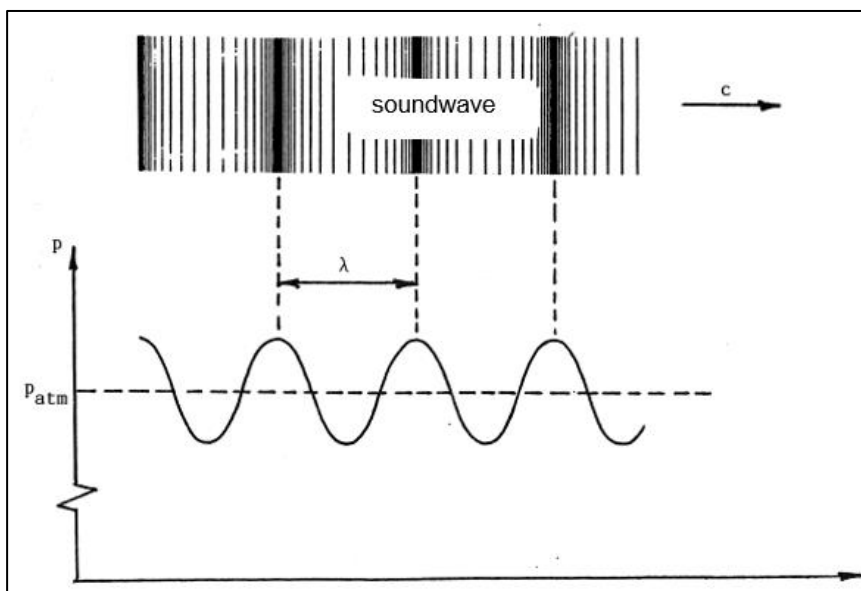


Figure 2: Soundwave of a pure tone / sin signal [4]

The soundwave shown in Figure 2 is a pure tone. This soundwave has a sinusoidal representation. Soundwaves like this do rarely occur in the real world. Most of the industrial sound that we hear are combinations of tones and noise. These soundwaves can no longer be represented by sinusoidal waves.

c = speed of the soundwave, (in dry air 343 m/s at 20 °C)

λ = wavelength = the distance the wave travels during one period

f = frequency = $\frac{1}{T}$ (with T = one period) in Hz

The frequency is the number of cycles within a specific time interval. $1 \text{ Hz} = 1 \text{ s}^{-1}$

2.1.2 Sound Pressure Level SPL / The decibel dB

The sound pressure level (SPL) is one of the most used parameters to compare sound sources.

It uses a logarithmic scale in decibel (dB). It basically compares the radiated sound power to a reference sound power. [4]

$$SPL = 10 \log \left[\frac{P}{P_r} \right] \text{ with } P_r = \text{reference power} = 10^{-12} \text{ W}$$

2.1.3 Acoustic sound power and sound pressure

The sound power P is “*the total airborne sound energy radiated by a sound source per unit of time. Sound pressure, on the other hand, is the result of sound sources radiating sound energy that is transferred into a specific acoustical environment and measured at a specific location. Sound power is the cause, and sound pressure is the effect.*” [5]

“Sound Power and Sound Pressure Explained,” BRÜEL & KJÆR, [Online]. Available: <https://www.bksv.com/en/knowledge/blog/sound/sound-power-sound-pressure>”

The mathematical definition of sound power is given by the following formula:

$$P = F * V$$

Where F is the sound force along a unit vector u in the direction of the sound wave propagation, V is the particle velocity along the same unit vector u . [6]

2.1.4 Acoustic impedance

The acoustic impedance (Z) is an important physical characteristic related to the propagation of sound through a medium. The acoustic impedance is given by the ratio of the wave's acoustic pressure to its volume velocity. The unit of acoustic impedance is the Pascal second per cubic meter, also called an acoustic Ohm.

“Acoustic impedance is very similar to electrical impedance. Electrical impedance or electrical resistance also measures how easily current can pass to a specific conductor. So the acoustic impedance is a measure of the ease with which a sound wave propagates through a particular medium. More specific, acoustic impedance is useful in discussing waves in confined mediums, such as tubes”.

[7] “Sound-physics Impedance,” Britannica, 12 May 2021. [Online]. Available: <https://www.britannica.com/science/sound-physics/Impedance>. [Accessed 12 April 2022].

When soundwaves go from air to a plastic barrier there will be a change of acoustic impedance. This change causes reflection and a limited transmission. This parameter is used by the standards to calculate the specific acoustic impedance ratio.

The mathematical definition of the characteristic specific acoustic impedance is given by the following formula:

$$Z = \rho * c \text{ where } \rho \text{ is the volumetric mass density and } c \text{ is the sound velocity [8]}$$

2.1.5 Absorption, reflection and diffusion

Sound absorption happens when we turn sound energy into heat or movement of a specific part. The sound waves create deformation in the sound barrier, this deformation costs energy. The larger the deformation the more energy the sound barrier can absorb.

“The sound absorption coefficient is the ratio of sound power entering the surface of the test object (without return) to the incident sound power for a plane wave at normal incidence”. [9]

S. MacDonald, “Sound Absorption,” Siemens, [Online]. Available:

<https://community.sw.siemens.com/s/article/sound-absorption>. [Accessed 25 04 2022].

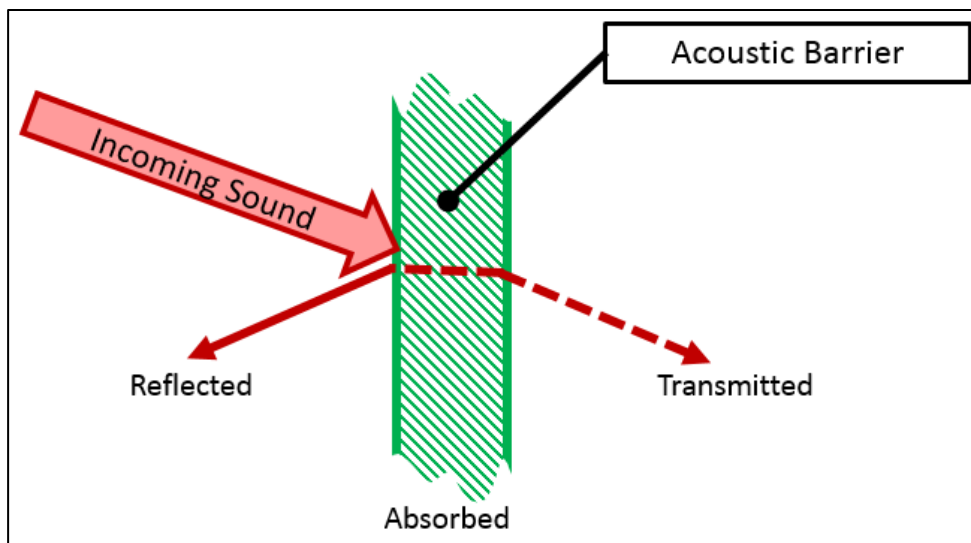


Figure 3: Principle of sound absorption [10]

Figure 3 shows that the sound can either be absorbed, reflected, or transmitted. The proportion of absorption, reflection, and transmission is different for every type of sound signal/frequency. This can be observed in Figure 4. Here multiple samples out of an acoustic foam material with changing thickness are tested for their absorption coefficient in function the frequency.

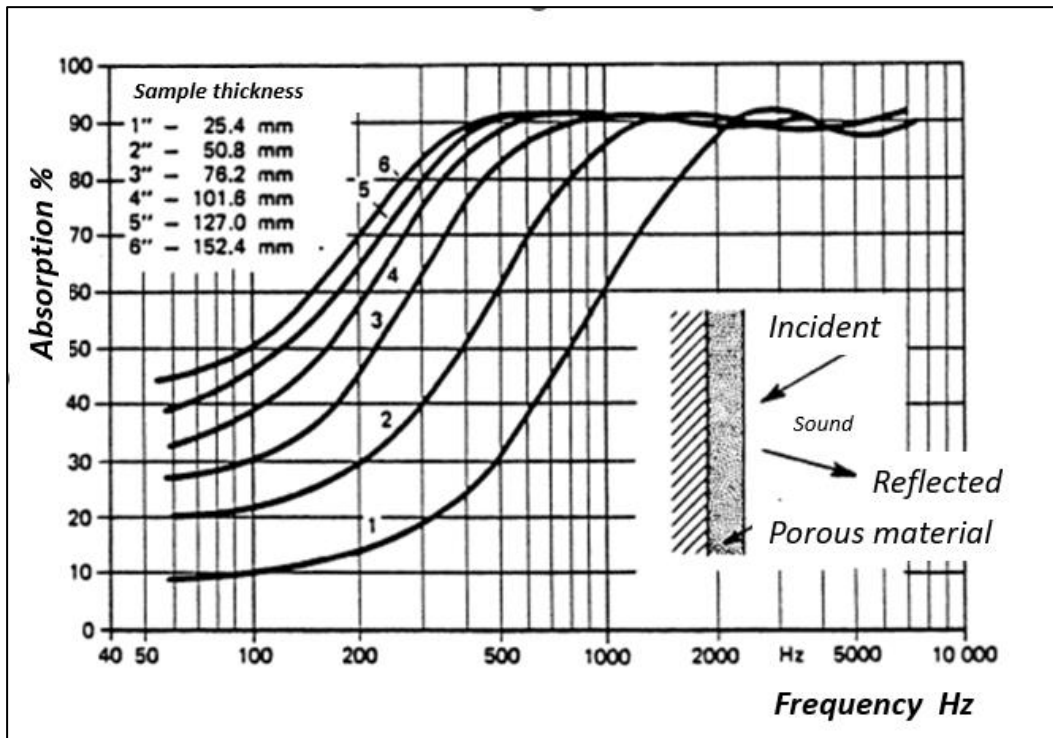


Figure 4: The absorption coefficient for the same test specimen is dependent on the sound signal frequency. [4]

The higher the absorption coefficient, the more sound is absorbed. Alfa ranges from zero to one. If alfa is equal to one, all the sound is absorbed.

$$\alpha = \text{absorption coefficient} = \frac{\text{Absorbed acoustic energy}}{\text{Incident acoustic energy}}$$

To design good acoustic barriers it is necessary to know which variables create maximum absorption or reflection. Listed below are the main checkpoints to keep in mind when designing.

Material composition: The exact material that is used for an acoustic barrier plays a big role. Some materials like foam are porous and are easily deformed elastically, which creates greater absorption. The polymer filament used in the 3D printers has very similar acoustic properties so that the material composition is not studied in this thesis.

Material thickness/geometry: Solid barriers will cause more reflection of the sound waves. Complex geometry, for example, thin curved surfaces will be better at diffusing the sound waves since they have a larger specific surface area.

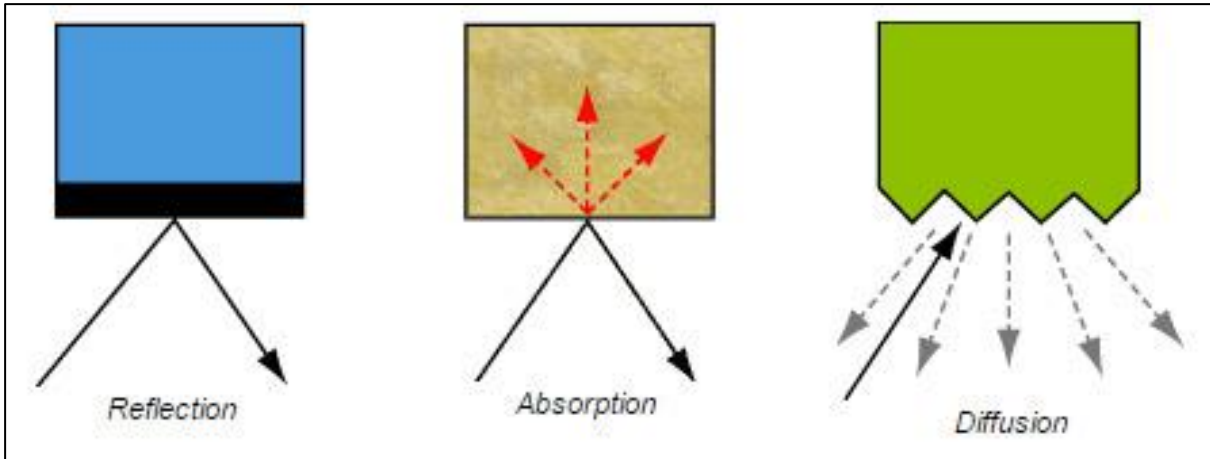


Figure 5: Types of soundwave propagation from air to a barrier [11]

Diffusion in acoustics is also a way of reflection. But the main goal here is to reflect the acoustic energy at various angles, as shown in figure 5. This breaks up planar sound waves. This type of barrier will be studied in this thesis.

2.1.6 White noise sound signal

“White noise is a random signal having equal intensity at different frequencies, giving it a constant power spectral density.” [12] See Figure 6. So white noise is a combination of different frequencies of audible sound, the signal can be heard by the human ear.

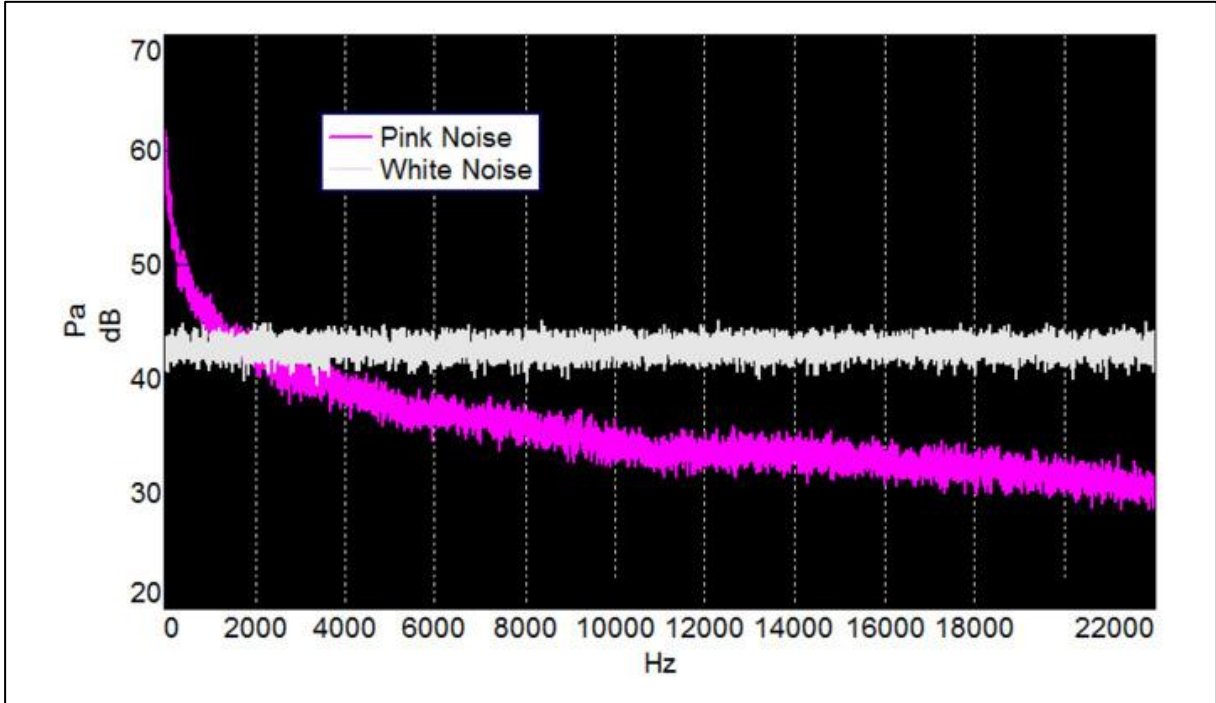


Figure 6: Example of a narrowband FFT of a white noise signal [13]

2.1.7 Chirp sound signal

This is a signal in which the frequency increases (up-chirp) or decreases (down-chirp) with time. An up-chirp sound signal can be seen in Figure 7. In some sources, the term chirp is used interchangeably with sweep signal. [14]

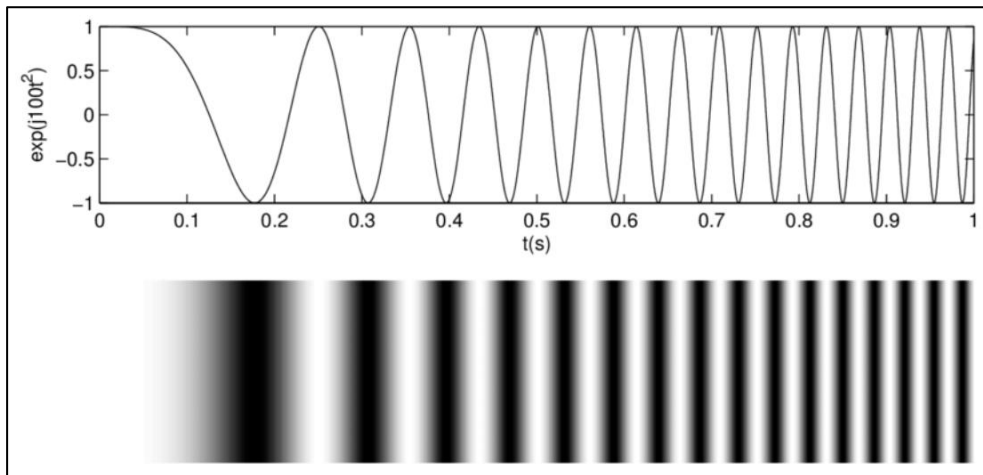


Figure 7: Example of a sin sweep, in particular an up-chirp signal [15]

2.1.8 Standing plane waves

A standing wave is according to the definition (IEC 801-23-15): “A periodic wave having a fixed distribution in space that is the result of interference of progressive waves of the same frequency and kind”. [16]

A standing wave, also known as a stationary wave, is a wave that oscillates in time but whose peak amplitude profile does not move in space. The peak amplitude of the wave oscillations at any point in space stays constant with respect to time, and the oscillations at different points throughout the wave are in phase, this is visible in figure 8. [17]

There are limits when it comes to generating acoustic plane waves inside tubes. These limits depend on the tube dimensions and on the sound generator.

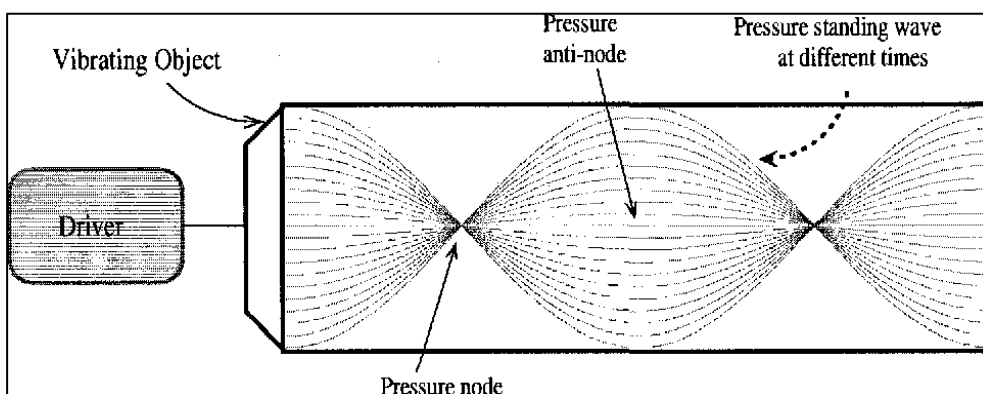


figure 8: Model of a plane wave created in a tube [18]

3 INTRODUCTION TO ACOUSTIC MEASUREMENTS

The best way for testing the acoustic properties on a small scale is by using an impedance tube. The impedance tube (also known as Kundt Tube) measurement obtains the normal incidence absorption coefficient and reflection factor. The results can be used to compare the acoustic performance of different samples.

3.1 The Kundt / impedance tube test setup

Figure 9 displays the impedance tube available in the lab. This tube is constructed according to the **ISO 10534 / ASTM E2611** standard. The tube has an uniform inner diameter of 100 mm. There is a speaker mounted on one side of the tube. This speaker can produce planar sound waves with different parameters. The other side of the tube is opened or it can be closed by a thick steel backplate. This setup is constructed with four microphone positions. Two in front of the sample and two behind. The used test setup can produce three different signals. The first one is white noise, this white noise is generated between two frequencies. In the MATLAB code, they are called f_1 and f_2 . The second signal that our speaker can produce is a pure tone or a sine wave. The frequency of the sine wave can be adjusted in the code as well. The last signal that the speaker can produce is a chirp signal. This test setup is relatively new, since it was built by the university as a project. This study will be testing the capabilities of this setup.

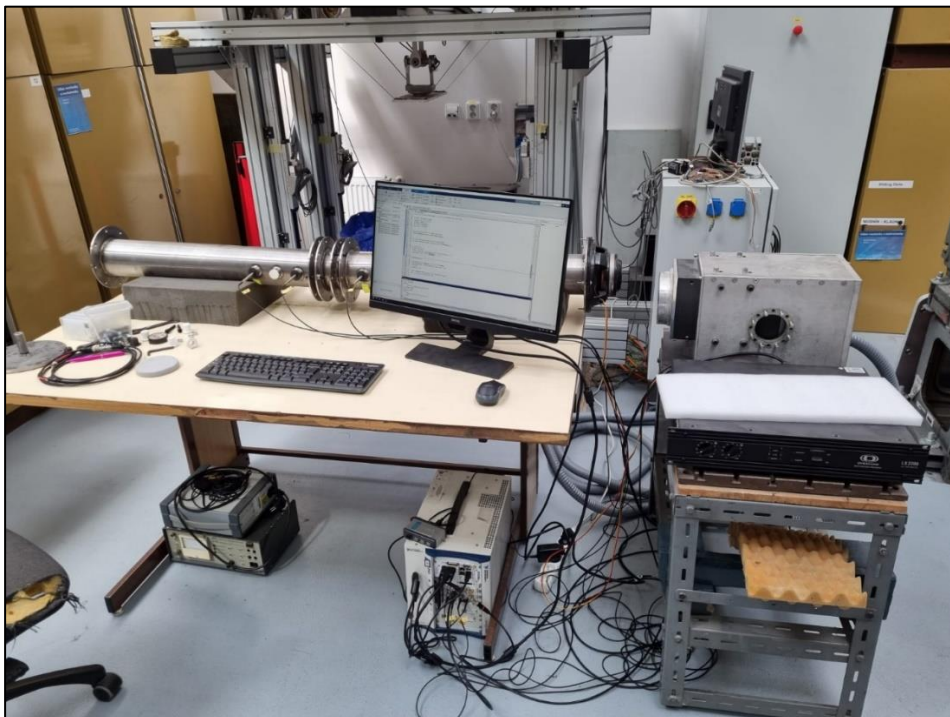


Figure 9: The impedance tube lab setup built by CTU.

3.1.1 Component overview

The available test tube in the laboratory is as described in the ISO 10534 and E2611-19 standards. The standards provide information about the components requirements. They also explain the used mathematical equations to convert the measured pressure signals from the microphones to useable acoustic parameters. These calculations are clarified in the data processing section. Figure 11 shows the samples that are normally tested using impedance tubes and Figure 10 shows an component overview of the two-microphone setup.

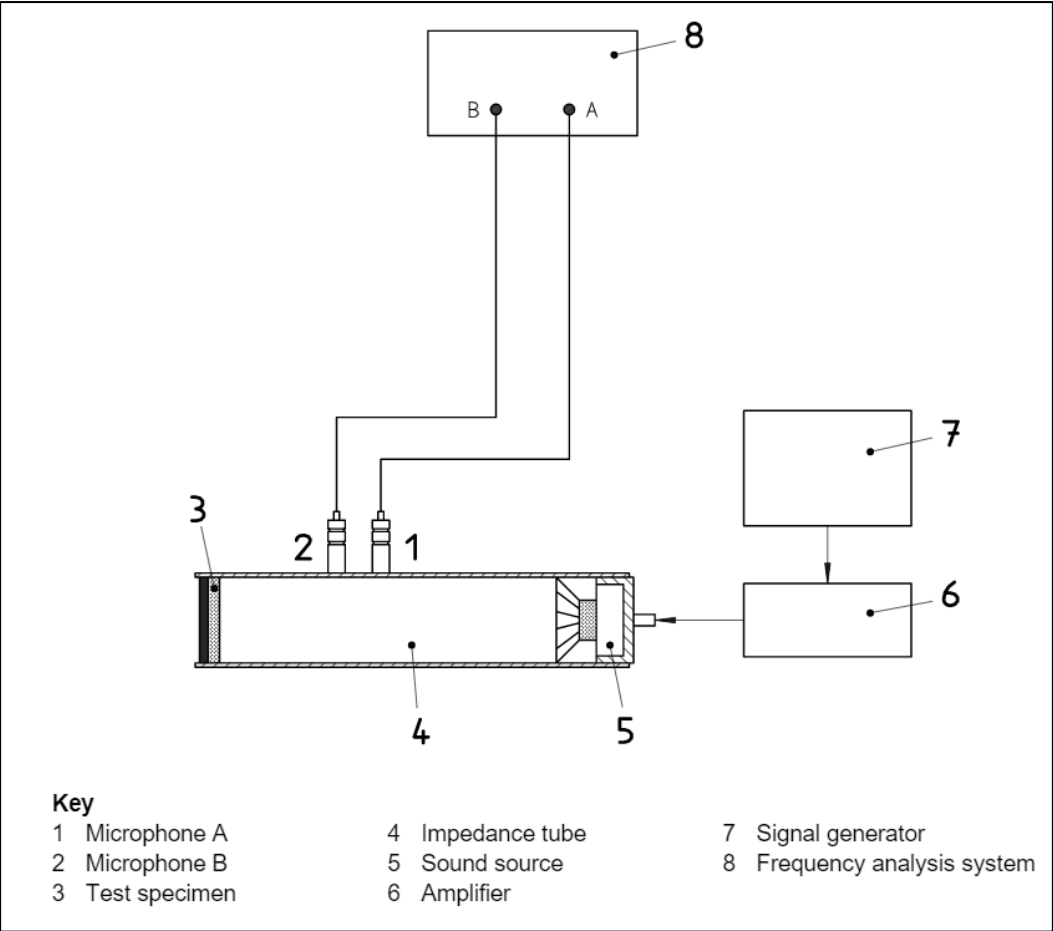


Figure 10: Two microphone impedance tube setup [9]



Figure 11: Typical acoustic test samples, with a sample cutter. [19]

3.2 ISO 10534-2 and E2611-19 standards

This section summarises the information gathered from the ISO and American standard. The ISO standard describes the use of a two microphone impedance tube to determine the reflection/absorption coefficient and the impedance ratio of the test sample. The main components of a two microphone impedance tube can be seen in Figure 10 and Figure 27. There are two ways of calculating these parameters listed in the standard. The first one is the standing wave method and the second one is called the transfer function method. The setup available in the laboratory has four microphones. So the equations in ISO 10534-2 can be used, here only two microphones in front of the sample are needed. The American E2611-19 standard does describe the use of a four microphone test setup. According to the following paper [20] there is very little difference between the 4-mic or 2-mic method. The result of this paper are shown in Figure 12.

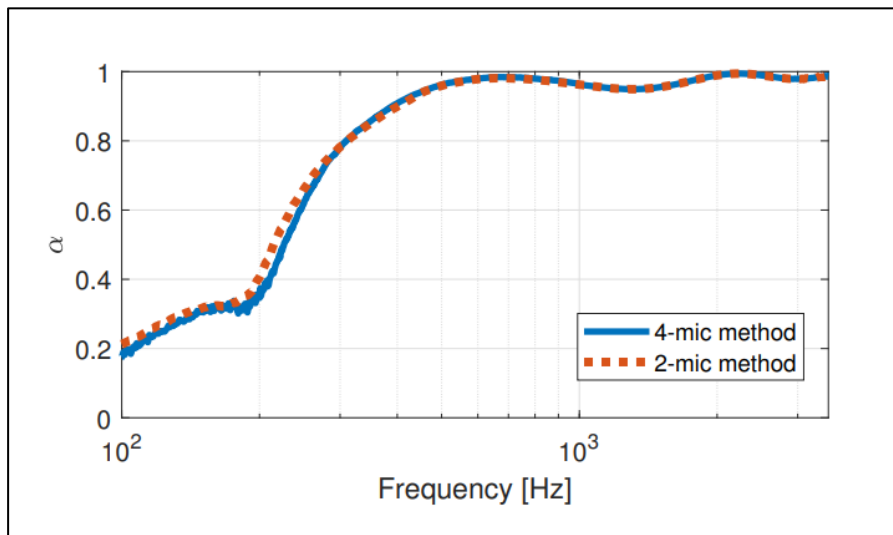


Figure 12: Acoustic absorption factor α determined by both 4 and 2 microphone setups. [20]

All the most important information out the standards is listed below.

3.2.1 Two microphone principle

The sample is mounted at one end of a straight rigid smooth and airtight impedance tube. This can be seen in Figure 10. Plane waves are generated in the tube by a sound source (random or pseudo-random sequence), and the sound pressures are measured at two locations near to the sample. The complex acoustic transfer function of the two microphone signals is determined and used to compute the normal incidence complex reflection factor, the normal incidence absorption coefficient and the impedance ratio of the test sample. [9] This is done by performing a fast fourier transform (FFT) on the measured microphone signals.

3.2.2 Four microphone principle

The principle of the four microphone measurements is very similar to the two microphone setup. The four microphone setup does allow you to determine more acoustic parameters. One of those additional parameters is the sound transmission coefficient. This coefficient gives an indication of how good a sample can contain the acoustic energy. It is the fraction of the transmitted sound power on the incident sound power.

This exact method is not used in this thesis since the MATLAB script available in the lab is not capable yet of performing the required calculations. But the current setup can calculate the transfer functions between the microphones. The transfer functions measured represent the acoustic pressure signals from one location relative to another location. So for example, H_{31} represents the pressure signal at location 3 relative to location 1. In this context, the transfer functions refer to the complex ratio of the Fourier transform of two signals.

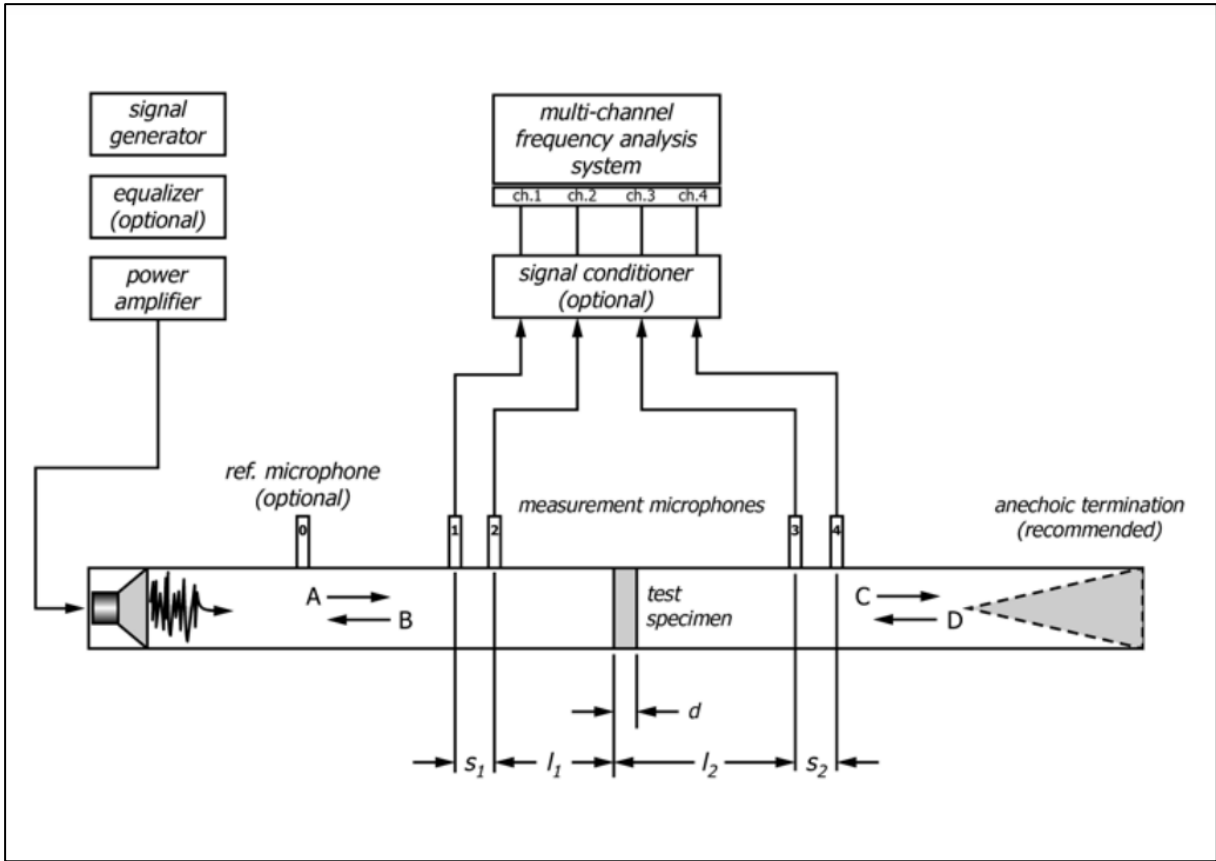


Figure 13 : Four microphone setup, the transfer function measured represents the acoustic pressure signals at location 3 relative to location 1. [21]

4 MATERIALS AND METHODS TO ACOUSTIC MEASUREMENTS

This sections describes all the practical materials, methods and calculations used to carry out the measurements.

4.1 Sound source

It is important to check the technical information of the speaker attached to the Kundt tube. This speaker will have a specific frequency range in which it can be used reliably. This information is shown in Figure 14. The speaker is connected to a Dynacord LX2200 PA Power Amplifier. This amplifier ramps up the control signal to create the required sound signals.



The image shows a Beyma 8LW30 Low Frequency Transducer speaker. The speaker is a circular, black, professional-grade unit with a visible yellow voice coil and a black cone. It is shown from a top-down perspective. The product name and model number are printed on the top of the speaker's frame.

TECHNICAL SPECIFICATIONS

Nominal diameter	200 mm	8 in
Rated impedance		8 Ω
Minimum impedance		6,9 Ω
Power capacity ¹		250 W _{AES}
Program power ²		500 W
Sensitivity	95 dB	1W / 1m @ Z _N
Frequency range		70 - 6.000 Hz
Recom. enclosure vol.	10 / 30 l	0,35 / 1,1 ft ³
Voice coil diameter	62,4 mm	2,5 in
Bl factor		12 N/A
Moving mass		0,022 kg
Voice coil length		16 mm
Air gap height		7 mm
X _{damage} (peak to peak)		23 mm


Figure 14: Used speaker on the Kundt tube built by CTU, note the marked frequency range

4.2 Microphones

The microphones used are made by IsemCon. They need a constant current power supply. This is done by connecting them with CCP connector cables to the embedded controller from National Instruments. The signals picked up by the controller are in V. Each microphone has a different sensitivity, this sensitivity is listed in the microphone frequency response measurement report provided by IsemCon. The EMM-7101 CSTB version is used, the info from this version is shown in a red box in Figure 15.

EMM-7101 series

(* ICP™, IEPE, DeltaTron™, CCP, ISOTRON™ compatible)



TYPICAL APPLICATIONS

- ✓ Multi-channel measurements
- ✓ Single-channel measurements
- ✓ Sound-power and sound-field analysis
- ✓ Low-cost in-car measurements
- ✓ Industrial Acoustics

The iSEMcon® Array Microphone EMM-7101-CSTB is an economically priced prepolarized microphone for single and multi channel measurements in arrays and matrices. It is a full featured product with integrated CCP-Preamplifier and programmed TEDS-chip (Template 27). The long 4" body minimizes the sound field influence from holding clamp or array mechanics.

ACTUAL SIZE

works from
Constant Current Power (CCP)
Phantom Power (PH)
By the use of an connector adapter
(no signal converter necessary)

FEATURES CSTB-Version

- ✓ Frequency range **10...20000Hz**
- ✓ Sensitivity **30mV/Pa** typ.
- ✓ Signal polarity: positive
- ✓ Dynamic range 30... >125dBspl
- ✓ 3% distortion limit >**130dBspl** typ.
- ✓ Built-in **TEDS** (template 27)
- ✓ **Calibration** chart and data included on CD
- ✓ Excellent amplitude and phase matching
- ✓ **SMB** connector
- ✓ **CCP or Phantom Power**
- ✓ Dimensions: diameter 1/4" (7mm) length w/ connector 4" (101mm)
- ✓ Weight **0.3oz (9grams)**

DIFFERENCE CHTB Version

- ✓ Sensitivity **6mV/Pa** typ.
- ✓ Signal polarity: positive
- ✓ Dynamic range 30... >140dBspl
- ✓ 3% distortion limit >**145dBspl** typ.

Figure 15: EMM 7101 microphones, long housing for mounting to limit the influence from the plastic clamp holder. The used CSTB version has a sensitivity of 30 mV/Pa.

iSEMcon®		Microphone Frequency Response Measurement Report		iSEMcon GmbH • Alexanderstr.66 • 68519 Viernheim Germany • www.iSEMcon.de • sales@iSEMcon.de	
Microphone Manufacturer:	iSEMcon GmbH	Model:	EMM-7101-CSTB		
Serial No.:	0315004				
Measurement Date:	12.01.15	Temperature:	20,9 °C / 69,62 °F		
Humidity:	35 %r.F. / r.H.	Pressure:	1012 mbar / 14,68 psi		
Phantom Power	Microphone sensitivity:	Reference microphone	Brüel & Kjaer 4133		
Supply voltage / Impedance	mV @ 94dBspl,1kHz	Sound calibrator	Quest CA-22		
Ref: 21V/4mA	26.10				

Figure 16: Microphone frequency response report, linked to every microphone serial number.

For example: Microphone 4 (serial No.:0315004) gives a signal from 26.1 mV when it observes a sound pressure level (SPL) of 94 dB.

Figure 17 and Figure 18 show the used microphone placement. The microphone holder should have a flush fit to the tube in order not to degrade the quality of planer wave.



Figure 17: Microphone mounted in plastic holder that is installed in the tube using a friction fit and petroleum jelly. The microphone stick out is measured here.



Figure 18: Mounted microphones

4.3 Boundary conditions

Good data can only be accomplished by being consistent when using the impedance tube. This is especially important when comparing samples. That is why this section is added to describe the used way of performing and preparing a good test.

Tube support: The tube is resting on high-density foam. This foam isolates the tube from any vibrations passing through the lab building. The foam needs to be spaced out evenly so that the tube is well supported and levelled out, this is shown in Figure 19. Good levelling is important to maintain acoustic plane waves. Any misalignment may result into uncontrolled reflection on the tube walls. This results in bad data.

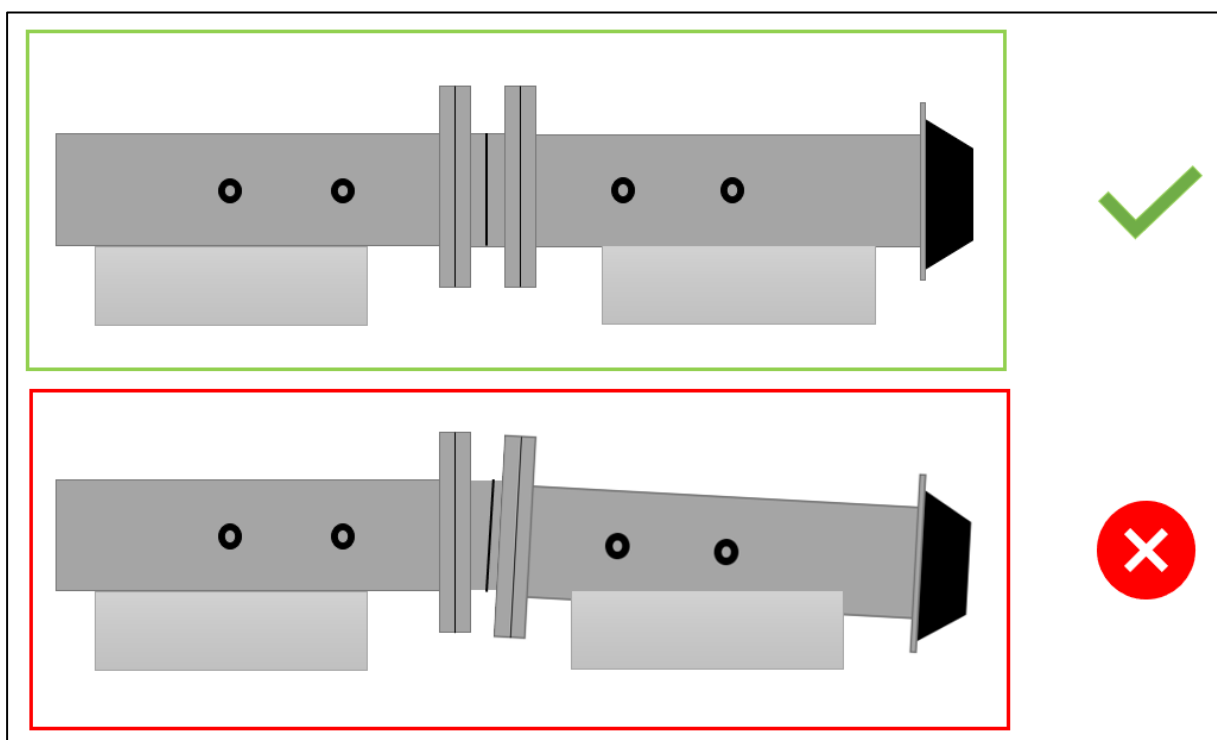


Figure 19: Good support makes for a proper seal and alignment of the impedance tube

Environment: All the tests are performed when no machines are running in the background, this is done to make sure that the microphones do not pick up any undesired sound or vibration.

Sample mounting and tube closing: The samples are mounted in a separate holder which is bolted to the main tube. This holder is placed in the middle of the impedance tube. All the samples have to be mounted in the same place. This place is in the middle of the sample holder since the distance between the microphones before and after the sample should be kept within the same range. This is measured by using a depth gauge.

The holder is used according to the E2611-19 standard: [21]

“6.3.2 Detachable Holder—As a detachable unit, the holder must make an airtight fit with the end of the tube opposite the sound source. The holder must conform to the interior shape and dimensions of the main part of the tube. The connecting joint must be finished carefully and the use of a sealant, such as petroleum jelly or silicone grease, is recommended.”

All the samples need to be installed in the holder similarly. This is performed by first checking and creating an airtight seal inside the holder. The seal is created by first placing O-rings inside the groves that are made into the samples, and then covering the sides with petroleum jelly to create an air-tight friction fit. This is visible in Figure 20 and Figure 21. The petroleum jelly (Vaseline) also serves as a lubricant to speed up the installation of the samples.



Figure 20: O-rings (size inner \varnothing 95 mm, thickness 2mm) and petroleum jelly are applied.

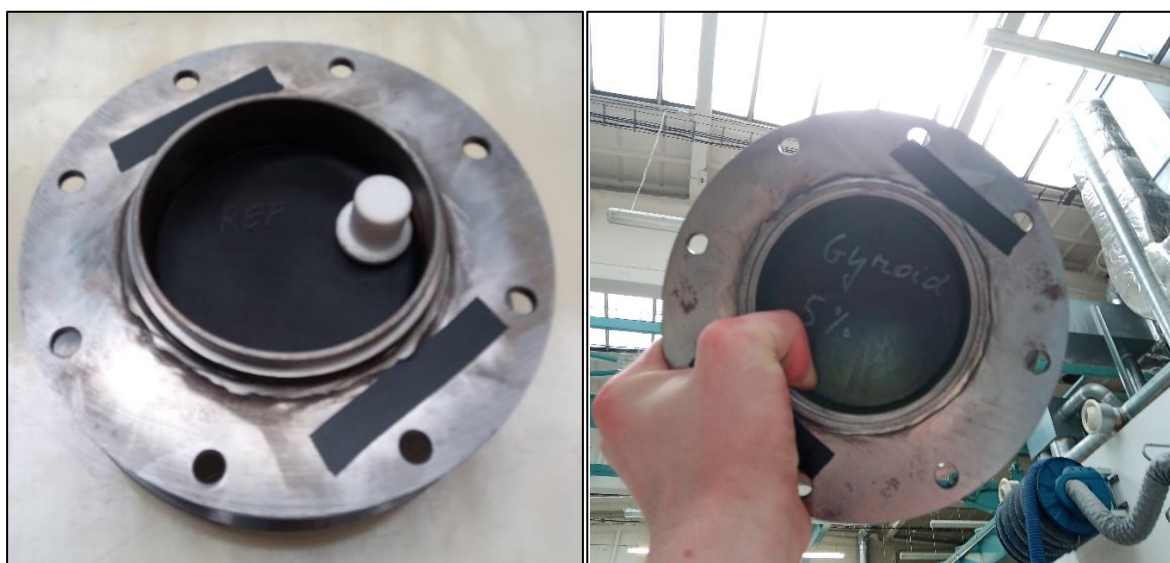


Figure 21: Procedure of checking the depth of a sample by using a plastic depth gauge. The depth is always checked from the same surface marked with two strips of tape.

Figure 21 also shows how the seal is checked. The sample holder is held up to a light source and then the sample circumference is checked for any gaps. If there are any gaps observed, then a small rubber band is added underneath the O-rings. The flat surface of the sample is always installed parallel to the face that is used to check the depth of the barrier sample.

The surfaces that are interacting to close the tube are finished on a lathe and have a tight fit. The flanges welded to the tube have multiple holes, not all of these holes were used to fasten the tube together, this is visible on Figure 22. Only two bolts on every flange connection is sufficient. The used bolts are placed 180° apart from each other and tightened with a similar torque. Before the tube is closed a small amount of Vaseline is applied to the closing rim, this creates an even better seal.

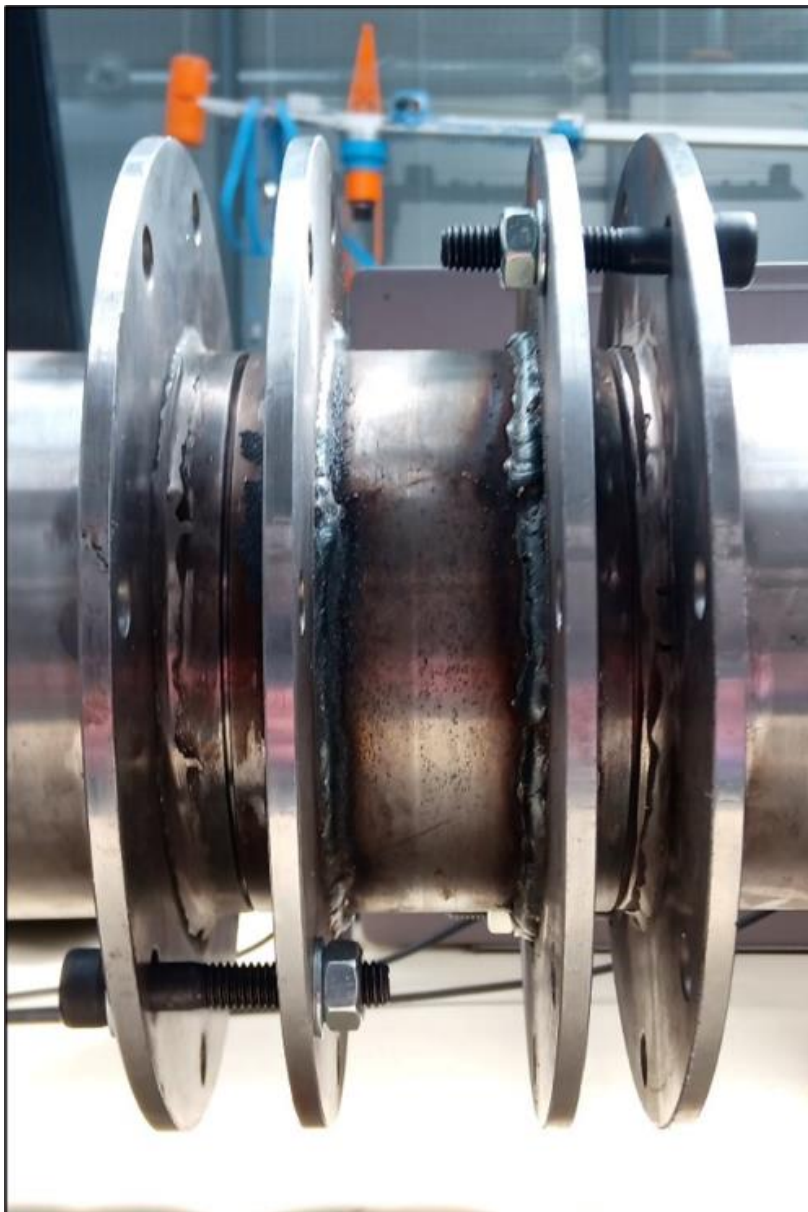


Figure 22: Properly closed impedance tube, the gap between the interfering parts has to be consistent around the whole circumference.

Microphone positioning: Always kept constant between the different microphones. See Figure 17, here the placement can easily be verified by using a calliper. The microphones cannot stick-out, this would diffuse the standing acoustic waves generated by the speaker. They have to be installed flush with the inner tube top. See Figure 24.



Figure 23: Microphone stick out seen from the inside of the tube (note here the microphones are sticking out too far.)

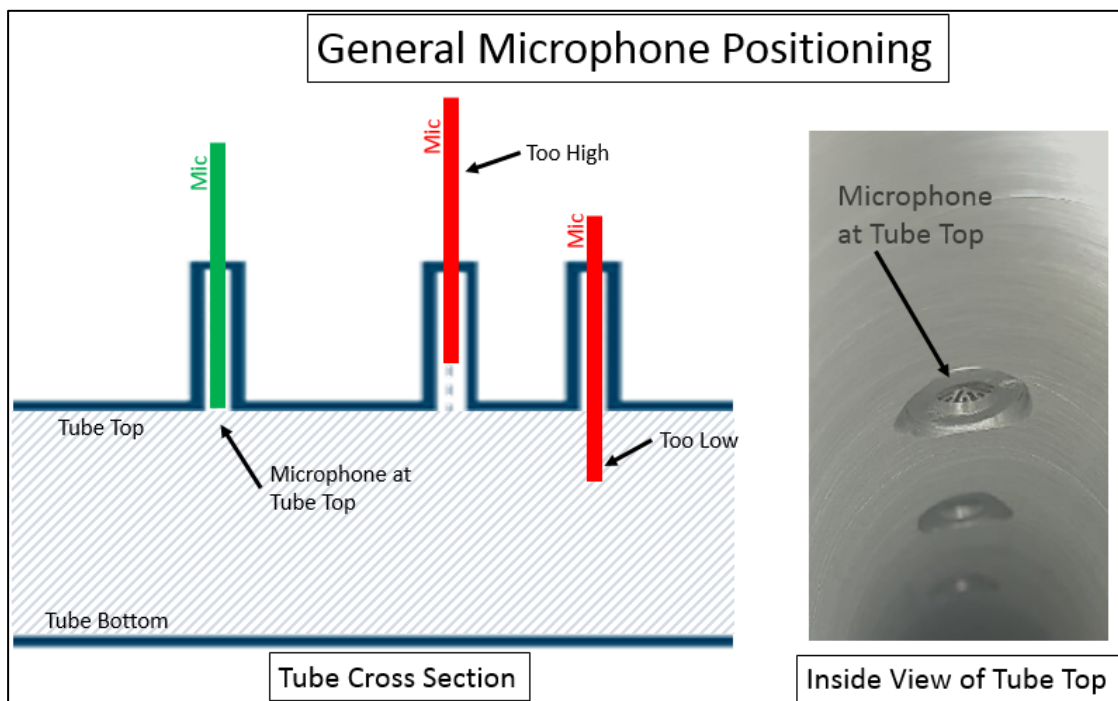


Figure 24: Good microphone placement [19]

Controller used: National Instruments PXIe-1062Q with a maximum system bandwidth of 3 GB/s. So this controller can handle 3 GB of data per second. This is why this controller is used to have a large sampling rate. The sampling rate can be controlled with the MATLAB script. This controller is running Windows with MATLAB.

Tube termination: The impedance tube used can be closed with a 20 mm thick steel backplate. The tube can also be opened, when using the four microphone principle. This represents an anechoic termination. Anechoic means that there are no acoustic waves being reflected back into the tube. The tube is pointed away from any hard and reflective objects, It is pointed in open space. An acoustic camera from SoundCam was used to verify this. This camera has 62 microphones and is normally used to locate sound sources. The speaker of the test tube produced a 1600Hz signal, this was easier to visualize and this sound signal is still a plane wave inside the tube.

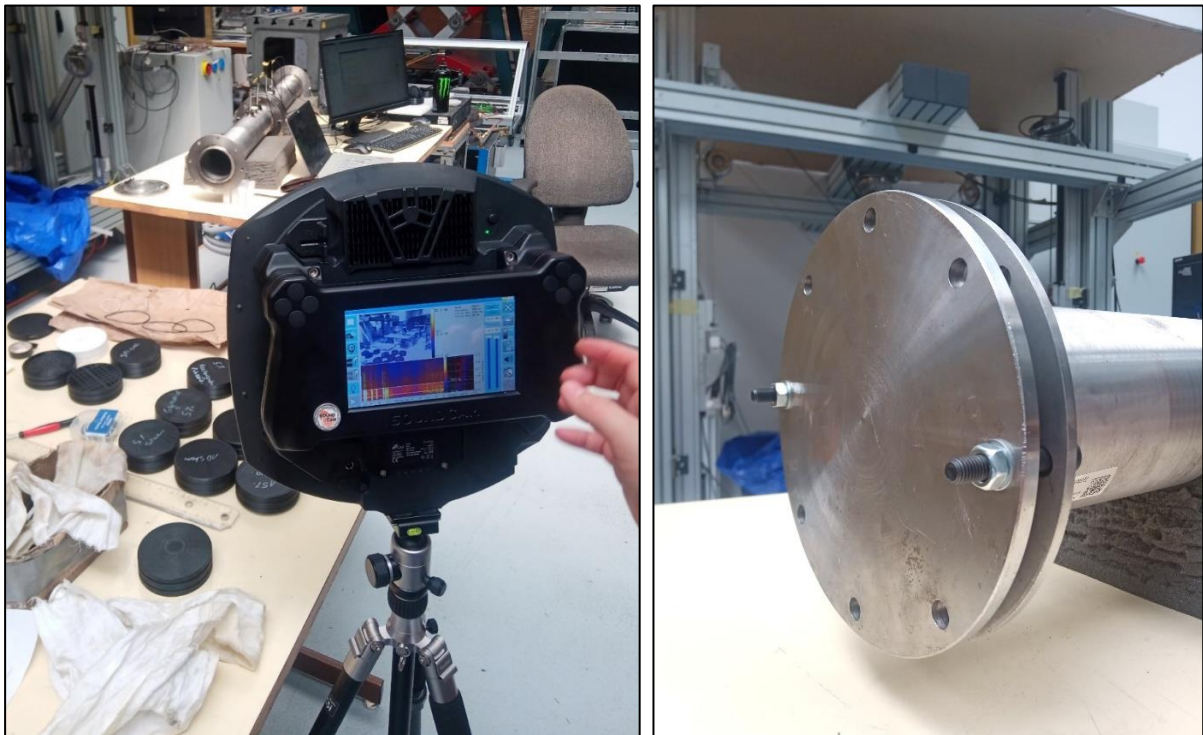


Figure 25: Left : Acoustic camera pointed at the impedance tube the verify the acoustic energy leaving the tube. Right: Tube closed with a solid steel backplate.

Figure 28 and Figure 29 show the results of the camera. The installed sample is the infill comparison model with 15% Hilbert infill. There is very little acoustic energy coming out of the tube when the sample is installed. So an open tube can be used for 4 microphone measurements if the background is kept constant. But it was decided to use a close tube, since this creates more constant measurements.



Figure 26: Used two microphone setup in the lab, The sample is always placed in the same place and backed by a 20 mm thick steel plate.

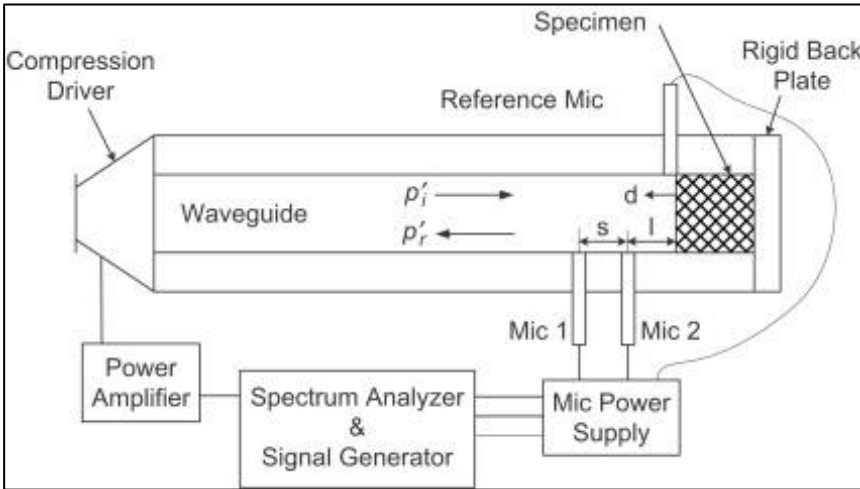


Figure 27: Principle diagram of a two microphone measuring setup. [22]

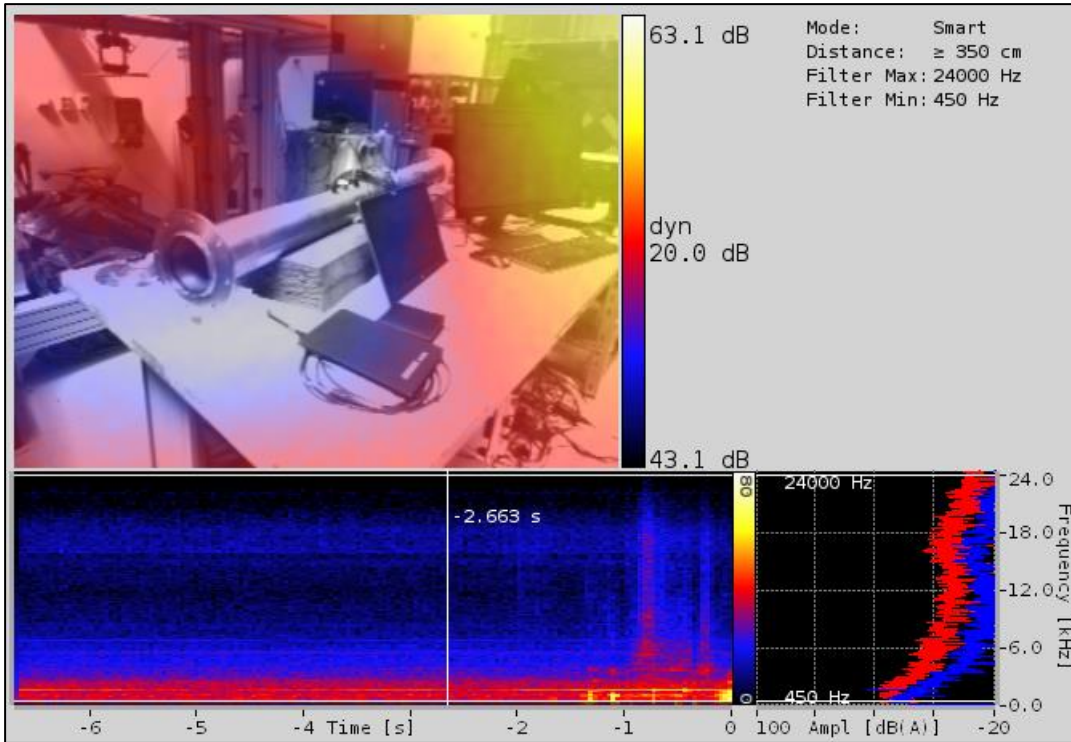


Figure 28: Screenshot from the camera display with a sample installed in the impedance tube. The sound measured is mostly ambient sound energy reflected from the back wall of the laboratory.

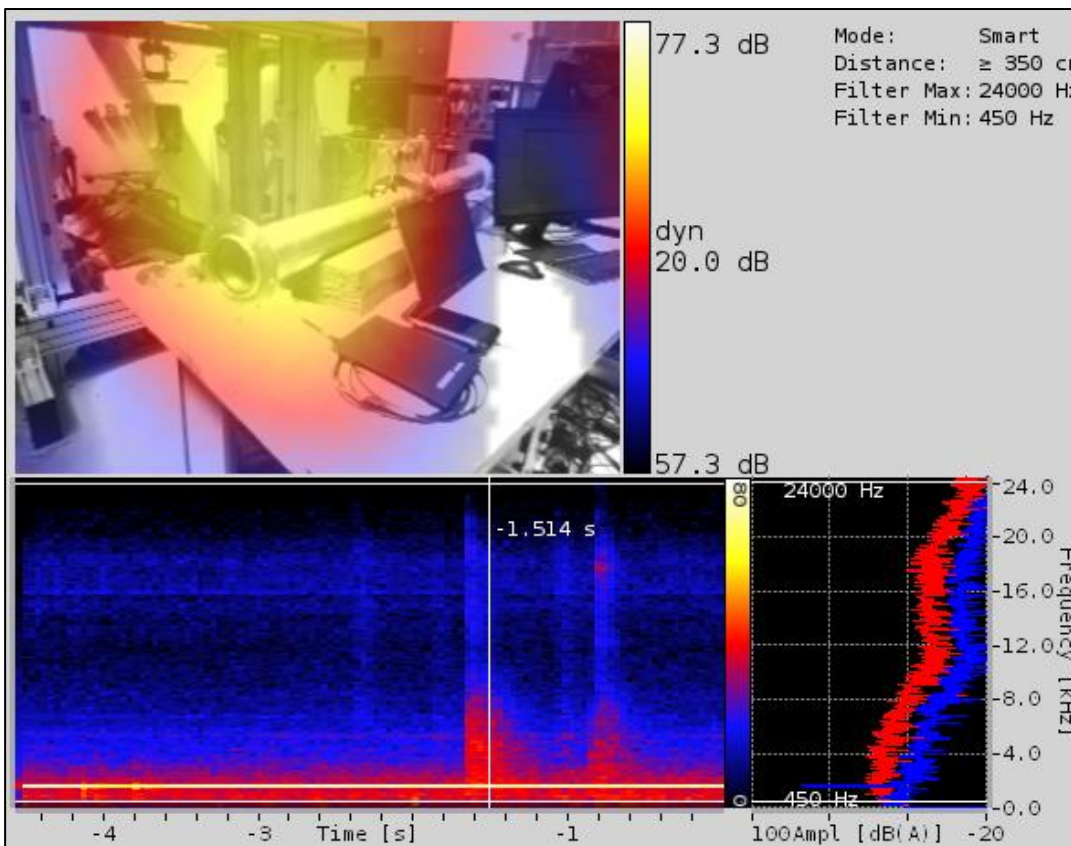


Figure 29: Screenshot from camera display with NO sample installed.

4.4 MATLAB script

This section briefly describes the use and potential options inside the MATLAB code used to measure the sound pressures inside the impedance tube.

To control the speaker mounted on the impedance tube a MATLAB script is used. This code creates the different sound signals and picks up the microphone data during the whole measurement duration. A constant measurement duration (10s) and sampling rate (10000) are used for all my tests/samples. The parts of the code listed below in Figure 30 and Figure 31 show the parameters that can be changed. As already mentioned above there are three signals that can be created. A pure tone, the sine signal, a white noise signal, and a chirp signal.

```
47 %% measurement setup and signal generation
48
49 % SAMPLING RATE
50 - d.Rate = 10000; % Hz, 1 to 204 kHz available
51
52 % MEASUREMENT DURATION
53 - time2measure = 10; % seconds
54
55 % FREQ RANGE for white noise and chirp signal generation
56 - f1 = 100; % Hz
57 - f2 = 1000; % Hz
58
59 % FREQUENCY for sine signal
60 - sineFreq = 500; % Hz
61 - timeStep = 1/fix(d.Rate);
62 - numSamples = fix(time2measure*d.Rate);
63
64 % generating white noise from f1 to f2, range +- 1 volt * gain
65 - gain = 1;
66 - wnf1 = f1; % Hz
67 - wnf2 = f2; % Hz
68 - whiteNoise = gain*genBilySumNIDAQRange (fix(d.Rate), numSamples, wnf1, wnf2);
69
70 % generating chirp signal
71 - chirpSig = gain*chirp(linspace(0, time2measure, numSamples), f1, time2measure, f2);
72 - chirpSig = chirpSig*rms(whiteNoise)/rms(chirpSig);
73 % normalizing rms ~ energy to match the levels of white noise
74
75 % sine signal
76 - sineTime = 0:timeStep:time2measure-timeStep;
77 - sineSig = sin(2*pi*sineFreq*sineTime);
78 - sineSig = sineSig*rms(whiteNoise)/rms(sineSig); % normalizing rms
```

Figure 30: Signal creation in MATLAB

```

99      %% measuring
100     % run this section (CTRL+ENTER) to perform measurement and save data
101
102     % SELECT THE OUTPUT SIGNAL
103     % output signal selection
104 -   outsig = whiteNoise;
105     % outsig = chirpSig';
106     % outsig = sineSig';
107
108
109     % run the measurement for input and output
110 -   [meas,timeMeasStarted]= readwrite(d,outsig);
111
112
113     % to run the measurement when not using output
114     % [meas,timeMeasStarted]= read(d,seconds(time2measure));
115
116
117     % saving data
118     % DATA FILE NAME
119 -   fname = "Kundt_01_"+string(datetime,'yyyy-MM-dd_HH-mm-ss');
120 -   save(fname,"meas","mCh","mChRange","-v7.3")
121

```

Figure 31: The signals can easily be selected by making the active (removing comment %)

For the experiments, it was decided to use the **sine signal and white noise signal**. The reason for this choice is listed in the following paper [23]. *A sine sweep signal (the chirp signal) is not ideal for the measurements because some frequencies of the sine sweep might resonate parts of the test setup, this could result in useless data.*

A white noise signal is also a good representation of industrial noise that the barriers should be able to block.

4.5 Preferred testing frequencies

Traffic or industrial noise is louder in the low frequency range of 10~ Hz to 1000 Hz, so for a barrier to be effective it must perform well in this range.

The upper frequency limit f_u depends on the diameter of the tube, the microphone spacing, and the speed of sound. In order to maintain plane wave propagation, the upper frequency limit is defined according to the **E2611-19 standard** as follows: [21]

$f_u < \frac{Kc}{d} \quad \text{or} \quad d < \frac{Kc}{f_u}$	f_u = upper frequency limit, Hz, c = speed of sound in the tube, m/s, d = diameter of the tube, m, and K = 0.586.
---	--

$$\frac{0.586 \cdot 330}{0,1} \cong 1930 \text{ Hz} \quad \text{So } f_u \text{ has to be smaller than } 1930 \text{ Hz.}$$

The lower frequency limit f_l is determined by the spacing of the microphones and the accuracy of the analysis. The microphone spacing shall be greater than one percent of the wavelength corresponding to the lower frequency of interest.

The test will be performed using two signals. A sine signal and a white noise signal. The following frequencies are used. Sine signal = 500 Hz and White noise with $f_1=100$ Hz and $f_2=1000$ Hz. The frequency f_1 has to be checked if it is not too low for the used test setup.

Microphone spacing s (see Figure 32 and Figure 10) is 0,13 m.

The wave length λ for a sound signal of 100 Hz going through dry air is 3,44 m. One percent of 3,44m is 0,0344 m. So the microphone spacing s has to be greater than 34 mm which is the case in the used test setup. Meaning that the frequency of 100 Hz can be used.

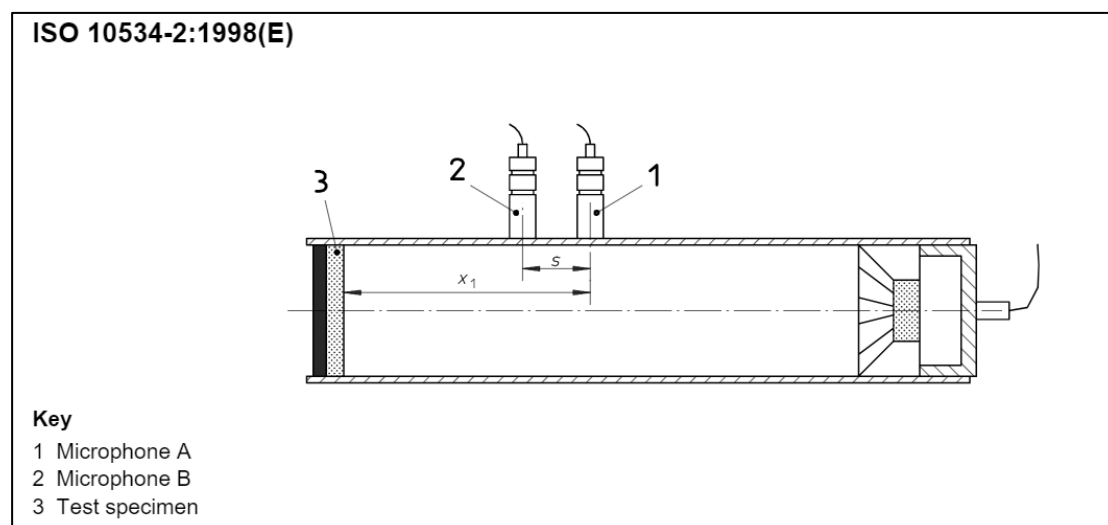


Figure 32: Two microphone test setup, note the microphone spacing s . [9]

4.6 Calculating acoustic parameters

To calculate the acoustic parameters using the two microphone transfer function method it is necessary to first clarify some specific definitions and symbols. They are explained in the ISO 10534-2 standard and listed below in Figure 39 [9]:

2 Definitions and symbols

For the purposes of this part of ISO 10534 the following definitions apply.

2.1

sound absorption coefficient at normal incidence

α

ratio of sound power entering the surface of the test object (without return) to the incident sound power for a plane wave at normal incidence

2.2

sound pressure reflection factor at normal incidence

r

complex ratio of the amplitude of the reflected wave to that of the incident wave in the reference plane for a plane wave at normal incidence

2.3

reference plane

cross-section of the impedance tube for which the reflection factor r or the impedance Z or the admittance G are determined and which is usually the surface of the test object, if flat

NOTE The reference plane is assumed to be at $x = 0$.

2.4

normal surface impedance

Z

ratio of the complex sound pressure $p(0)$ to the normal component of the complex sound particle velocity $v(0)$ at an individual frequency in the reference plane

2.5

normal surface admittance

G

inverse of the normal surface impedance Z

2.6

wave number

k_0

variable defined by

$$k_0 = \omega/c_0 = 2\pi f/c_0$$

where

ω is the angular frequency;

f is the frequency;

c_0 is the speed of sound.

NOTE In general the wave number is complex, so

$$k_0 = k_0' - jk_0''$$

where

k_0' is the real component ($k_0' = 2\pi/\lambda_0$);

λ_0 is the wavelength;

k_0'' is the imaginary component which is the attenuation constant, in nepers per metre.

2.7

complex sound pressure

p

Fourier Transform of the temporal acoustic pressure

2.8

cross spectrum

S_{12}

product $p_2 \cdot p_1^*$, determined from the complex sound pressures p_1 and p_2 at two microphone positions

NOTE * means the complex conjugate.

2.9

auto spectrum

S_{11}

product $p_1 \cdot p_1^*$, determined from the complex sound pressure p_1 at microphone position one

NOTE * means the complex conjugate.

2.10

transfer function

H_{12}

transfer function from microphone position one to two, defined by the complex ratio $p_2/p_1 = S_{12}/S_{11}$ or S_{22}/S_{21} , or $[(S_{12}/S_{11})(S_{22}/S_{21})]^{1/2}$

2.11

calibration factor

H_c

factor used to correct for amplitude and phase mismatches between the microphones

Figure 33: Specific definitions and symbols used in ISO 10534-2 [9]

The calculations will be performed by a MATLAB script that performs FFT (Fast Fourier Transform) to convert the measured pressure signals to transferfunctions. The following parameters in Figure 34 and Figure 35 can be determined by using the equations in MATLAB. More information about the exact script can be found in the data processing section. This script is provided by CTU. The purpose of my thesis is to implement the existing script not to improve it.

7.7 Determination of the reflection factor

Calculate the normal incidence reflection factor (see annex D):

$$r = |r|e^{j\phi_r} = r_r + jr_i = \frac{H_{12} - H_1}{H_R - H_{12}} e^{2jk_0x_1}$$

where

r_r is the real component;

r_i is the imaginary component;

x_1 is the distance between the sample and the further microphone location;

ϕ_r is the phase angle of the normal incidence reflection factor;

H_1 and H_R are defined in annex D.

7.8 Determination of the sound absorption coefficient

Calculate the normal incidence sound absorption coefficient:

$$\alpha = 1 - |r|^2 = 1 - r_r^2 - r_i^2$$

Figure 34: Calculating the reflection factor and absorption coefficient. See the appendix for annex D [9]

7.9 Determination of the specific acoustic impedance ratio

Calculate the specific acoustic impedance ratio:

$$Z / \rho c_0 = R / \rho c_0 + jX / \rho c_0 = (1 + r) / (1 - r)$$

where

R is the real component;

X is the imaginary component;

ρc_0 is the characteristic impedance.

Figure 35: Calculating the specific acoustic impedance ratio. $\rho * c_0$ is the characteristic impedance of the air inside the tube. Z is the acoustic impedance of the sample. See appendix. [9]

5 INTRODUCTION TO 3D PRINTING

5.1 FDM 3D printing

FDM 3D printing or Fused Deposition Modelling is 3D printing technique that uses material extrusion. [24] A model is printed layer by layer, the main principle of FDM printing is shown in Figure 36. There is a specific workflow that is used when designing 3D printed parts. The first step is creating a CAD model, all the CAD models used in this research are designed using SolidWorks. Most of the slicer software cannot work with the CAD file extension created by SolidWorks for example. This is why the CAD models are converted into STL files when the design is done STL is an acronym for Standard Tessellation Language. SolidWorks simplifies the CAD model by meshing and covering it with triangles. The STL-file is then uses by the slicer software to create G-code.

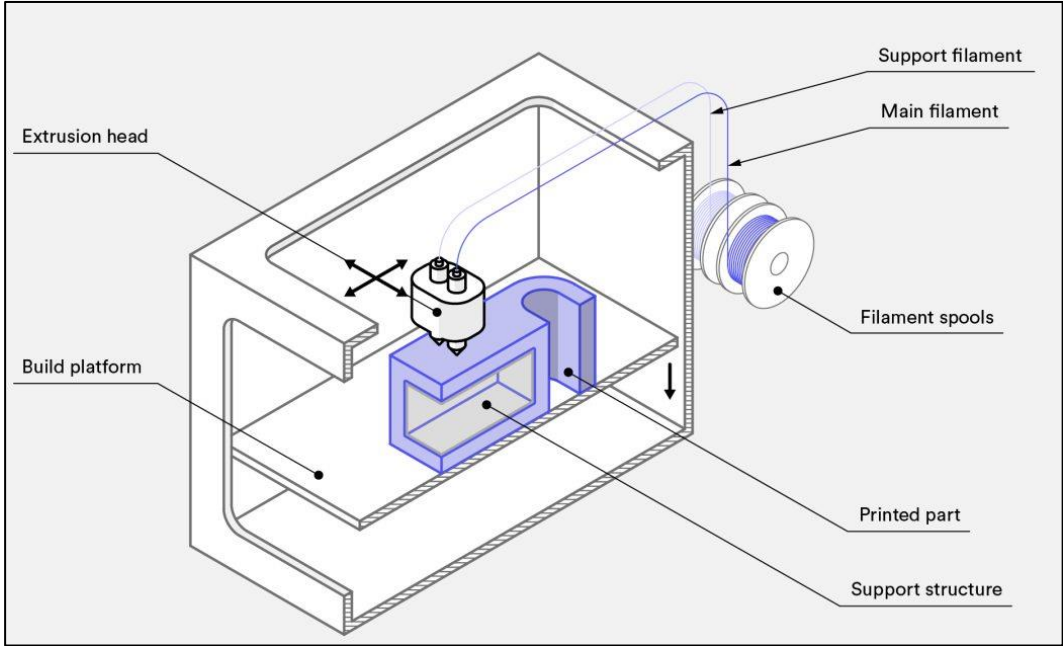


Figure 36: Principle of FDM 3D printing [24]

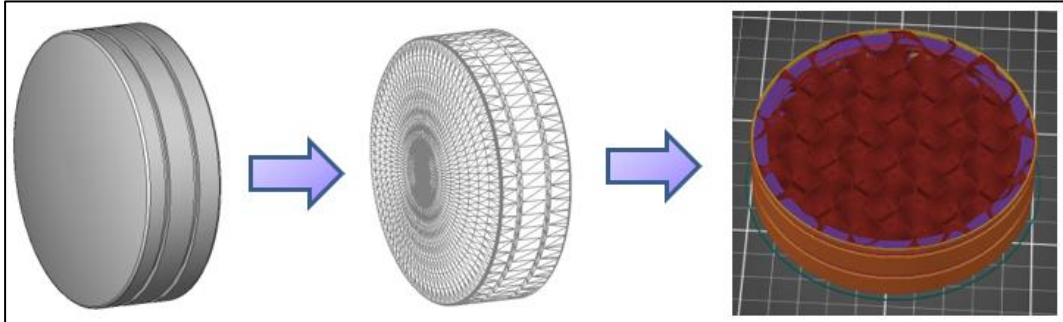


Figure 37: The CAD model is converted to STL and then used by CAM/slicer software to create a G-code.

Notice in Figure 37 that the resolution of the STL-file changes. Places that have more details get a higher tessellation.

5.2 Important 3D printing terms

There is a lot to consider when preparing models for a FDM 3D printer. Some terms need special attention in this study. They are summarized below.

Layer height: is the height of the individual slices/thickness of each layer. Layer height is the main factor affecting both the printing time and the vertical resolution of your model. The first layers that are printed are always higher. This will improve adhesion and general tolerances.

Wall thickness: In Prusa slicer, the wall thickness can be changed either in the vertical or horizontal direction. The used terms in the software are, vertical shells and horizontal shells. An example of this is shown in Figure 38 and Figure 39.

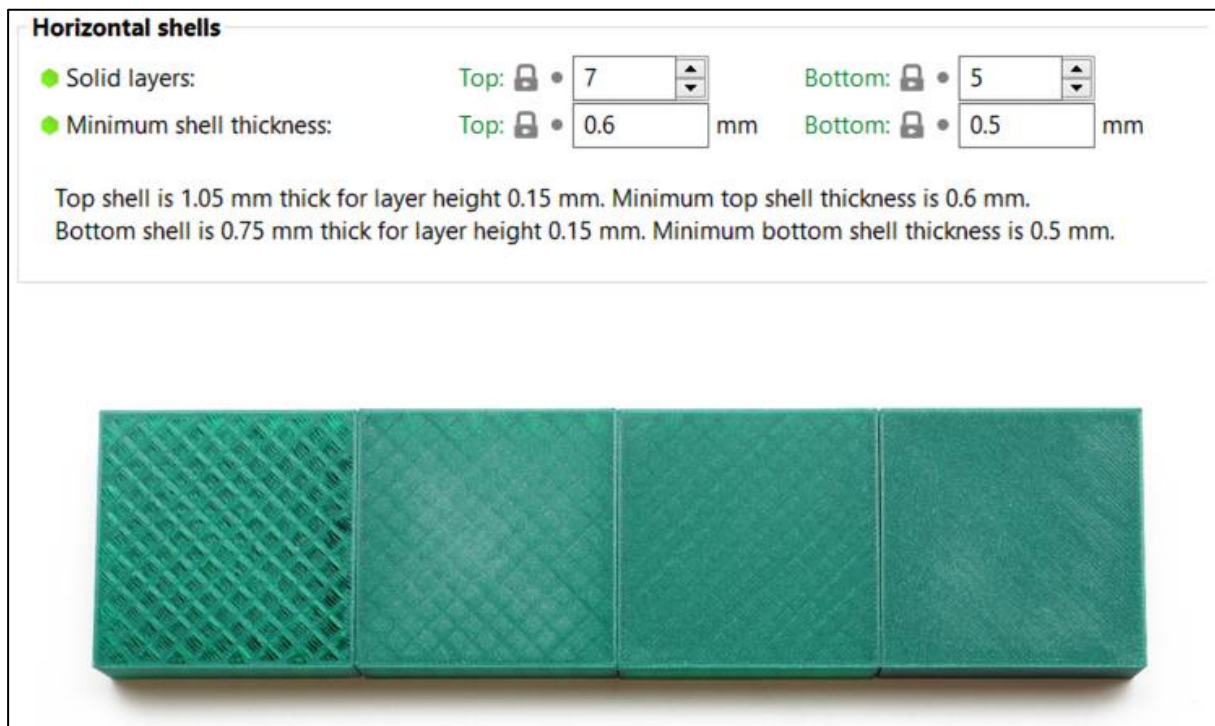


Figure 38: Example of setting up the horizontal wall thickness. From left to right, 1, 2, 3, and 5 top layers, printed at 0.1 mm layer height. [25]

Setting up the vertical shells/wall thickness is done in a similar way.

Infill: All models that are modelled as solids can be made hollow in the slicer software using infill. This study will compare the different infill geometries and densities available for the same solid base model. An example of an square rectangular infill can be seen in Figure 38.

Filament: This is the plastic feeding wire material used by the extruder of the printer to create the models.

5.3 PrusaSlicer

The PrusaSlicer software is used to convert the STL-files into a G-code. The G-code is the scripted language used by the 3D printer to create a extrusion nozzle path. PrusaSlicer is utilized since it is compatible with the Prusa printers and because it has advanced options to change the infill and wall thickness of the acoustic barriers STL-models. The exact advanced options and infill settings applied to the barriers are explained in the production section.

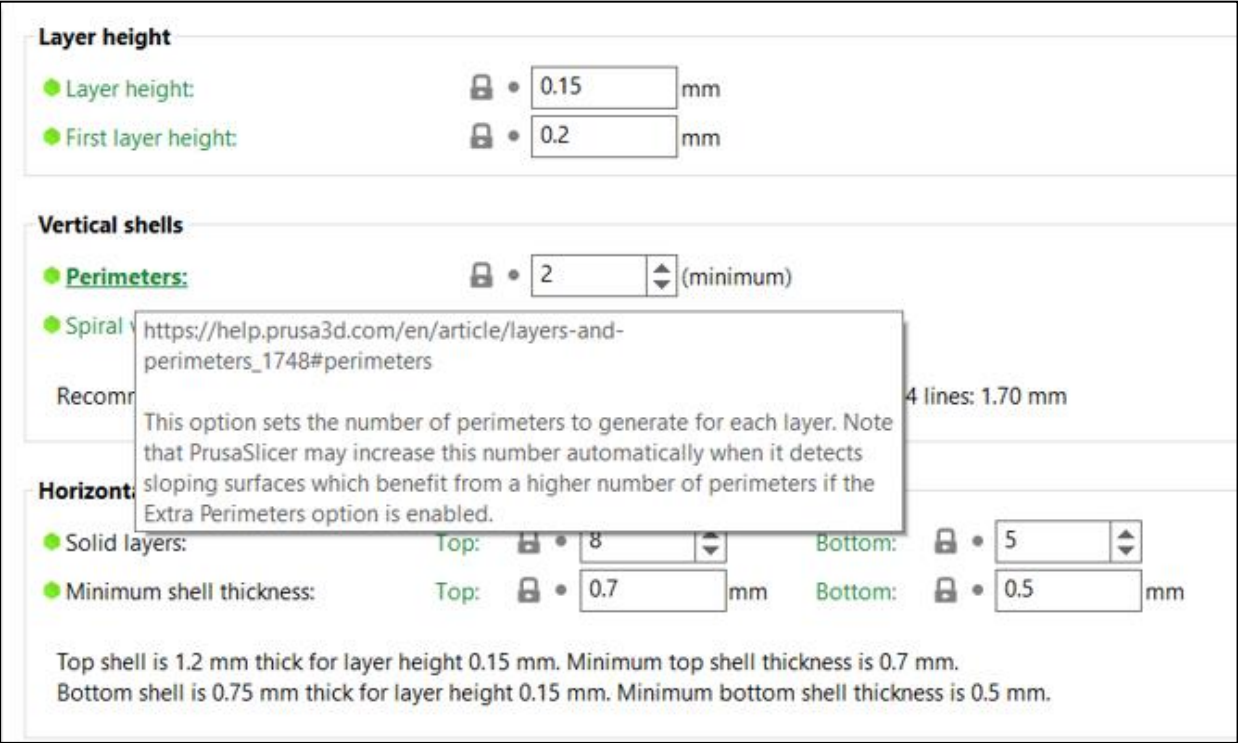


Figure 39: The Prusa software automatically chooses setting but change can be made to create extra thin wall features. All the green parameters are explained in the online user manual of the software.

6 DESIGN OF ACOUSTIC BARRIER STRUCTURES

Finding the best geometry that is able to absorb or reflect different soundwaves is not easy. There is very little written research available about 3D printed sound barriers. So tests about how far to go with wall thickness and other design variables like infill geometry will be studied. The sections below describes how to design test samples that respect the FDM 3D printing limitations.

6.1 Acoustic metamaterials

Acoustic metamaterials can be made fast using 3D printing or mechanical machining. They do not have to be super complicated to obtain better sound proofing results than the standard porous sound isolating foams. The main difference between acoustic metamaterials and normal sound isolation materials like polyurethane foams, is the fact that the air permeability is better in the metamaterials. Metamaterials are designed for slowing down the soundwaves. This is done by diffusing the soundwave not only on the striking surface of the barrier but also inside the barrier. Figure 40 is an example of such a barrier. So, a metamaterial could consist of air and a complex infill geometry.

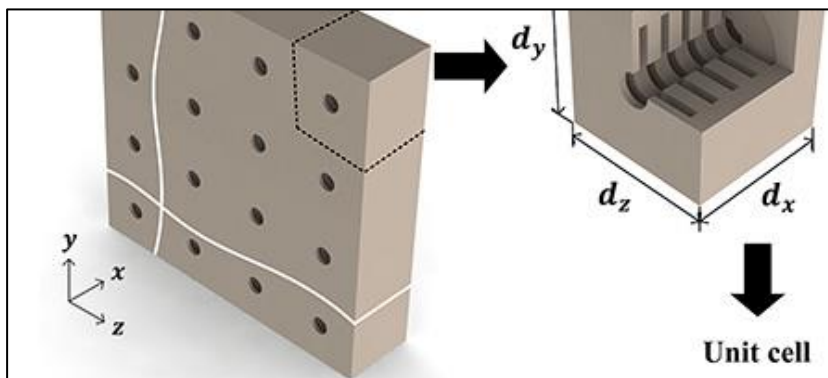


Figure 40: Example of a metamaterial made out of one base material with repeating unit cells. [26]

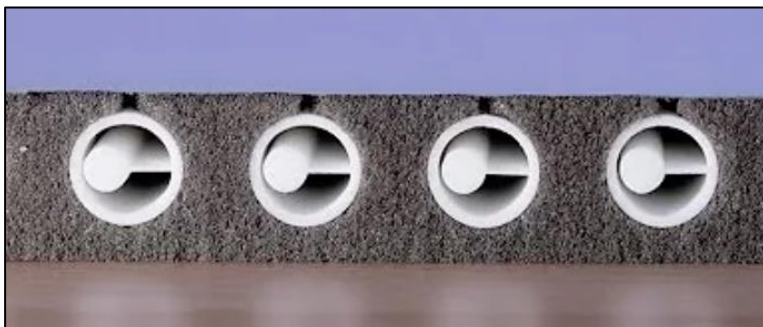


Figure 41: Example where multiple materials are used to create an acoustic metamaterial. [27]

Metamaterials could also be made out of multiple materials combined together, Figure 41 shows such a material. Here foam and solid plastic are working together to absorb and diffuse sound waves. But this thesis is focusing on single material 3D printed designs. Designs structures with periodically rearranging objects can have interesting impacts on the propagation of sound waves. These periodical rearrangements of a specific geometry can form sonic crystals, Figure 42 shows examples of such patterns that can be 3D printed.

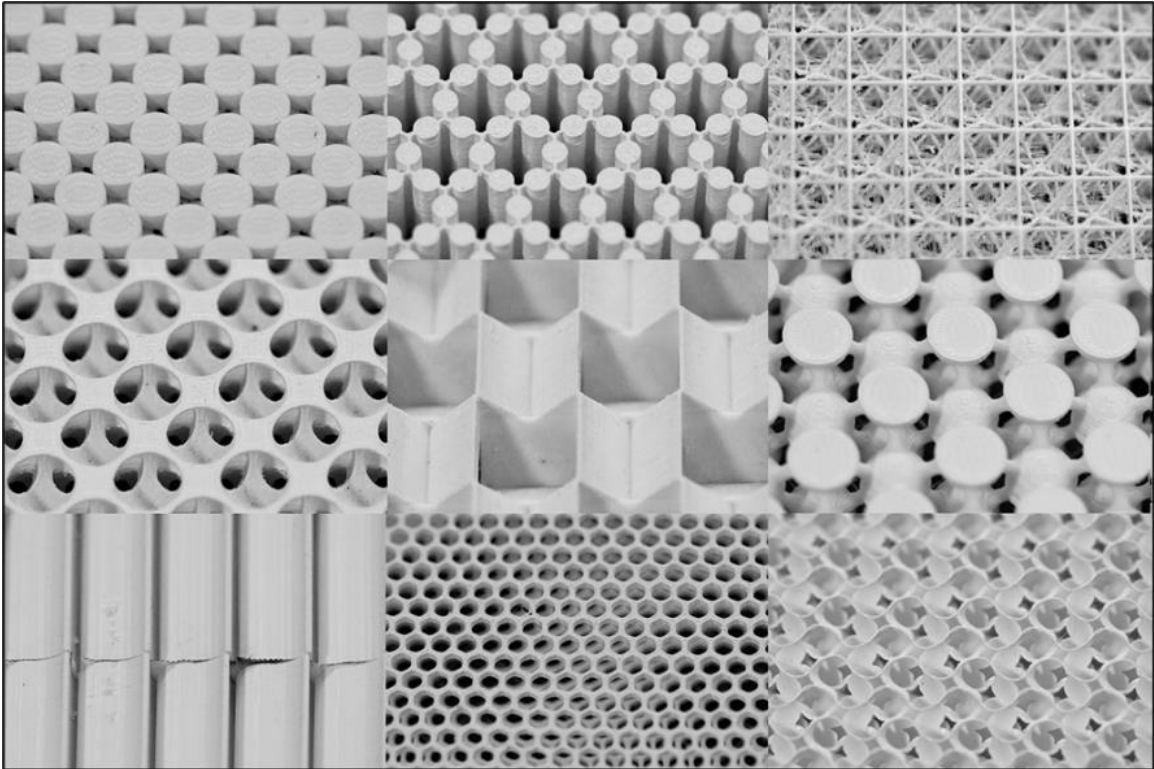


Figure 42: Examples of 3D printed metamaterials used as acoustic diffusers. [28]

6.2 CAD Models

Creating CAD models that could provide interesting results is not an easy task. The models should have a similar volume and weight to compare the overall effectiveness. They need to be easy to print and need to have similar dimensions and weight. They also need grooves to add O-rings to create a good seal inside the sample holder of the impedance tube. The exact dimensions of all the models can be found in the technical drawings added to the appendix and all the models are designed using SolidWorks.

Reference model

A reference model is used to check the effectiveness of just a straight sheet of plastic. This model has an overall thickness of 3 mm. All these features are made using the revolve function.

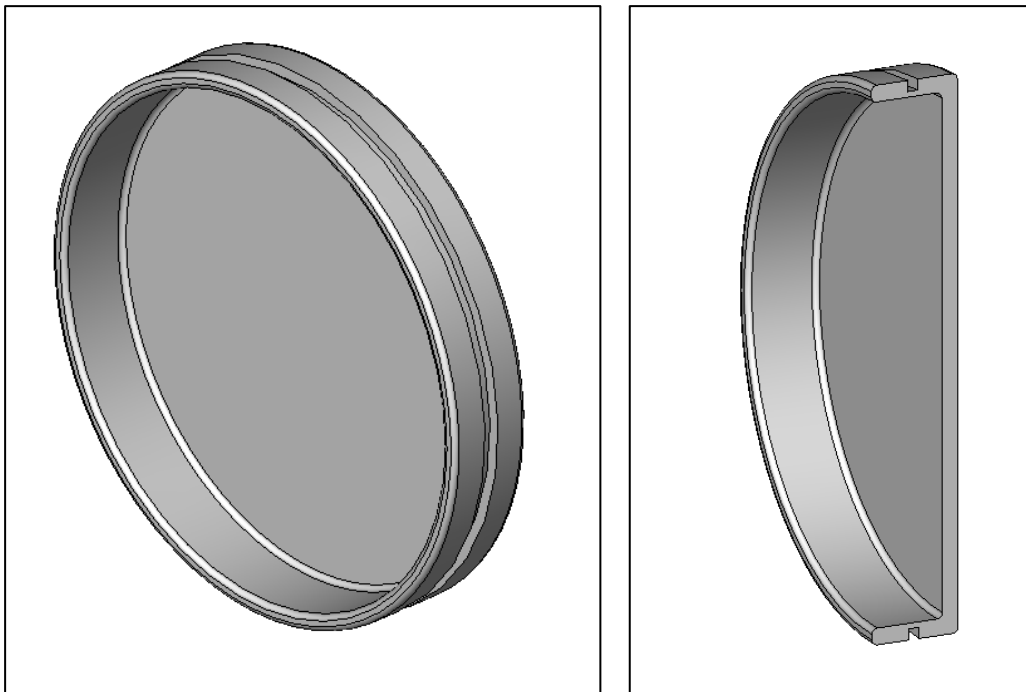


Figure 43: Reference sample CAD model with section view

Infill comparison model

This model is modelled as a solid, later in the slicer software it will be possible to hollow out this model by using different infill types and infill densities. Some infill materials might have better properties when it comes to diffusing / absorbing acoustic energy, that is why this model is created. The exact types of infill will be described in the next section. This model is also created using the revolve function.

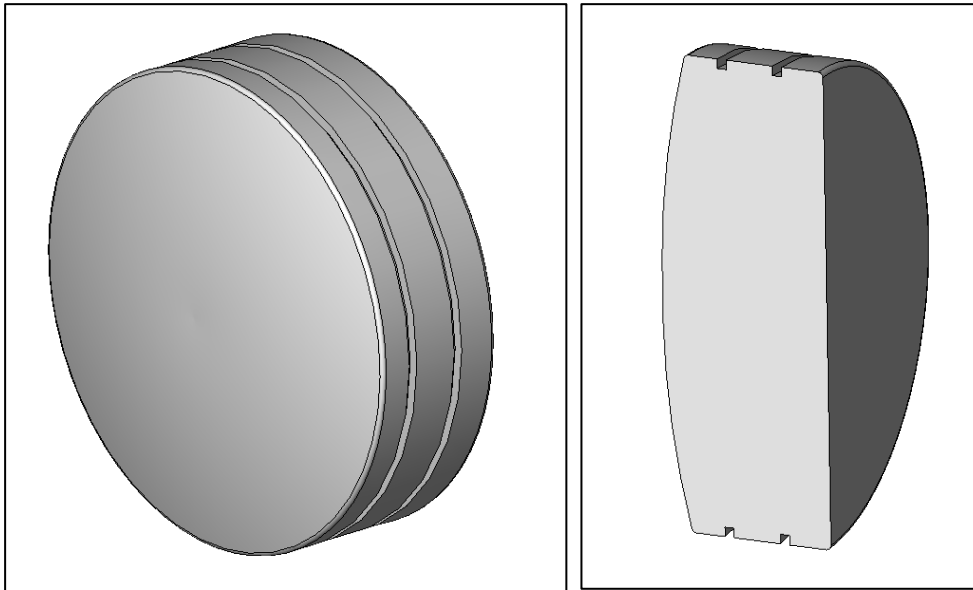


Figure 44: Solid CAD model used to test infill geometries

Thin wall model

This model has multiple identical curved surfaces all lined up besides each other. The design is based on the unit cell seen in Figure 40. There is a central hole in the middle which allows for more airflow inside the barrier. The wall thickness of curved inner surfaces can be changed to study the impact on the acoustic properties. The tested sample will be printed first with the thinnest possible wall thickness, for this an infill might be required. This model is also designed using the revolve function.

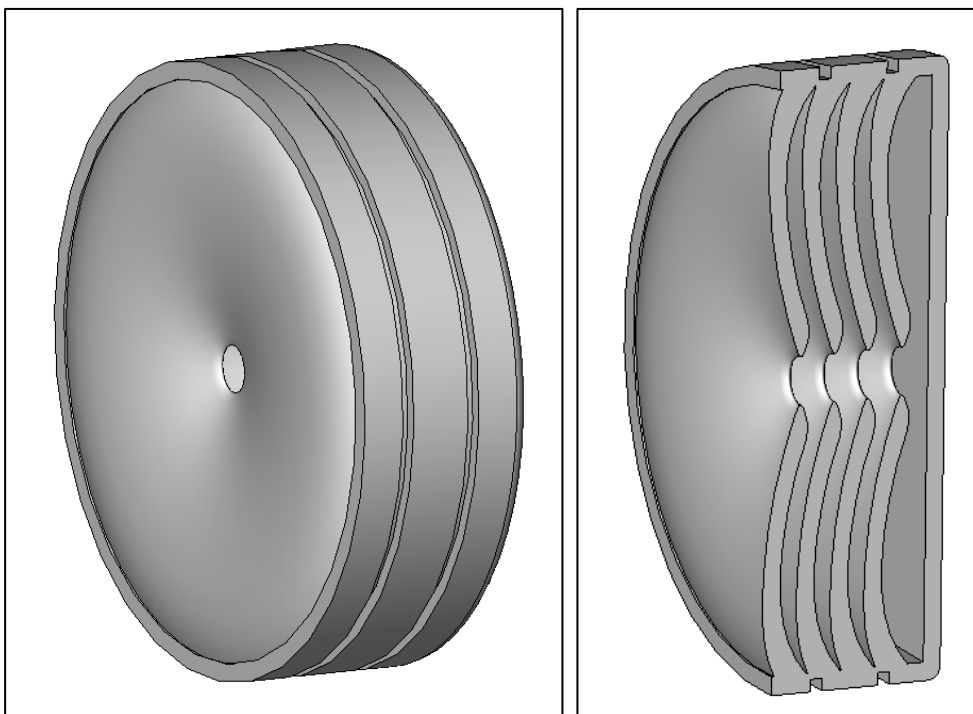


Figure 45: CAD model of a thin wall metamaterial

Thick wall model

This model consists of thicker walls and has a sharp straight edged geometry. But this structure has many angled cavities. These cavities should redirect the sound waves and cause a lot of reflection. Note that all my barriers have a solid back plastic wall. The thickness of this wall is the same as the reference piece (3mm). This wall will be the bottom (start of the print) when the models are being 3D printed. The outer shell is again created using the revolve function. The inner angled structures are extruded using additional sketch planes that were created in the model.

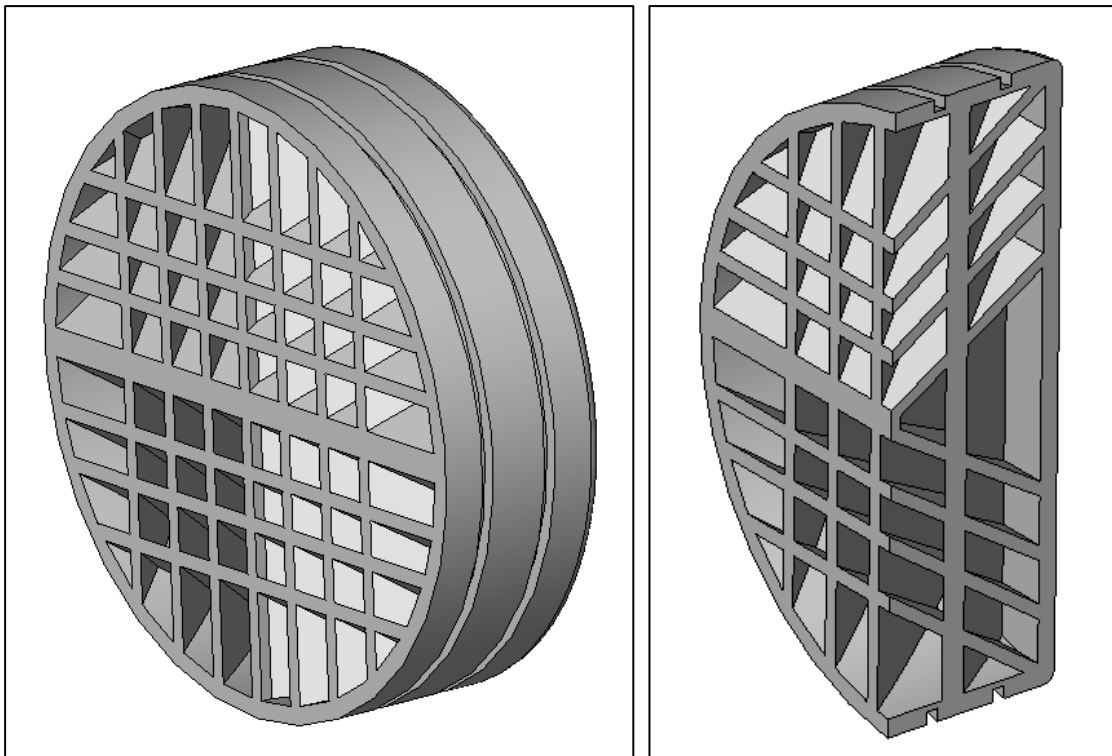


Figure 46: Thick wall cavity CAD model

Cavity barrier model

This design and the thin wall model listed above are designed to test the facts listed in the patent by: Valášek, M.: Acoustic Barrier, PCT Patent Pending. The model has a thin curved top surface with highly curved inner support ribs. The model is also created using the revolve function. After this additional holes are created to allow airflow inside the barrier.

The following section out of the patent describes the design rules that were used for both models that do not test the available infill structures.

A solution of an acoustic barrier according to this invention is based on the knowledge that planar surfaces (have infinite radii of curvature) radiate the acoustic energy more than curved surfaces (a finite radius of curvature) and surfaces containing straight lines (one infinite radius

or radii of curvature with a different sign) radiate the acoustic energy more than surfaces not containing straight lines (radii of curvature with the same sign). So cylindrical, conical and straight surfaces are unsuitable. Thin-walled structures radiate acoustic energy less than thick-walled ones because they are lighter and contain mass points (given by an assumed cut-out of a structure) with a lower weight. A thin-walled structure can have problems with the structure stability and a deformation under loading, therefore it is equipped with reinforcing ribs. [2]

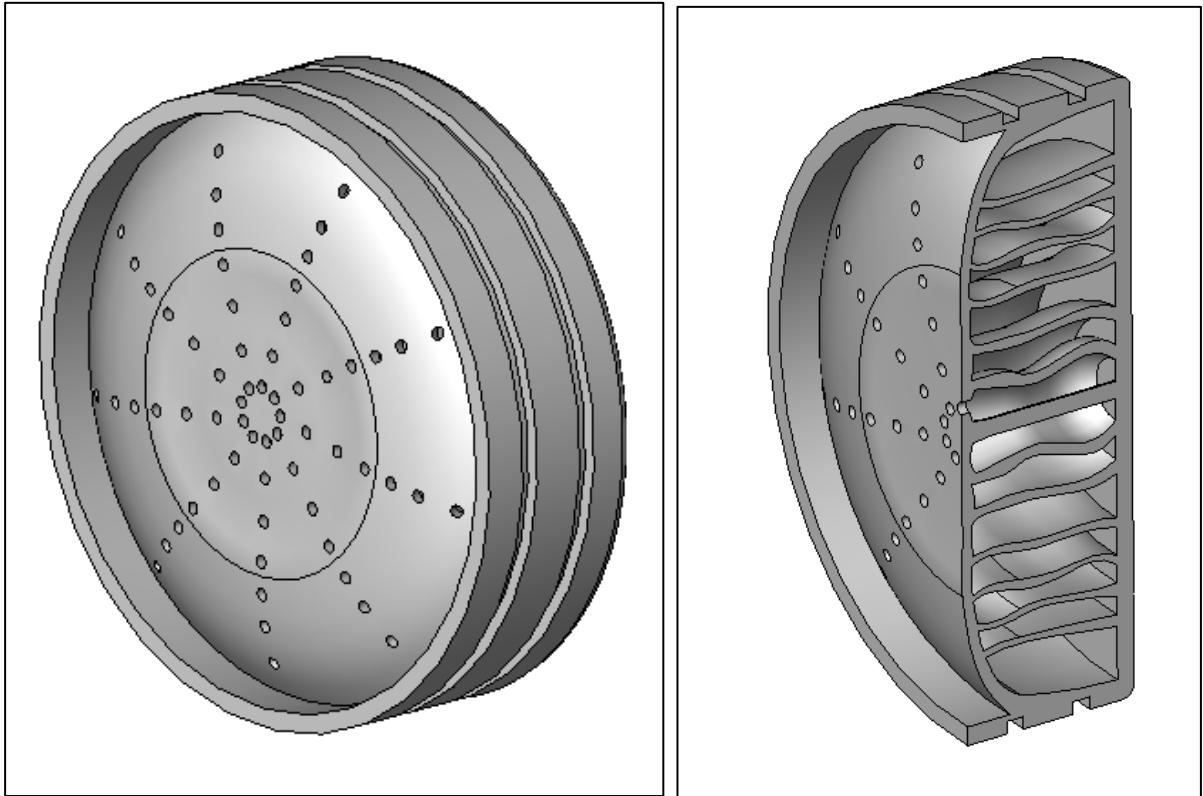


Figure 47: CAD model of the cavity barrier, note the curvature of the support ribs in the section view.

6.3 STL conversion

All the CAD files listed above have been converted to STL file by using the same settings in SolidWorks. Figure 48 shows the settings available in SolidWorks. The settings in SolidWorks are automatically calculated when selecting a desired resolution. The STL-conversion can then be previewed and checked.

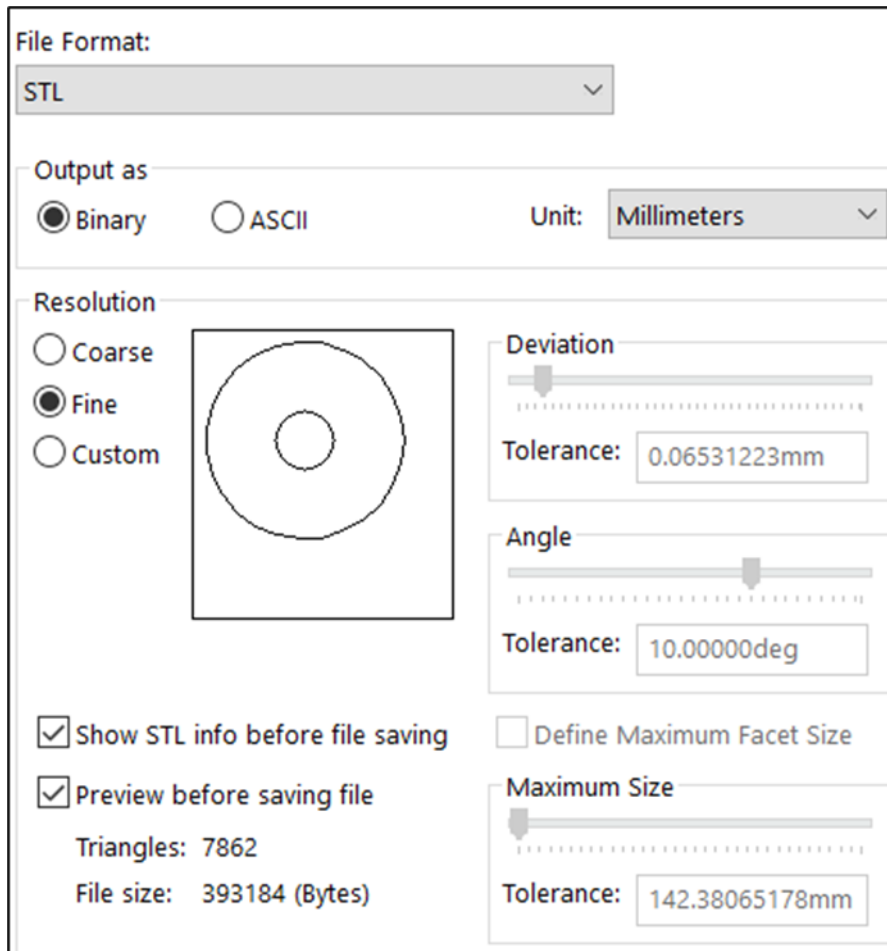


Figure 48: Exact STL conversion settings

7 PRODUCTION OF THE ACOUSTIC BARRIERS

This section describes how the samples are printed. All the samples used in this research are printed on Prusa Cartesian 3D printers. The layer height depends on the installed nozzle diameter and printer settings. The nozzle diameter used on all the samples is 0.4 mm.

Reference sample

This sample is used for comparison with the designs according to the patent. It is printed completely solid out of PETG filament. The sample weight is calculated by the slicer software, the reference sample weighs 29,9 g.

Samples for infill comparison

The printing process of all the samples was performed on the same model of 3D printer. The prints all start with a flat bottom. The used layer height is 0.2 mm. The flat starting bottom of all the prints has a thickness of **0.8 mm** (four solid layers). After this the printer starts with creating the infill. The different types of infill that were printed can be seen in Figure 49.

Infill type	Infill density	Material	Sample weight (g)		
Hilbert	5%, 10% ,15%	PETG	55,3	69,9	84,7
Rectangular	5%, 10% ,15%	PETG	55,6	70,2	84,6
Gyroid	5%, 10% ,15%	PETG	54,3	68,7	82,6
Octogram	5%, 10% ,15%	PETG	55,5	70,6	85
Archimedean	15%	PETG	82,5		

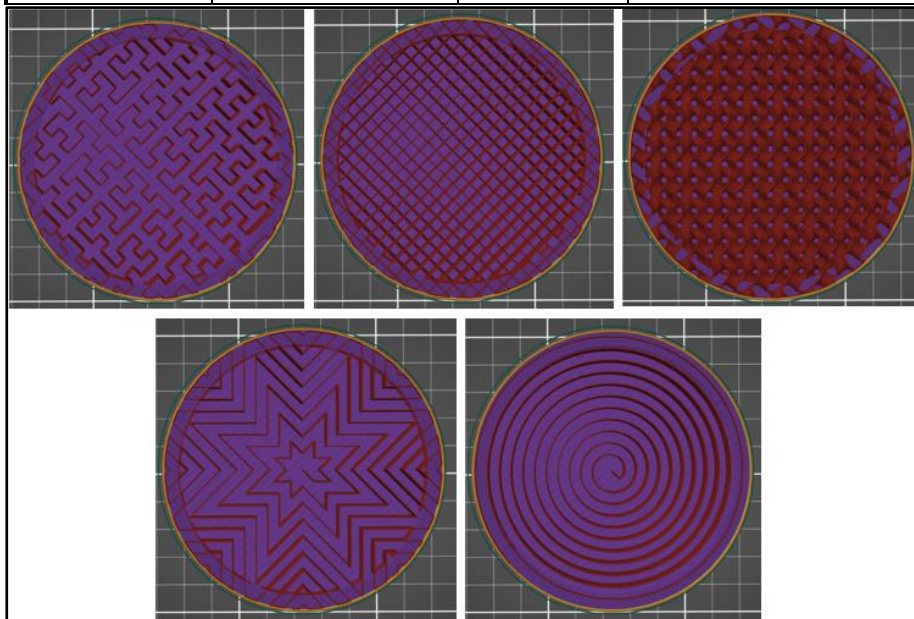


Figure 49: Used infill types (at 10%) from left to right: Hilbert, Rectangular, Gyroid, Octogram and Archimedean chords

The samples are always grouped and printed together. After the print is done they are marked to make identification easier. Figure 50 shows the used printing layout.

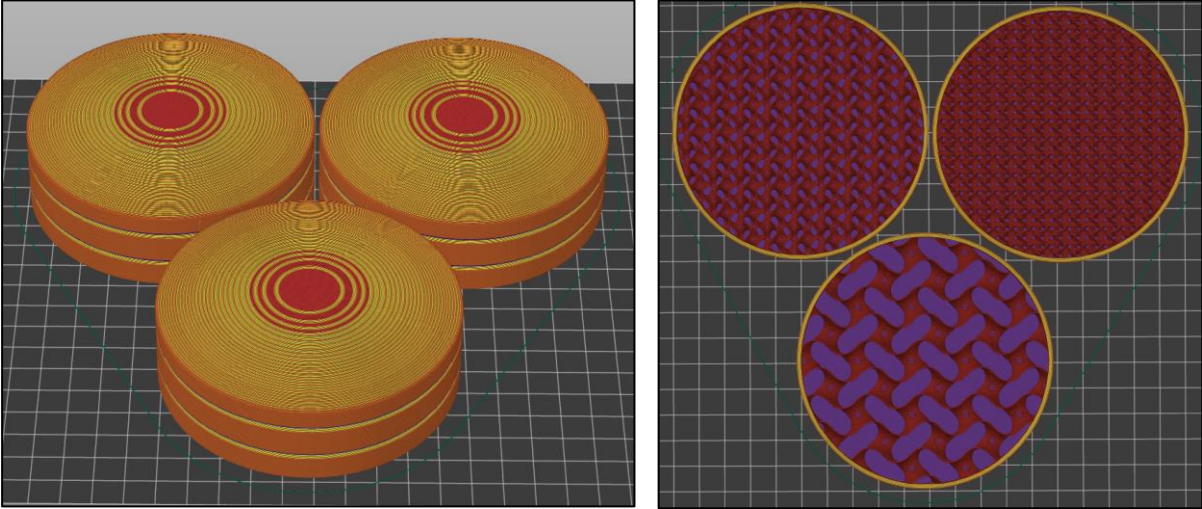


Figure 50: Example of G-code creation for the Gyroid samples, 5-10-15 % infill, total print time 12h 34m.

During printing the samples were checked if the infill was being printed successfully. But still some samples were cut open to verify the infill, this can be seen on Figure 51.

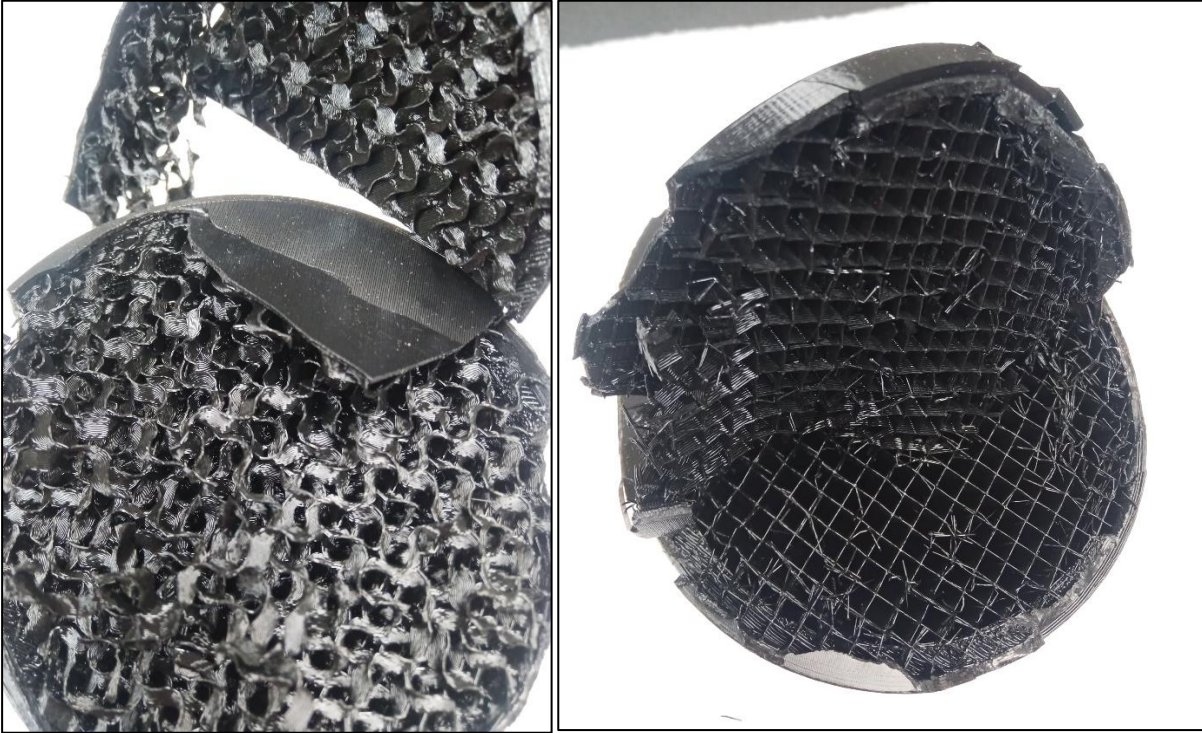


Figure 51: Extra samples were printed to cut open and verify if the infill was printed successfully. Left: gyroid infill 10 % Right: rectangular infill 10%

Samples designed according to the patent guidelines

The samples that are designed according to the patent are more delicate to print. They have thin walls and the overhang is set at the maximum. No support material was used, since the slicer software indicated that it was possible to print them without support. The printing process of the thin wall sample can be seen in Figure 52. Notice the thin wall thickness and the low percentage line infill (5%) between the walls. The vertical walls have (according to PrusaSlicer see Figure 53), a thickness of 0.87 mm. The printed samples are listed in Table 1.

Name sample	Material	Normal plane wall thickness	Weight (g)
Thin wall barrier	PLA	0.9	78
Thick wall barrier	PETG	Printed solid	97
Cavity barrier	PETG	Printed solid	132,9

Table 1: 3D printed samples and their properties.

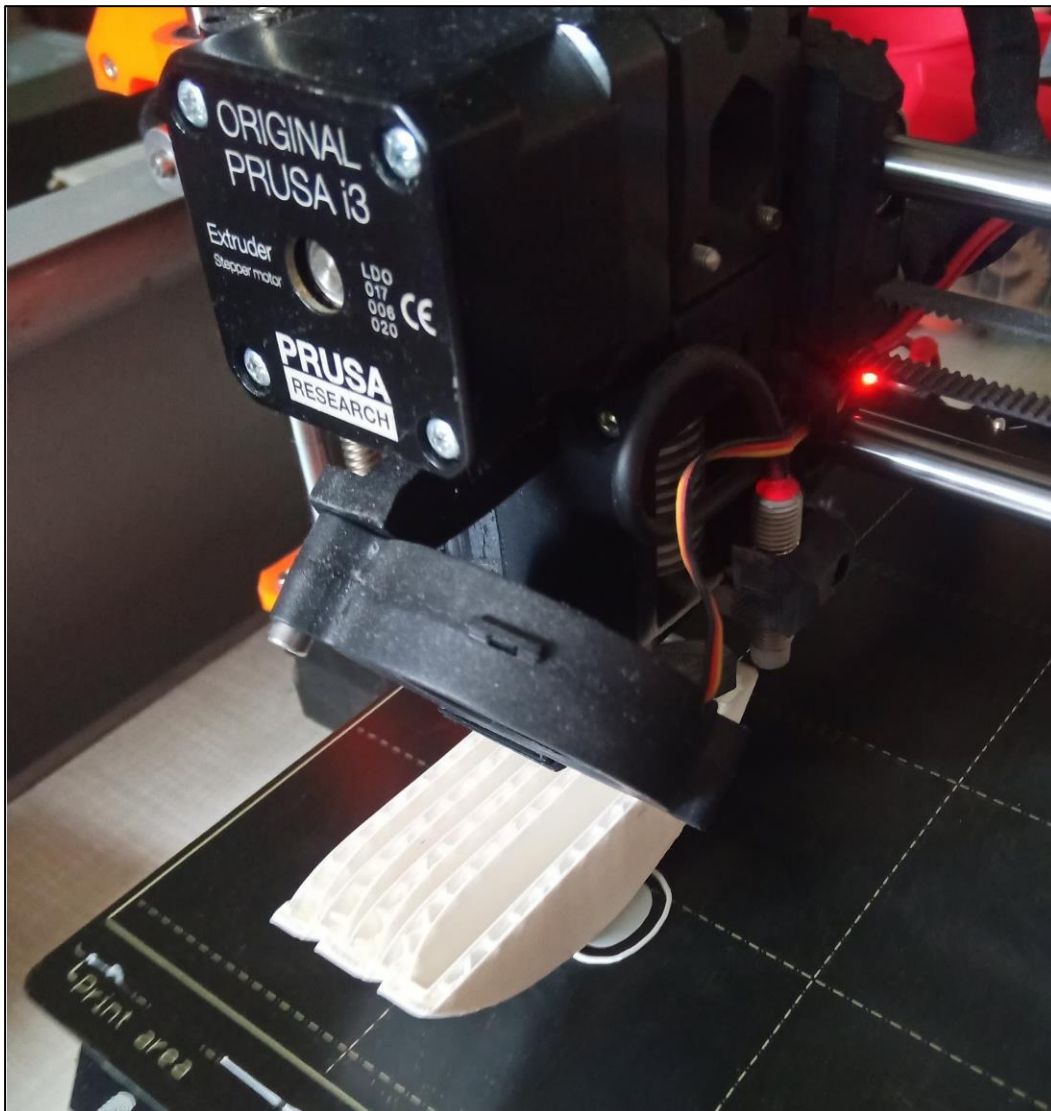


Figure 52: Printing process of the thin wall barrier with line infill



Figure 53: Vertical wall settings in PrusaSlicer



Figure 54: All the printed samples (reference sample is not included).

As already mentioned in the theoretical introduction, the absorption coefficients can be small since we are dealing with rather solid and highly reflecting samples. When the samples have similar results and do not show much variation it might be useless to keep testing all the different infills. So it was decided to test the most different samples first. First, the reference sample will be tested. Then the gyroid and rectangular infill will be compared. The thin wall model will also be tested and compared with the reference and infill samples of similar weight and volume. All the samples mentioned above are visible in Figure 54.

8 DATA PROCESSING

The measured data represents the acoustic pressure inside the Kundt tube. The measured values are in Volt. They can be converted to pressure (Pascals) by multiplying them with the microphone sensitivity. The sensitivity of the used microphones is 30 mV/Pa, see Figure 15. This conversion is not necessary since it influences all the signals in the same way. So the voltage values can be used directly. The measured data is then converted by using a Fourier transform (FFT) into the complex sound pressure. The complex sound pressure of microphone 1 and 2 is then used to calculate the cross and auto spectrum. See Figure 57. These spectrums are needed to calculate the transfer function from microphone position one to microphone position two. The MATLAB code used to perform the calculations is listed below and was provided by CTU.

```
1      % << imptru_READ_FILE.m >>|
2      % Read Data
3
4      function [Time, PRef, P1, P2, P3, P4]=imptru_READ_FILE(Jmeno);
5
6      load(Jmeno)
7
8      Time=meas.Time;
9      PRef=meas.Ref;
10     P1 = meas.Mic1;
11     P2 = meas.Mic2;
12     P3 = meas.Mic3;
13     P4 = meas.Mic4;
14
```

Figure 55: Reading the measured data file

```
3      function [ff, P1f, P2f, P3f, P4f, N, adr, Ifig]=imptru_PLOT_FrequencyDomain(Time, PRef, P1, P2, P3, P4)
4
5      Ifig=1;
6      a=diff(Time); dt=seconds(a(1)); T=seconds(Time(end));
7      F=1/dt; df=1/T; N=length(Time(:,1));
8
9      ff=(0:1:N-1)*df;
10     PRef=fft(PRef);
11     P1f=fft(P1); P2f=fft(P2); P3f=fft(P3); P4f=fft(P4);
12
13     adr=find(ff<1000);
14
15     Ifig=Ifig+1; figure(Ifig)
16     subplot(211)
17     Sxx= conj(PRef).*PRef/N;
18     semilogy(ff(adr), Sxx(adr), 'b'), xlabel('F [Hz]'), ylabel('SxxPref [?]', grid on
19     subplot(212)
20     SxxP1= conj(P1f).*P1f/N;
21     semilogy(ff(adr), SxxP1(adr), 'r'), xlabel('F [Hz]'), ylabel('SxxP1 [?]', grid on
22     eval(['print -dtiff -r400 Obr' num2str(Ifig)])
```

Figure 56: Calculating the complex sound pressures using **FFT** .

```

2 function [] = imptru_TransfearFunction(ff,P1f,P2f,P3f,P4f,N,adr,Ifig)
3 % Cross and auto spectrum
4 SxxP1= conj(P1f).*P1f/N;
5 SxxP2= conj(P2f).*P2f/N; SxxP12= conj(P1f).*P2f/N;
6 SxxP3= conj(P3f).*P3f/N;
7 SxxP4= conj(P4f).*P4f/N; SxxP34= conj(P3f).*P4f/N;
8
9 % transfer functions
10 H21=P2f./P1f; Hh21=SxxP12./SxxP1; Hhh21=sqrt(SxxP2./SxxP1);
11 H43=P4f./P3f;
12 H31=P3f./P1f;
13 coherP12=SxxP12.^2./(SxxP1.*SxxP2);

```

Figure 57: Top: Calculating the auto and cross spectrum. Bottom: Calculating the transfer functions according to the microphone positions.

```

30 RR=[]; j=sqrt(-1);
31
32 dx=0.130; x1=0.055+dx; x2=x1-dx;
33 for i=1:length(adr)
34 k=2*pi*ff(i)/346;
35 H=H21(i);
36 aa=H-exp(-j*k*dx);
37 bb=exp(j*k*dx)-H;
38 r1a=aa/bb*exp(j*2*k*x1); % determining the reflection factor
39 RR=[RR; ff(i) abs(r1a) ];
40 end

```

Figure 58: Calculating the reflection factor over the whole range according to ISO 10534-2.

```

53 alf=1-(abs(rr)).^2; % sound absorbtion coefficient (figure 8)
54 plot(RR(:,1),alf,'b'), grid on, hold on
55 set(gca,'Xlim',[200,900]);
56 set(gca,'Ylim',[-1/2,3/2]);
57 xlabel('Frequency [Hz]'); ylabel('α = absorption coefficient')
58 title('Absorption coefficient')
59 %probeer
60 eval(['print -dtiff -r400 Obr' num2str(Ifig)])
61 Z=(1+rr)./(1-rr); % Specific acoustic impedance ratio

```

Figure 59: Calculating the absorption coefficient according to ISO 10534-2.

After this the parameters are plotted in function of the used frequency range (white noise 100-1000Hz). The graphs are then used to compare the samples. The graphs contain a lot of noise. The script can definitely be improved to obtain better graphs.

9 TEST RESULTS

The samples are tested both using the two microphone and four microphone method. The two microphone method is used to calculate the reflection factor and absorption coefficient of the samples. Here some additional measurements were made as well. The four microphone method is used to compare the transfer functions calculated between the microphones. These functions indicate how much acoustic energy is going through the barriers.

9.1 Results of the two microphone method

In this section the reflection factor and absorption coefficient of the different samples are compared. This comparison is done using the sine signal (100-1000Hz). An the results are analysed within the range of 200 to 900.

After some initial testing it became clear that most of samples have a high reflection factors. This is because they have a hard surface where the sound waves are striking on. But still all the results vary slightly, some barriers have less reflection at specific frequencies.

After measuring the regular 3D printed samples, four additional situations were tested to verify that the results are correct and usable. The first two additional situations are: a measurement with really good absorbing material (glass wool) and a measurement where some absorbing material (glass wool) is added to the incident surface of the thin wall 3D printed sample. The last two additional samples test the impact of infill sample with the solid top is removed and when using a softer material (TPU filament).

Reference sample:

Figure 60 shows that the reference sample is a good sound reflector. The sample reflects the energy excited by the speaker almost completely back over the whole frequency range. Note that all the graphs mentioned below have a lot of noise. This noise is caused by not averaging the spectrums that are calculated using the FFT.

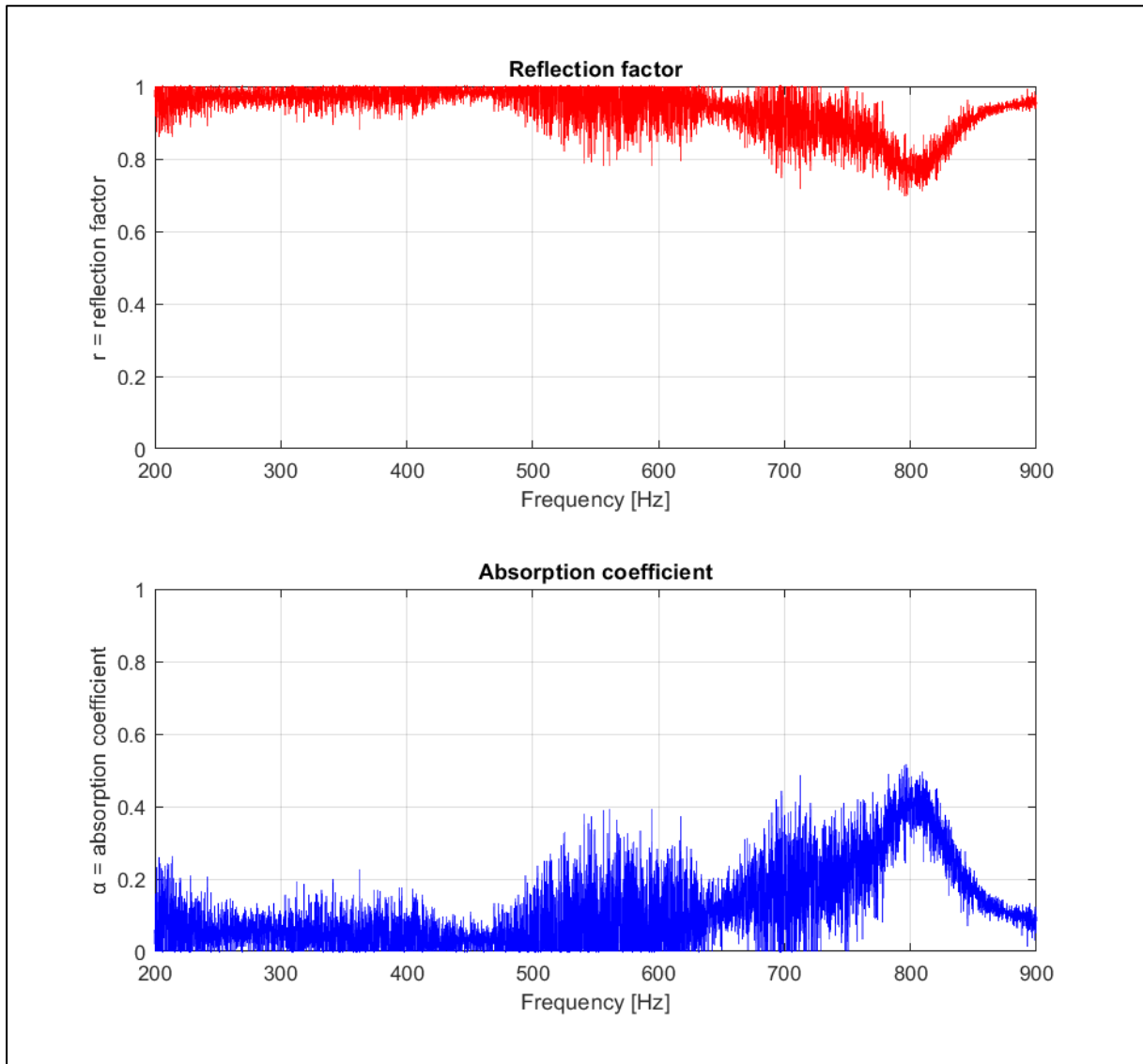


Figure 60: Reflection and absorption parameters of the reference sample with a white noise sound signal.

Thin wall sample:

This sample is overall a good reflector. See Figure 61, at a frequency of 300 Hz, the barrier is reflecting the sound less. This shows that the energy is diffused inside the barrier at this frequency.

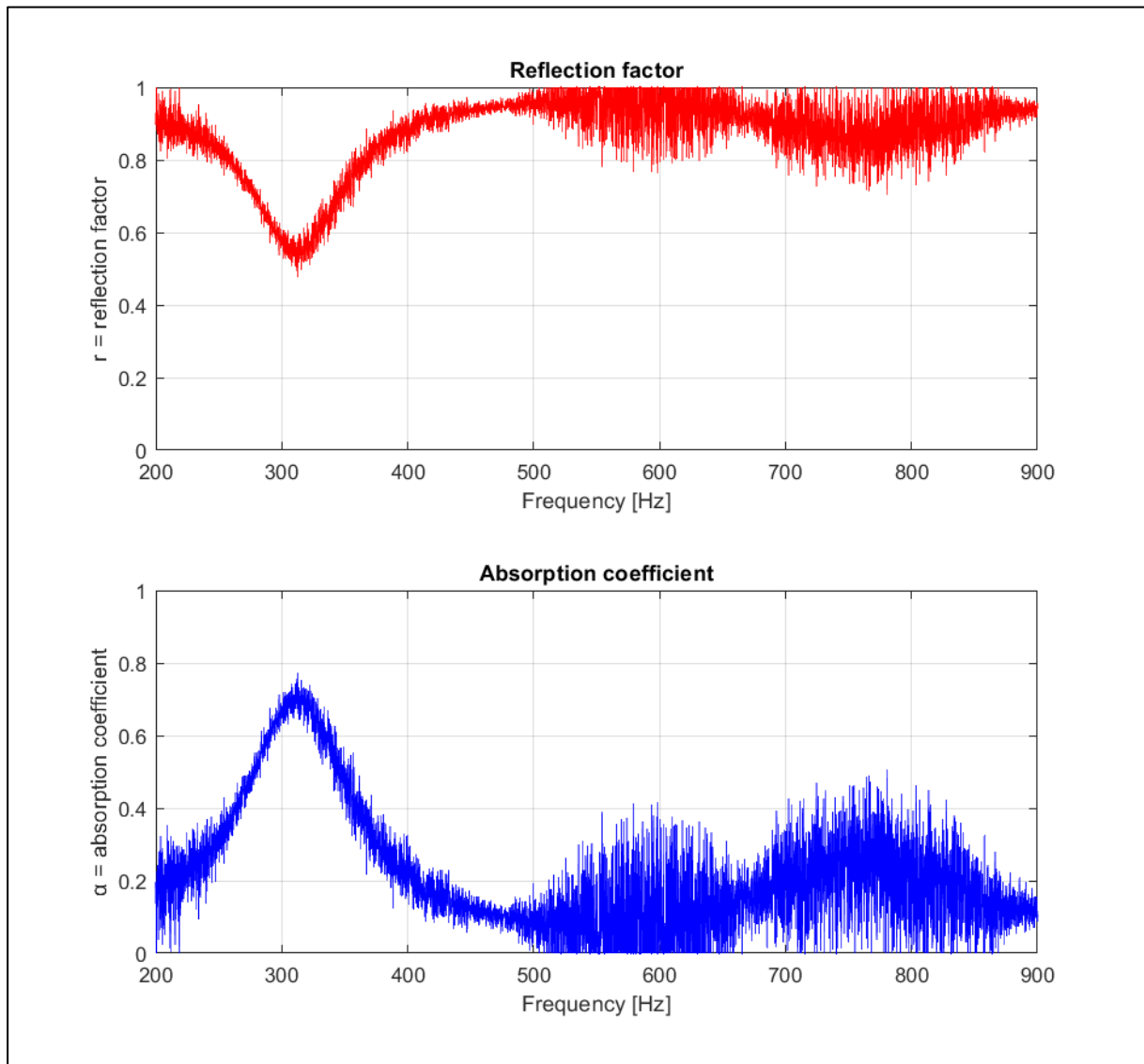


Figure 61: Reflection and absorption parameters of the thin wall sample with a white noise sound signal.

Thick wall sample:

This sample is reflecting the sound energy very well over the whole frequency range. See Figure 62.

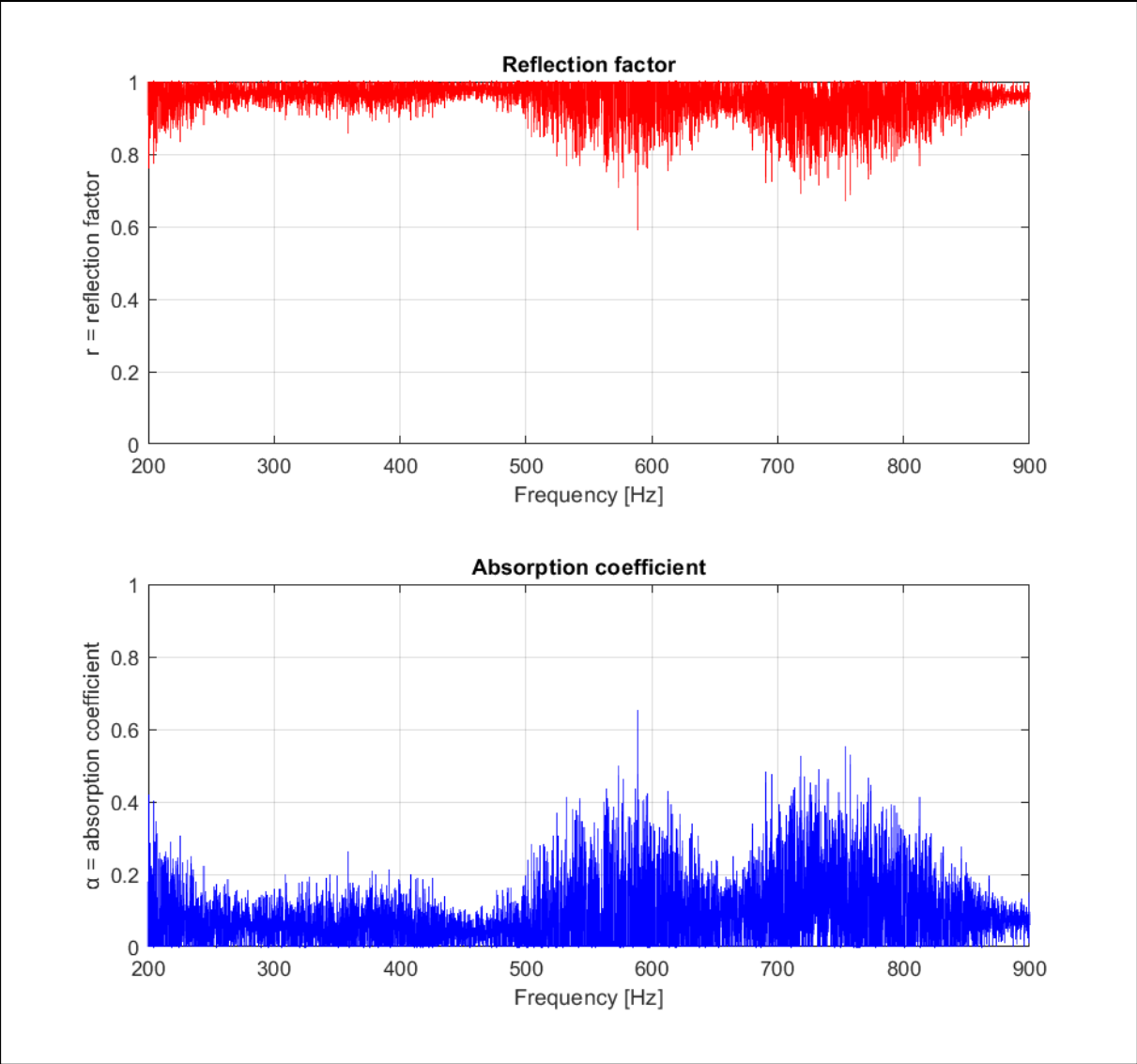


Figure 62: Reflection and absorption parameters of the thick wall sample with a white noise sound signal.

Gyroid 5 % infill sample:

This sample is reflecting the sound energy very well over the whole frequency range. This can be seen in Figure 63.

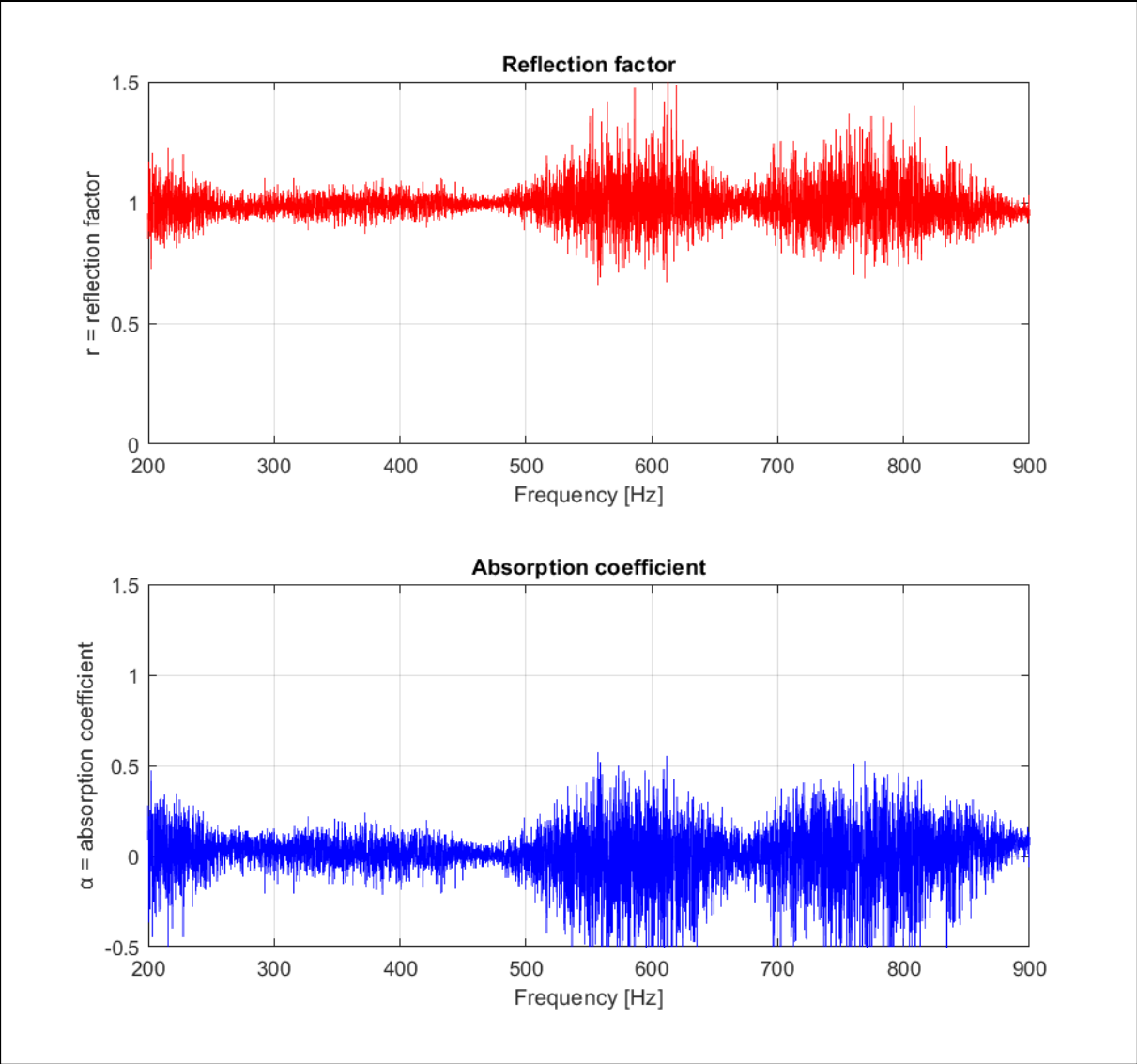


Figure 63: Reflection and absorption parameters of the 5% gyroid infill sample with a white noise sound signal.

Gyroid 15 % infill sample:

This sample is reflecting the sound energy very well over the whole frequency range. See Figure 64.

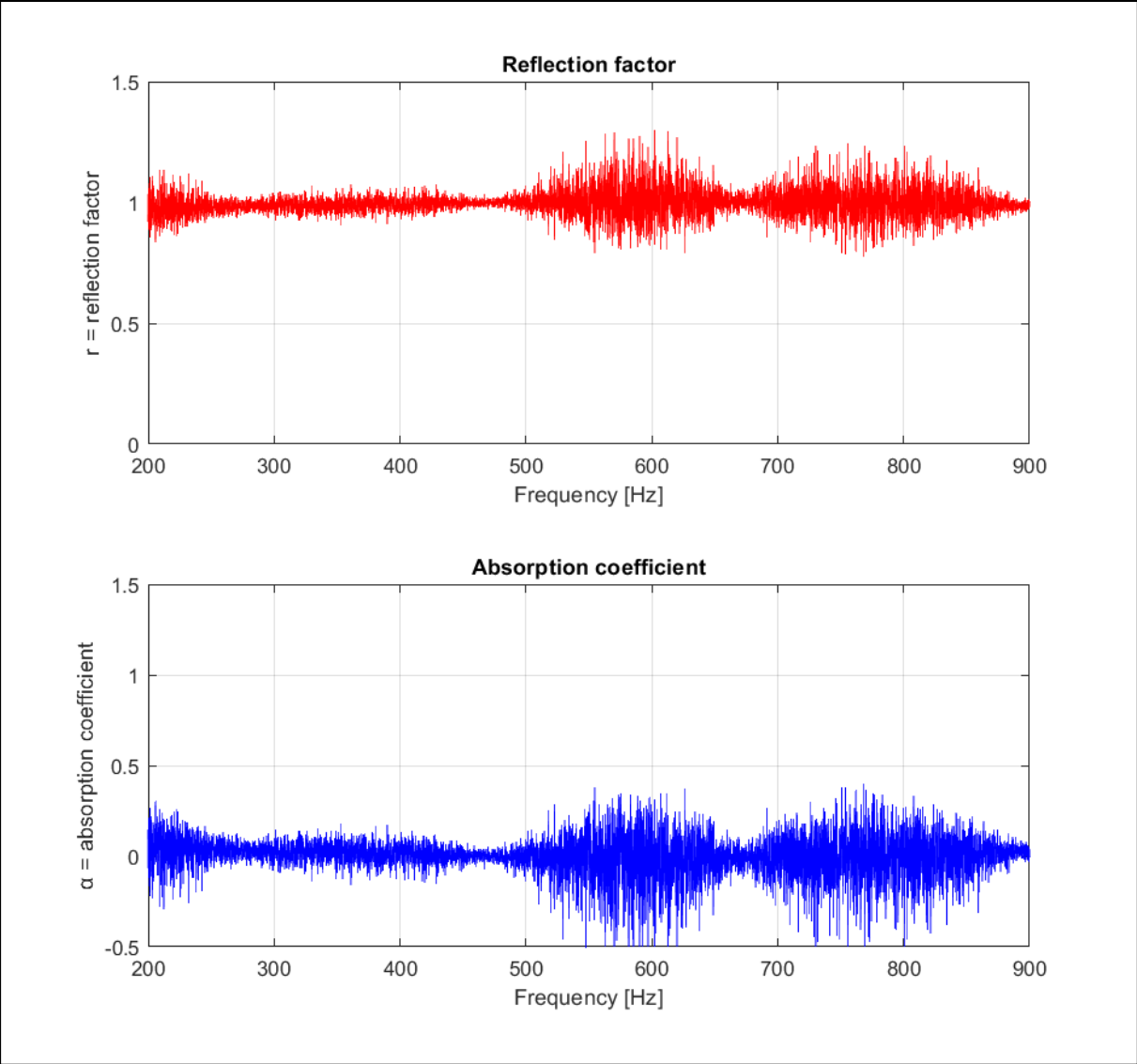


Figure 64: Reflection and absorption parameters of the 15% gyroid infill sample with a white noise sound signal.

Rectangular 5 % infill sample:

This sample is also reflecting the sound energy very well over the whole frequency range. At the high frequency the reflection factor starts to drop. This is shown in Figure 65.

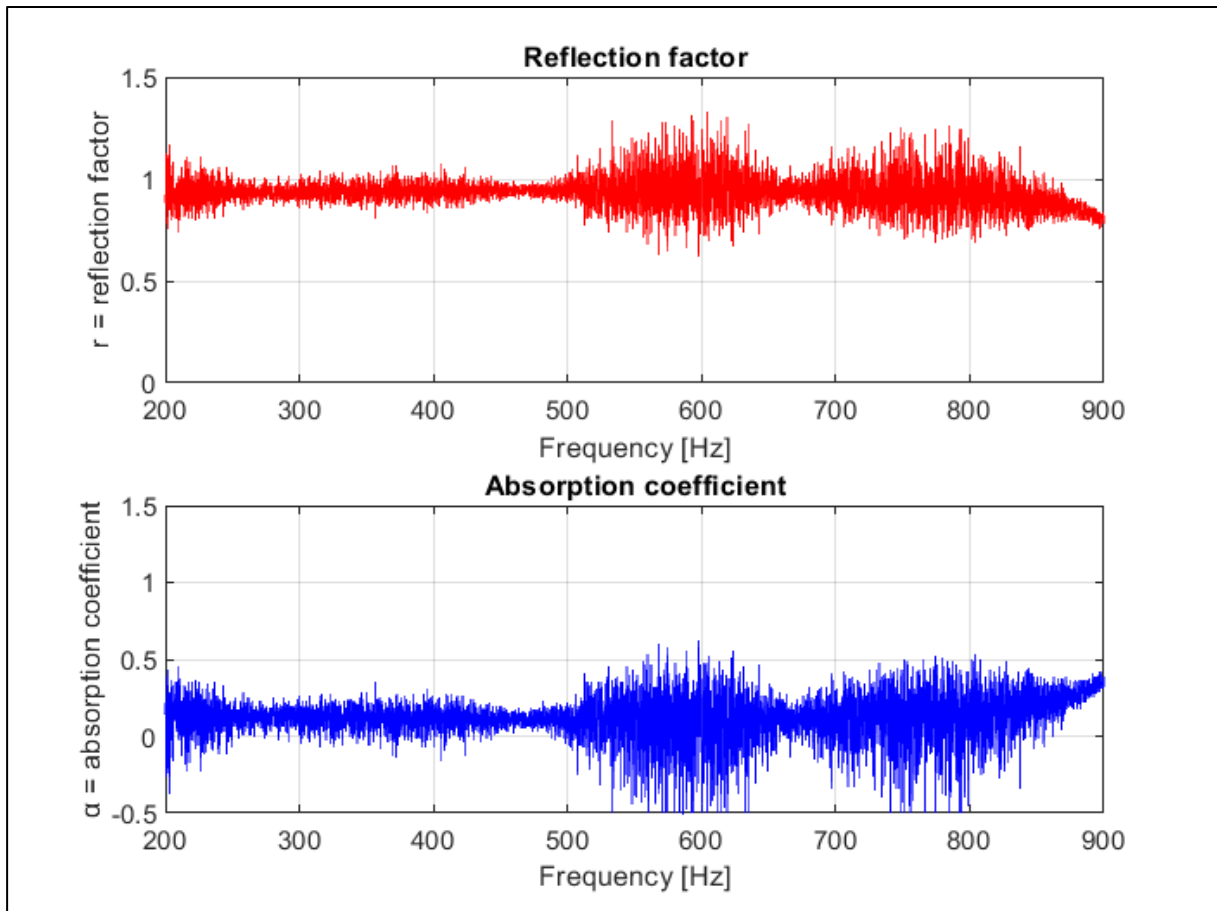


Figure 65: Reflection and absorption parameters of the 5% rectangular infill sample with a white noise sound signal.

Rectangular 15 % infill sample:

This sample is reflecting the sound energy very well over the whole frequency range. Again the graphs are quite noisy, see Figure 66.

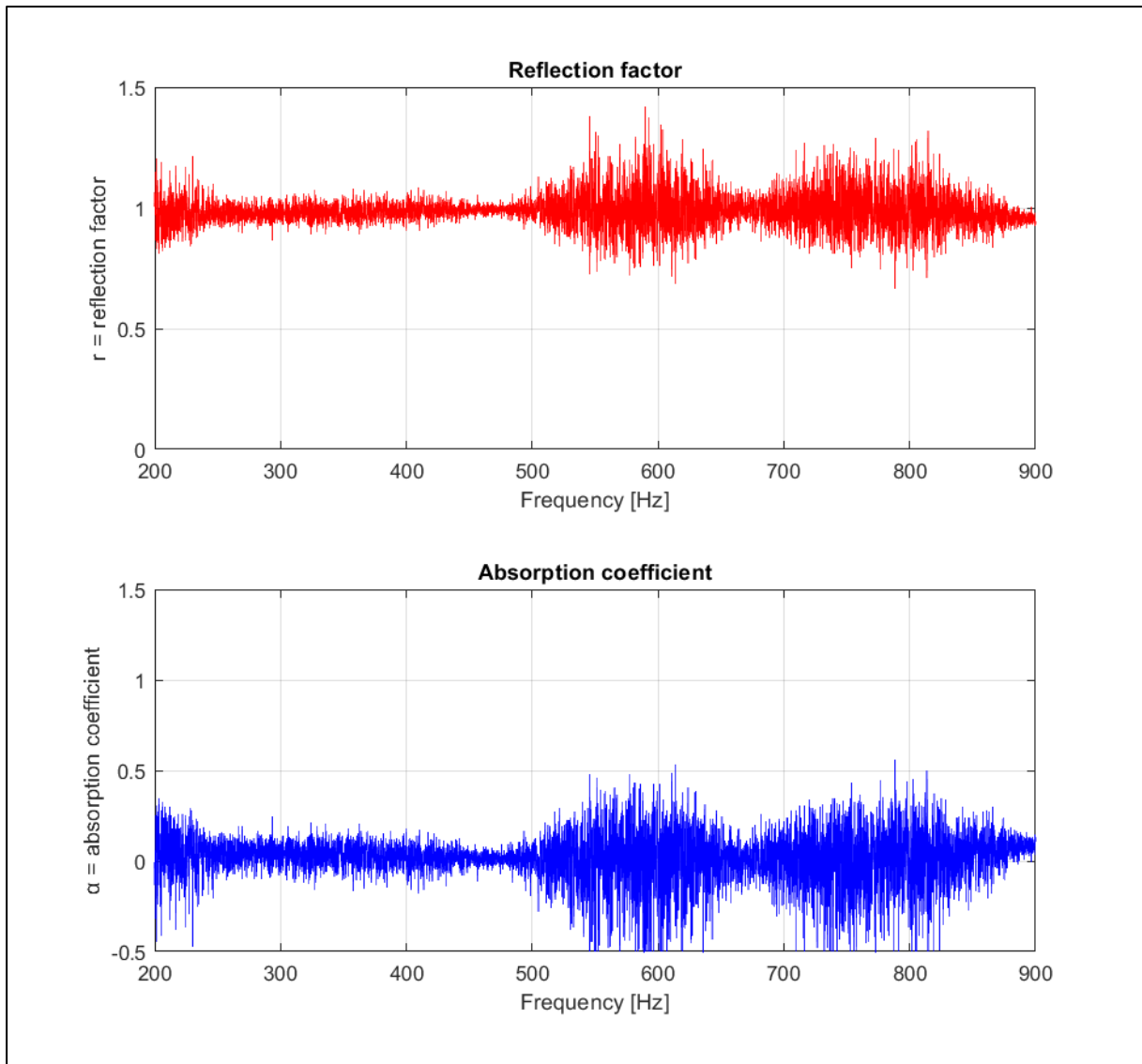


Figure 66: Reflection and absorption parameters of the 5% rectangular infill sample with a white noise sound signal.

Here the additional samples are listed to verify if the test setup is capable of measuring samples that are better at absorbing acoustic energy.

Additional sample 1: 60 mm of glass wool:

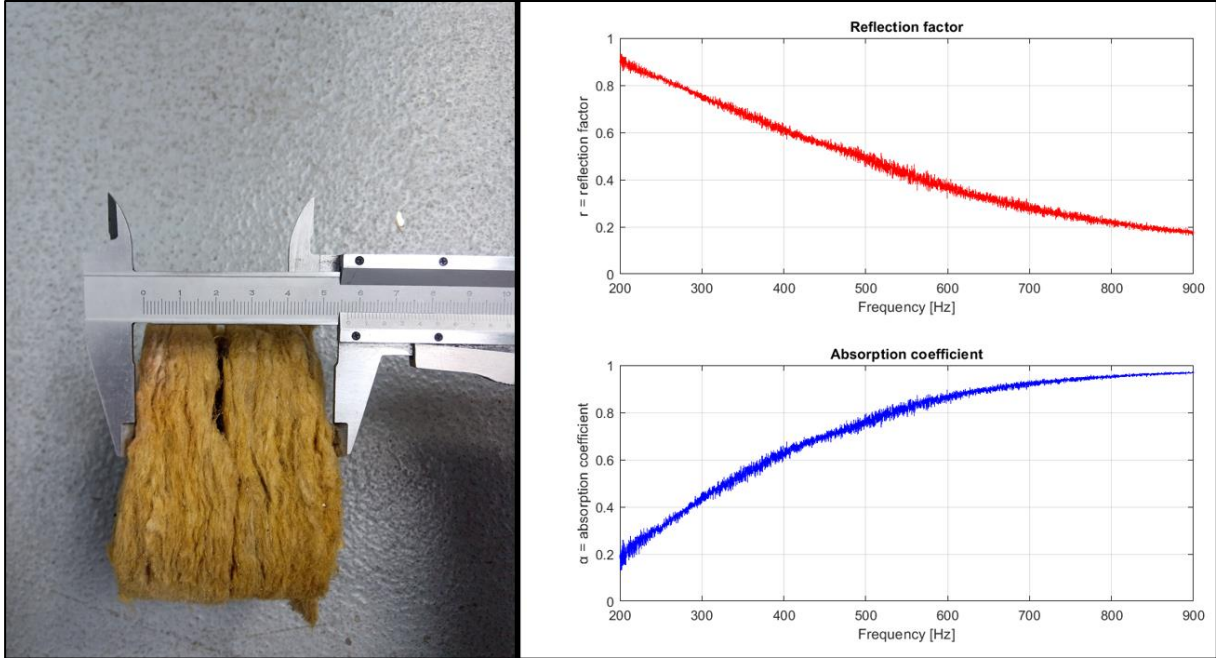


Figure 67: Reflection and absorption parameters of glass wool sample with a white noise sound signal.

Additional sample 2: 30 mm of glass wool + thin wall barrier:

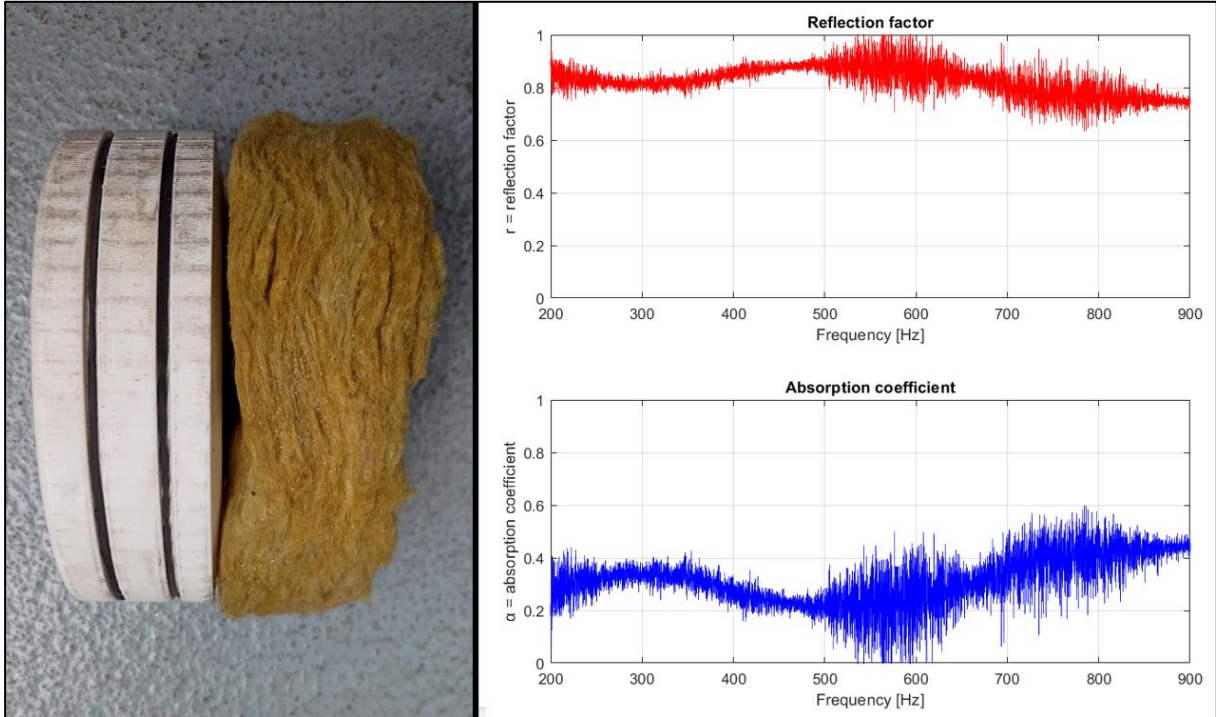


Figure 68: Acoustic parameters of a combined sample with a white noise sound signal.

Additional sample 3: Gyroid 5% infill open shell (PETG):

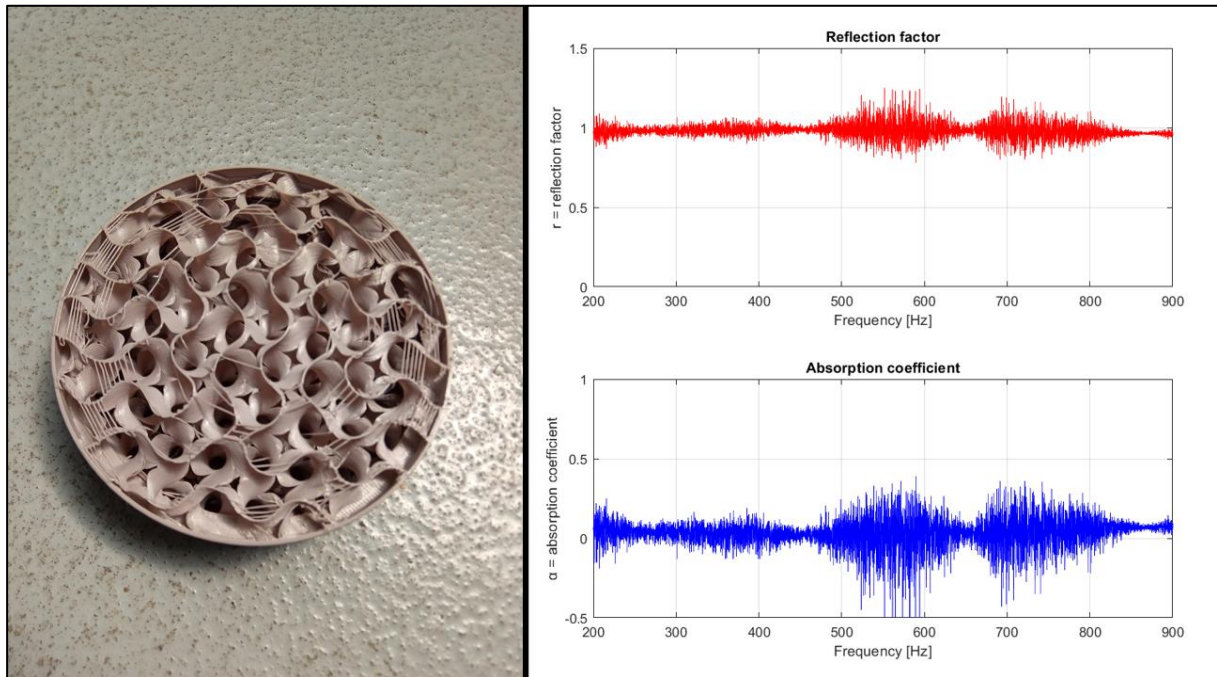


Figure 69: Acoustic parameters of a PETG 5% gyroid infill sample where the top is removed. A white noise sound signal is used.

Additional sample 4: Gyroid 5% infill open shell soft material (TPU):

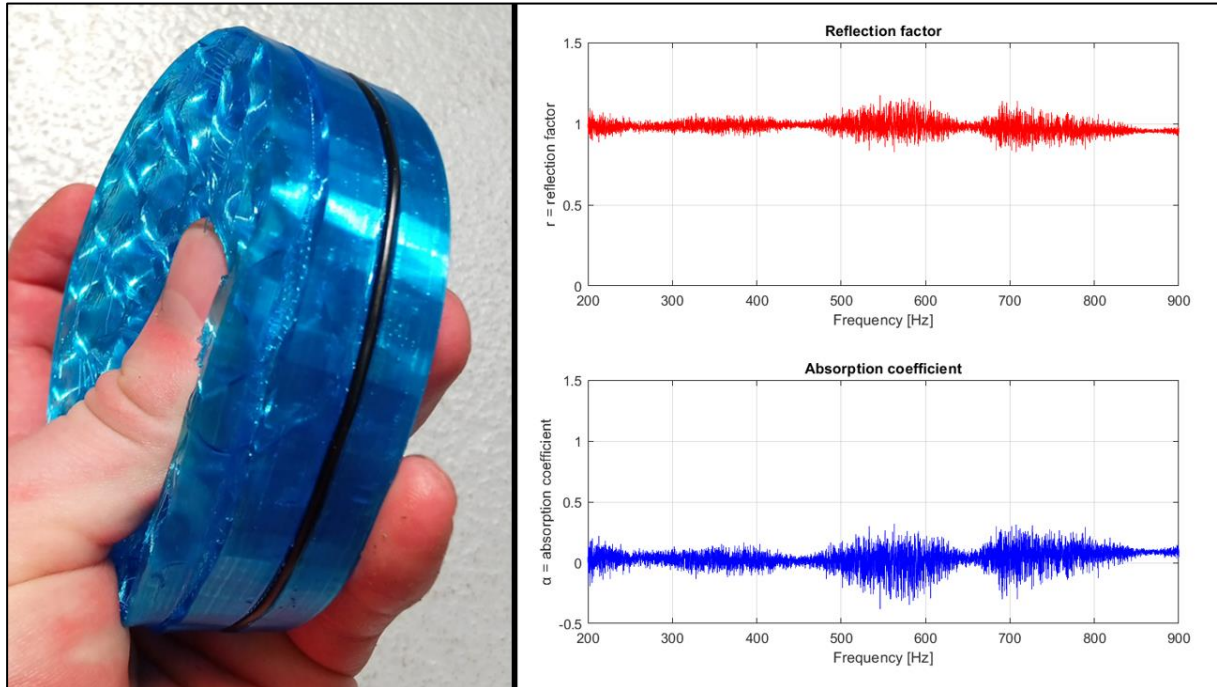


Figure 70: Acoustic parameters of a soft TPU 5% gyroid infill sample where the top is removed. A white noise sound signal is used.

9.2 Discussion of the two microphone method results

All the 3D printed samples turn out to be good at reflecting sound. Only the thin wall and the reference sample show a slight change of the reflection factor in frequency range from 200 – 900 Hz. This can be seen in Figure 60 and Figure 61.

The additional samples show that soft and porous materials like glass wool are way better at absorbing the acoustic energy. This is shown in Figure 67 and Figure 68. These measurements confirm that the impedance tube is a better instrument for comparing soft and porous samples. The samples where the solid top layer is removed still don't show any absorption. See Figure 69 and Figure 70. The used materials and geometry are still too stiff, there is no deformation so the energy cannot be absorbed. The samples are lined up in Figure 71.

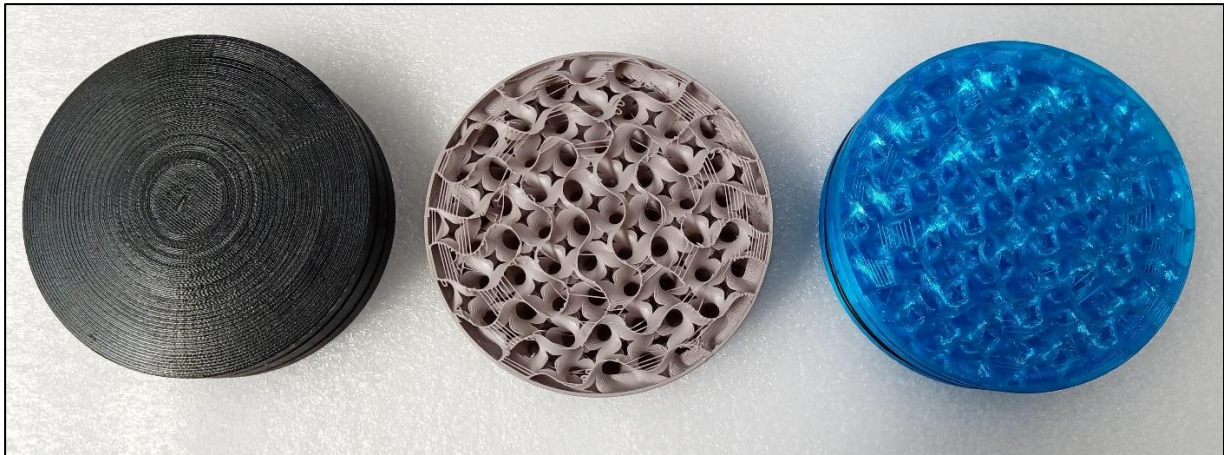


Figure 71: Left: solid top PETG sample with a gyroid infill 5%. Middle: open top PETG sample with a gyroid infill 5%. Right: open top TPU sample with a gyroid infill 5%.

9.3 Results of the four microphone method

By computing the transfer function between a microphone in front and a microphone behind the sample it is possible to compare acoustic energy that is blocked by the samples when they are tested with the same sound signal. This is shown in Figure 72. The used sound signal is the same white noise signal (100 – 1000 Hz) that is used in the two microphone measurements. The transfer functions H_{31} of the samples with the most different results will be compared here. The measurements are performed with the four microphone setup with hard backing. The transfer functions measured represents the acoustic pressure signals at location 3 relative to location 1. The location of microphone 1 and 3 is shown in Figure 13. By comparing these functions we can indicate which barrier is better at blocking the acoustic energy created by the speaker. The transfer functions are plotted and integrated to calculate the area under the graph. This value is then used to compare the different samples.

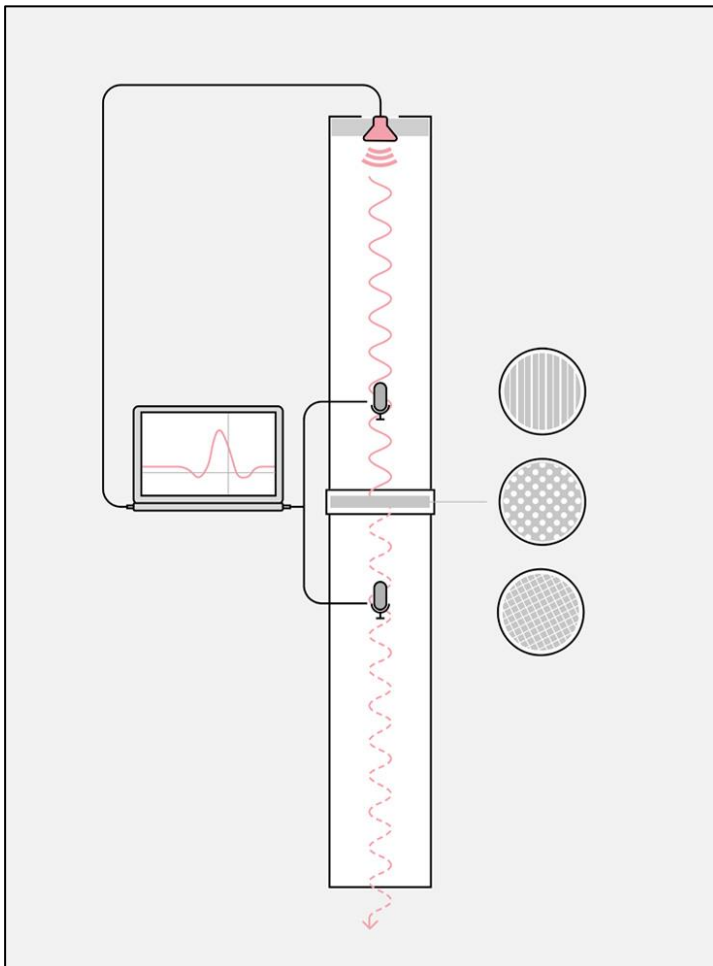


Figure 72: Representation of the used setup to determine which samples are better at blocking sound energy. [28]

Figure 73 shows the plotted transfer function H_{31} of the reference sample. The area underneath the curve is calculated and listed under the title of the graph.

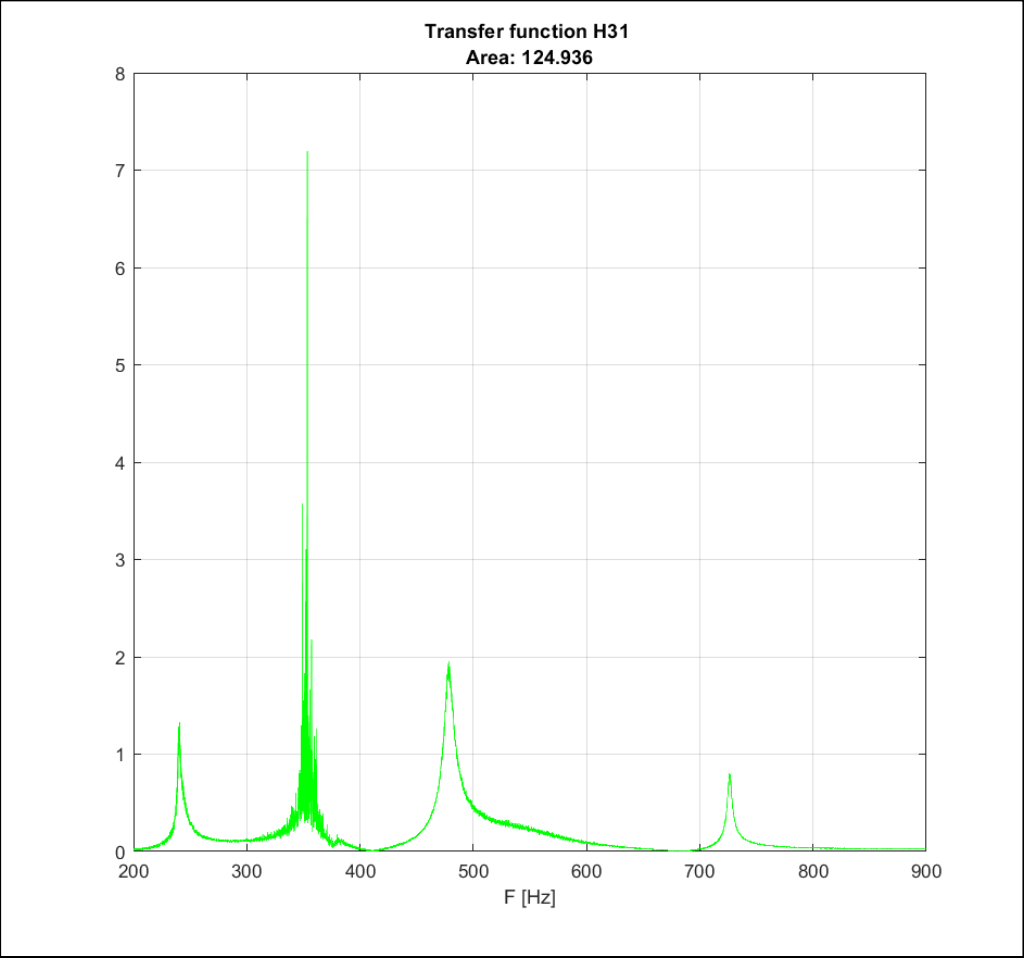


Figure 73: Plotted transfer function of the reference sample.

The results of the most interesting samples are listed in Table 2.

Name	Mass [g]	Area under transfer function H_{31}
Reference sample	29.9	124,9
Thin wall sample	78	93,4
Thick wall sample	97	27,0
Gyroid 5% infill	54,3	15,9
Gyroid 10% infill	68,7	23.3
Gyroid 15% infill	82,6	15,2
Rectangular 5% infill	55,6	97,1
Rectangular 10% infill	70.2	104,5
Rectangular 15% infill	84.6	54,1

Table 2: Comparison of the thin/thick wall samples and from the different infill samples.

9.4 Discussion of the four microphone method results

There is quite some difference in the integration results of the transfer functions calculated by the MATLAB script. It is important to note that these results are influenced by how well the samples are fitted inside the sample holder. All the samples were always installed with an airtight seal. The seal was always checked before any measurements were made.

But still after analysing this rough indication, it becomes clear that the gyroid infill is better at blocking the acoustic energy. This proves the fact that thin curved geometries don't radiate the acoustic energy as well as straight lines / surfaces.

CONCLUSION

Designing 3D printable acoustic barriers is a process where over-designing can easily be done. By this, I mean that most 3D printed structures that can be created are rather stiff. Solid or stiff parts will always reflect sound waves. There is very little difference between the reflection factors and absorption coefficients that were determined by using the two-microphone method. All the barriers are good sound reflectors.

But it becomes interesting when the sound travels through this solid structure or barrier. The used infill does affect the transfer of acoustic energy. This is proven by the four microphone test setup that was used. The gyroid infill is better at stopping the acoustic energy. This is because this geometry contains more curvature, which radiates the acoustic energy less. This knowledge can be applied when FDM 3D printing is used to create for example sound blocking covers. A sound-blocking cover that has a gyroid infill will be better at containing acoustic energy.

So it can be concluded that good polymer acoustic barriers should contain a lot of thin and curved features.

REFERENCES

- [1] *3D printing Handbook, ver. 3.11, Prusa Research Ltd, Prague 2019.*
- [2] *Valasek, M., Vampola, T.: Acoustic barrier, Utility pattern, 35819, UPV, Prague 2022.*
- [3] *Seybert, A.F. and Ross, D.F.: Experimental Determination of Acoustic Properties Using a Two-Microphone Random-Excitation Technique, J. Acoust.Soc. Am., Vol. 68, No. 3 pp. 907-921., 1998.*
- [4] D. Degryse, Artist, *Lesnota's Geluid en mechanische trillingen*. [Art]. KU Leuven, 2020.
- [5] "Sound Power and Sound Pressure Explained," BRÜEL & KJÆR, [Online]. Available: <https://www.bksv.com/en/knowledge/blog/sound/sound-power-sound-pressure>. [Accessed 2022 06 13].
- [6] Wikipedia, "Sound power," Wikipedia. [Online]. [Accessed 16 06 2022].
- [7] "Sound-physics Impedance," Britannica, 12 May 2021. [Online]. Available: <https://www.britannica.com/science/sound-physics/Impedance>. [Accessed 12 April 2022].
- [8] "Acoustic impedance," [Online]. Available: https://en.wikipedia.org/wiki/Acoustic_impedance. [Accessed 16 06 2022].
- [9] *ISO 10534-2 Acoustics- determination of sound absorption coefficient and impedance in impedance tube-Transferfunction method, 1998.*
- [10] S. MacDonald, "Sound Absorption," Siemens, [Online]. Available: <https://community.sw.siemens.com/s/article/sound-absorption>. [Accessed 25 04 2022].
- [11] Primacoustic, "Flexifuser Science," [Online]. Available: <https://www.primacoustic.com/flexifuser/science/>. [Accessed 31 05 2022].
- [12] "White noise," Wikipedia, [Online]. Available: https://en.wikipedia.org/wiki/White_noise. [Accessed 30 05 2022].
- [13] "White noise and Pink Noise in Spectral acquisition," Siemens community, [Online]. Available: <https://community.sw.siemens.com/s/question/0D54O000061xkhISAQ/what-is-white-noise-and-pink-noise-in-spectral-acquisition>. [Accessed 16 06 2022].

- [14] “Chirp,” Wikipedia, [Online]. Available: <https://en.wikipedia.org/wiki/Chirp>. [Accessed 30 05 2022].
- [15] “ENHANCEMENTS TO SYNTHETIC APERTURE RADAR CHIRP WAVEFORMS AND NON-COHERENT SAR CHANGE DETECTION FOLLOWING LARGE SCALE DISASTERS,” -Scientific Figure on ResearchGate., [Online]. Available: https://www.researchgate.net/figure/LFM-chirp-signal-phase-map_fig1_269366877. [Accessed 13 06 2022].
- [16] “Acoustic Glossary sound waves,” [Online]. Available: <https://www.acoustic-glossary.co.uk/sound-waves.htm#:~:text=Standing%20Wave%20a%20phenomenon%20when,combine%20and%20'resonance'%20occurs..> [Accessed 9 06 2022].
- [17] “Standing wave,” wikipedia, [Online]. Available: https://en.wikipedia.org/wiki/Standing_wave#Acoustic_resonance. [Accessed 9 06 2022].
- [18] M. Nabavi, “Numerical and experimental investigations of the acoustic standing wave resonator, pump, and micropump.,” 2008.
- [19] P.Schaldenbrand, SIEMENS, [Online]. Available: <https://community.sw.siemens.com/s/article/Measuring-Sound-Absorption-with-an-Impedance-Tube>. [Accessed 15 05 2022].
- [20] E. P. N.B. Roozen, “Uncertainty analysis of some acoustic and non-acoustic parameters derived from,” Laboratory of Acoustics, Soft Matter and Biophysics, Department of Physics and Astronomy,, KU Leuven, Celestijnenlaan 200D, 3001, 2022.
- [21] *E2611 – 19 Standard Test Method for Normal Incidence Determination of Porous Material Acoustical Properties Based on the Transfer Matrix Method.*
- [22] *Todd Schultz, Mark Sheplak, Louis N. Cattafesta, Uncertainty analysis of the two-microphone method, Journal of Sound and Vibration, Volume 304, Issues 1–2, Pages 91-109, 2007.*
- [23] *Suhanek, Mia & Jambrošić, Kristian & Domitrović, Hrvoje. (2008). Student project of building an impedance tube. The Journal of the Acoustical Society of America. 123. 3616. 10.1121/1.2934823..*

- [24] 3D-Hubs knowledge base, "What is FDM (Fused Deposition Modeling) 3D printing?," [Online]. Available: <https://www.hubs.com/knowledge-base/what-is-fdm-3d-printing/>. [Accessed 1 06 2022].
- [25] "Layers and perimeters," PRUSA knowledge base, [Online]. Available: https://help.prusa3d.com/article/layers-and-perimeters_1748#solid-layers-top-bottom. [Accessed 2 06 2022].
- [26] *Acoustic metamaterial panel for both fluid passage and broadband soundproofing in the audible frequency range* Jae Woong Jung, Jae Eun Kim and Jin Woo Lee, Jan 22, 2018.
- [27] "Metacoustics inovate solutions," [Online]. Available: <https://metacoustic.com/services/>. [Accessed 3 06 2022].
- [28] WertelOberfell, "Noise absorbing patterns," [Online]. Available: <http://www.werteloberfell.com/project/noise-absorbing-patterns/>. [Accessed 1 06 2022].
- [29] "How to create high quality STL files for 3D prints," Markforged, [Online]. Available: <https://markforged.com/resources/blog/how-to-create-high-quality-stl-files-for-3d-prints>. [Accessed 4 06 2022].
- [30] "Infill types and their properties," [Online]. Available: https://help.prusa3d.com/article/infill-patterns_177130#infill-types-and-their-properties. [Accessed 4 06 2022].

APPENDIX

ISO 10534-2:1998(E)

© ISO

Annex D (informative)

Theoretical background

The measuring method is based on the fact that the sound reflection factor at normal incidence r can be determined from the measured transfer function H_{12} between two microphone positions in front of the tested material, see figure 2.

The sound pressures of the incident wave p_1 and the reflected wave p_R are, respectively:

$$p_1 = \hat{p}_1 e^{jk_0 x} \quad (D.1)$$

and

$$p_R = \hat{p}_R e^{-jk_0 x} \quad (D.2)$$

where

\hat{p}_1 and \hat{p}_R are the magnitudes of p_1 and p_R at the reference plane ($x = 0$);

and $k_0 = k_0' - jk_0''$ is a complex wave number.

The sound pressures p_1 and p_2 in the two microphone positions are

$$p_1 = \hat{p}_1 e^{jk_0 x_1} + \hat{p}_R e^{-jk_0 x_1} \quad (D.3)$$

and

$$p_2 = \hat{p}_1 e^{jk_0 x_2} + \hat{p}_R e^{-jk_0 x_2} \quad (D.4)$$

The transfer function for the incident wave alone H_I is:

$$H_I = \frac{P_{2I}}{P_{1I}} = e^{-jk_0(x_1 - x_2)} = e^{-jk_0 s} \quad (D.5)$$

where $s = x_1 - x_2$ and is the separation between the two microphones.

Similarly, the transfer function for the reflected wave alone H_R is:

$$H_R = \frac{P_{2R}}{P_{1R}} = e^{jk_0(x_1 - x_2)} = e^{jk_0 s} \quad (D.6)$$

The transfer function H_{12} for the total sound field may now be obtained by using equations (D.3) and (D.4) and noting that $\hat{p}_R = r\hat{p}_1$, as:

$$H_{12} = \frac{p_2}{p_1} = \frac{e^{jk_0 x_2} + r e^{-jk_0 x_2}}{e^{jk_0 x_1} + r e^{-jk_0 x_1}} \quad (D.7)$$

Transposing equation (D.7) to yield r , and using equations (D.5) and (D.6), one has:

$$r = \frac{H_{12} - H_1}{H_R - H_{12}} e^{2jk_0x_1} \quad (\text{D.8})$$

The sound reflection factor r at the reference plane ($x = 0$) can now be determined from the measured transfer functions, the distance x_1 and the wave number k_0 which may include the tube attenuation constant k_0'' .

NOTE It is important that the transfer function is compensated for phase and pressure amplitude mismatch of the microphones when the two-microphone technique is used.

7.2 Determination of the sound velocity, wavelength and characteristic impedance

Before starting a measurement, the velocity of sound, c_0 , in the tube shall be determined, after which the wavelengths at the frequencies of the measurements shall be calculated.

The velocity of sound can be assessed accurately with knowledge of the tube air temperature from equation (5):

$$c_0 = 343,2 \sqrt{T / 293} \quad \text{m/s} \quad (5)$$

where T is the temperature, in kelvin.

The wavelength then follows from:

$$\lambda_0 = c_0 / f \quad (6)$$

The density of the air, ρ , can be calculated from

$$\rho = \rho_0 \cdot \frac{p_a T_0}{p_0 T} \quad (7)$$

where

T is the temperature, in kelvin;

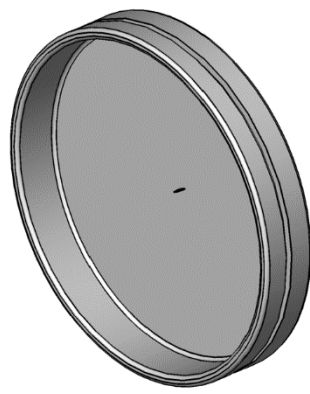
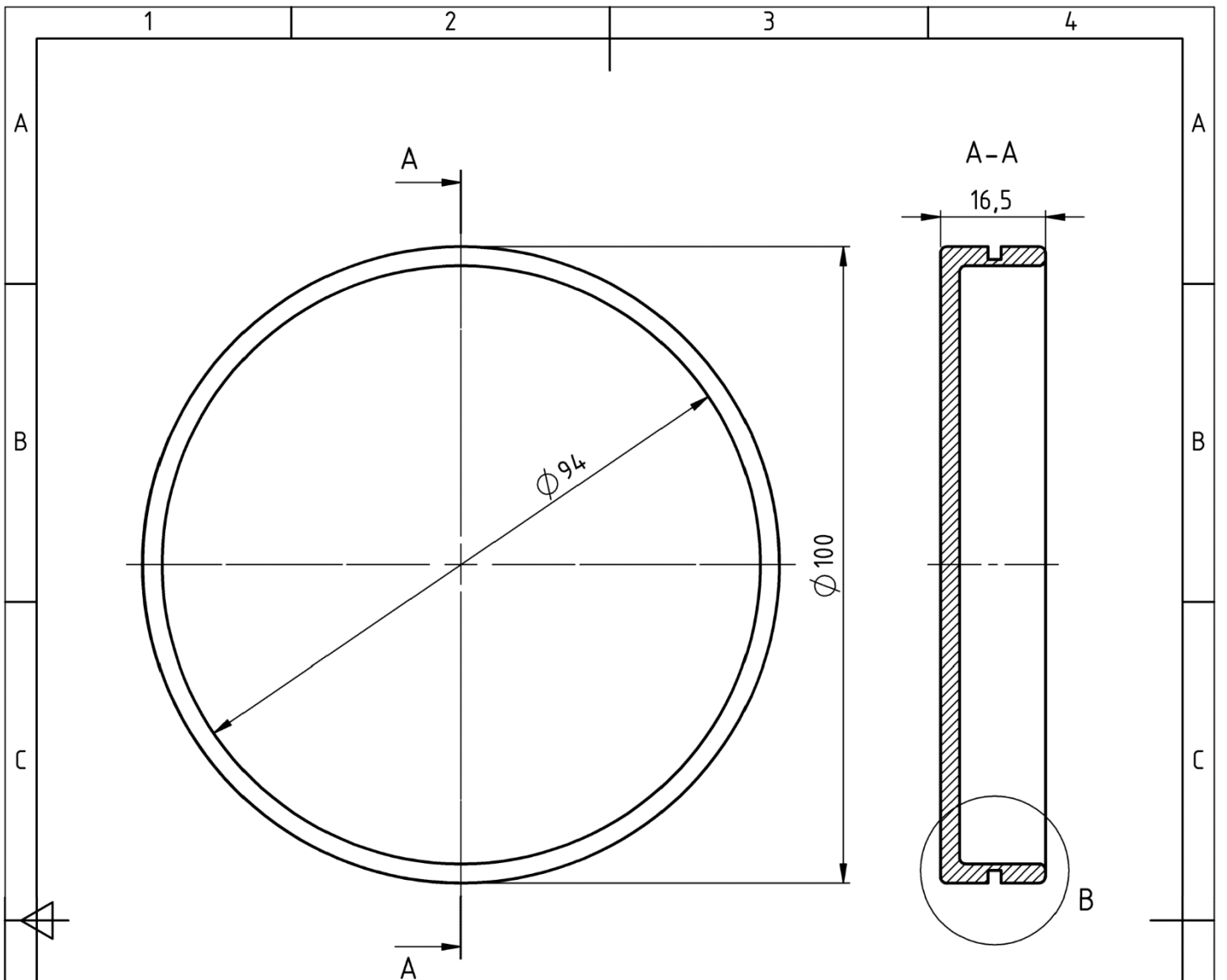
p_a is the atmospheric pressure, in kilopascals;

$T_0 = 293 \text{ K}$;

$p_0 = 101,325 \text{ kPa}$;

$\rho_0 = 1,186 \text{ kg/m}^3$.

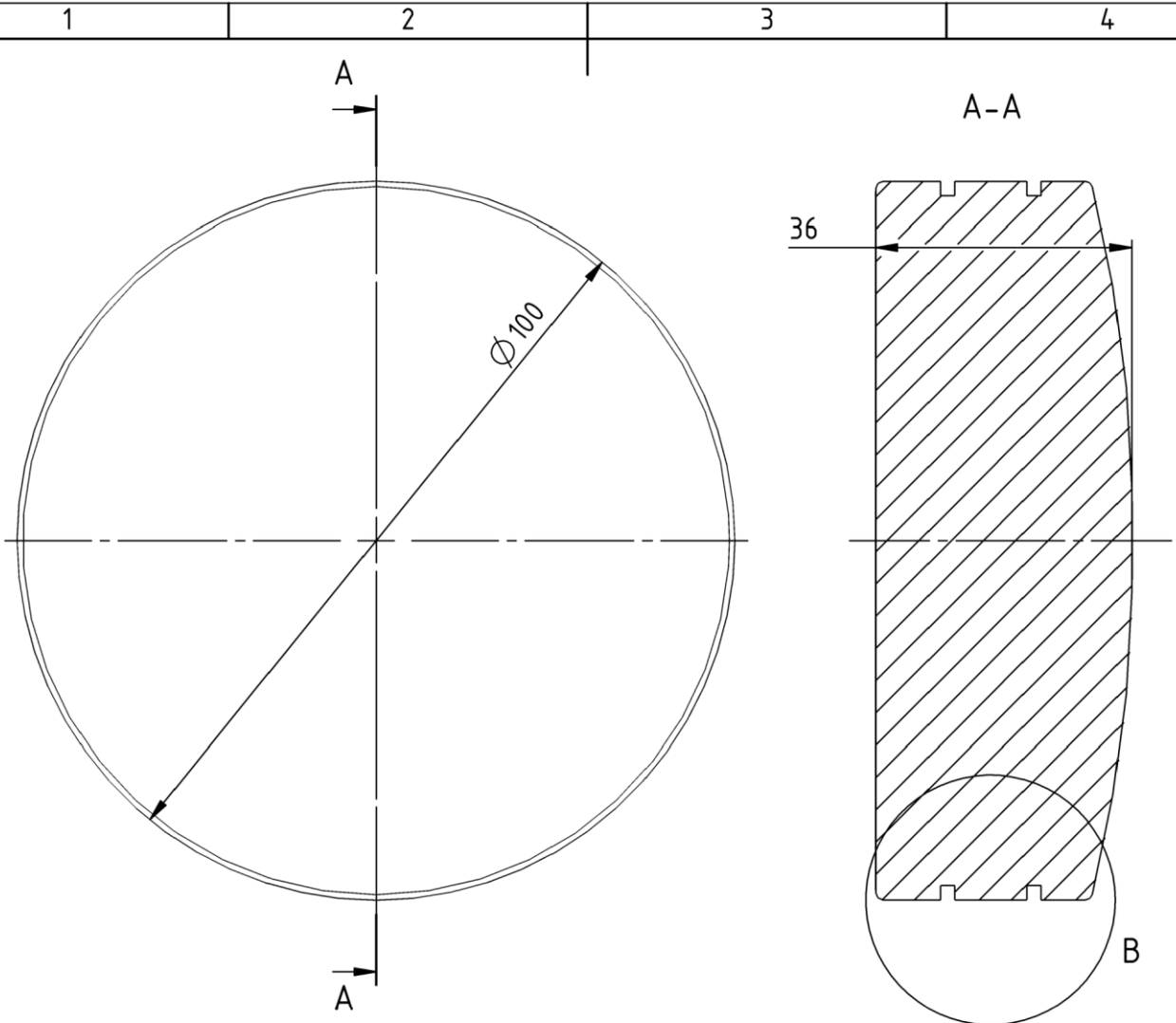
The characteristic impedance of the air is the product ρc_0 .



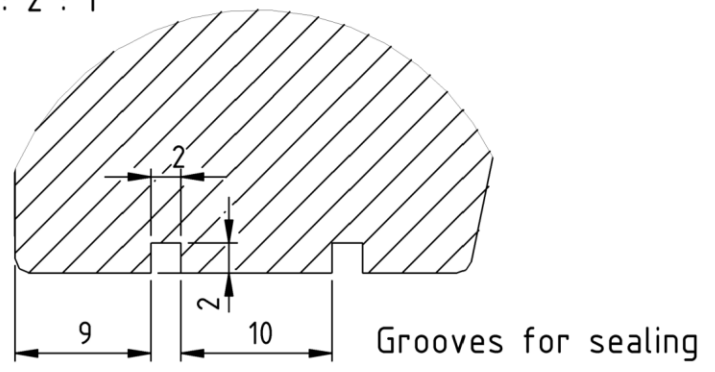
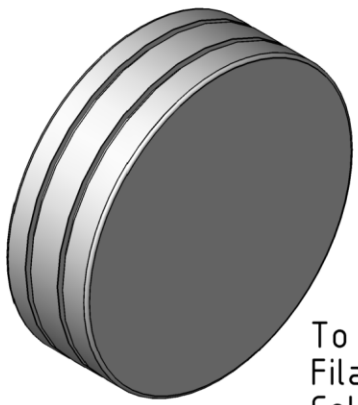
3D view

To be FDM 3D printed:
 Filament material: PETG
 Color: Black

Alg. tolerantie :			Getekend :	
PC-nr.	Reference barrier Planar sheet		Wolf Van Der Bauwhede	
Eenheid : mm			Klas :	Datum : 4/06/2022
		KU Leuven Technologiestrategie Gent		Schaal : 1:1
Faculteit Industriële Ingenieurswetenschappen			Formaat : A4	

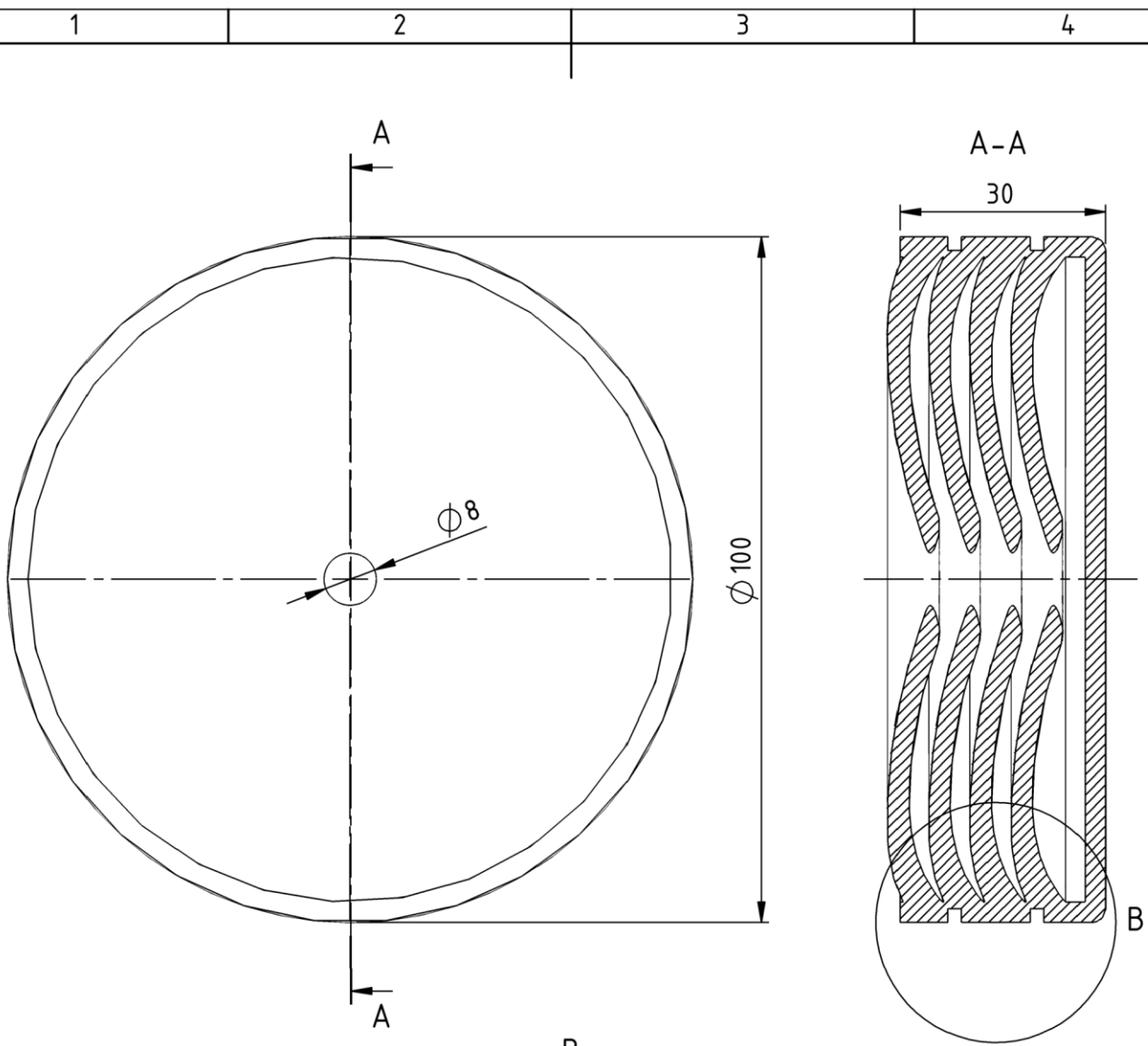


B
SCALE: 2 : 1



To be FDM 3D printed:
 Filament material: PETG
 Color: Black
 Use: Testing different infill geometries

Alg. tolerantie :		Getekend : Wolf Van Der Bauwhede	
PC-nr.	Infill comparison model		Klas :
Eenheid : mm		Datum : 4/06/2022	
		KU Leuven Technologiestudie Gent	Schaal : 1:1
Faculteit Industriële Ingenieurswetenschappen		Formaat : A4	



B
SCALE: 2 : 1

To be FDM 3D printed:
 Filament material: PETG or PLA
 Color: Black
 Use: Testing extra thin wall thickness

Alg. tolerantie :		Getekend :	Wolf Van Der Bauwhede
-------------------	--	------------	-----------------------

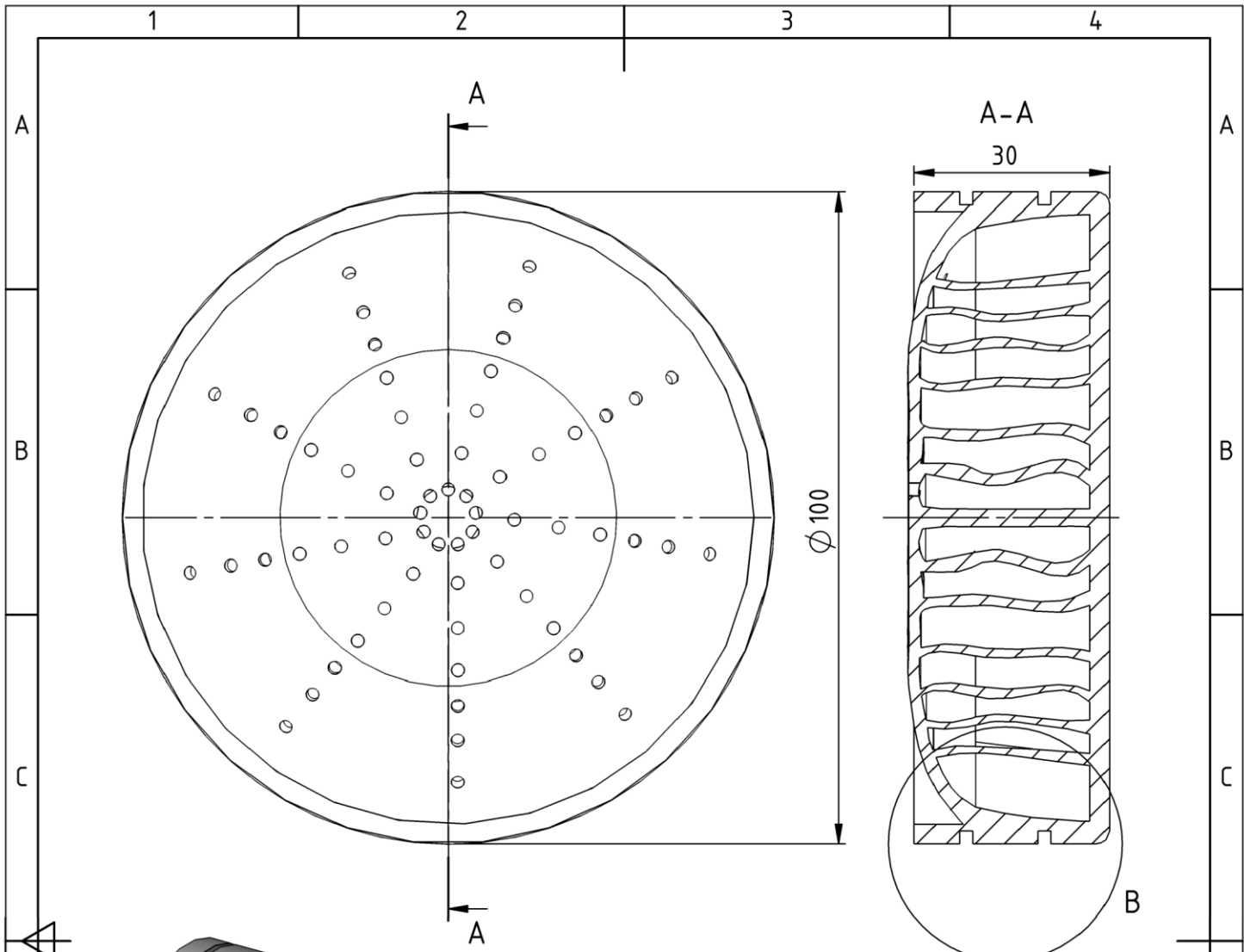
PC-nr.	Thin wall model
	Metamaterial curvature and thin walls

Klas :	Datum : 4/06/2022
--------	----------------------

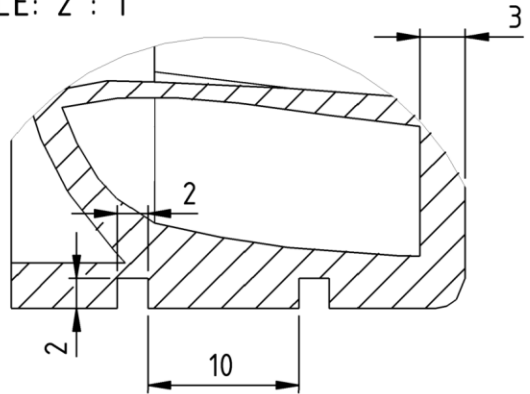
Eenheid : mm

KU LEUVEN
 KU Leuven
 Technologicampus Gent
 Faculteit Industriële Ingenieurswetenschappen

Schaal :	Formaat :
1:1	A4



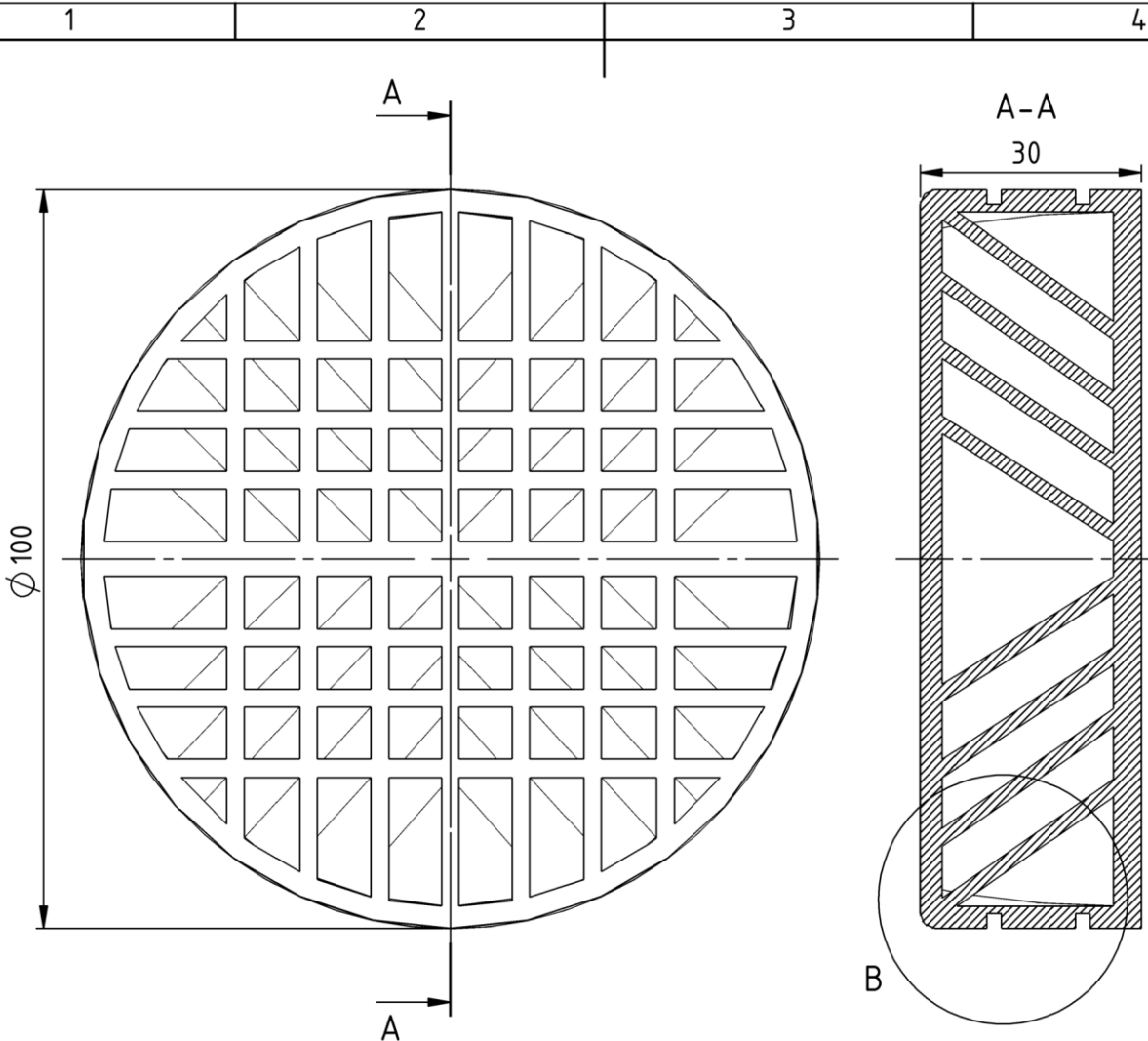
B
SCALE: 2 : 1



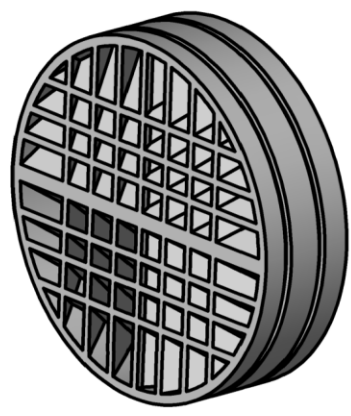
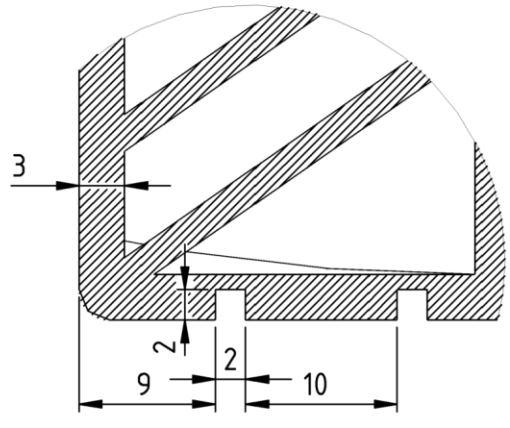
To be FDM 3D printed:
 Filament material: PETG
 Color: Black
 Use: Testing thin wall, curvature and air permeability

Alg. tolerantie :				Getekend :	
PC-nr.		Cavity barrier model High air permeability		Wolf Van Der Bauwhede	
Eenheid : mm				Klas :	Datum :
				4/06/2022	
Faculteit Industriële Ingenieurswetenschappen		KU Leuven Technocampus Gent		Schaal :	Formaat :
				1:1	A4

Tekeningnaam:Cavity barier



B
SCALE: 2 : 1



To be FDM 3D printed:
Filament material: PETG
Color: Black

Alg. tolerantie :		Getekend : Wolf Van Der Bauwhede	
PC-nr.	Thick wall model		Klas :
Eenheid : mm	 KU Leuven Technologicampus Gent Faculteit Industriële Ingenieurswetenschappen	Datum : 4/06/2022	Schaal : 1:1
		Formaat : A4	

